

‘A Fluorophore for the Future’

**Design and Synthesis of
Novel BODIPY Derivatives**

A thesis submitted in partial fulfilment of the requirements for the degree of

Master of Science in Chemistry

University of Canterbury

2017

Joseph Fee Bruce

"I have not failed.

I have just found ten thousand things that do not work"

Thomas Edison (1847-1931)

Acknowledgements

Firstly I would like to say thank you to everyone who has given me any wisdom, guidance, laughter or encouragement during my masters. Undeniably, both my moral and commitment have waivered at times as I have questioned myself, and through these interactions with all of you, I have persevered.

My supervisor, Dr Chris Fitchett: Your sheer aura as a chemist and mentor has kept me in the lab when I needed to be and for the knowledge you have passed on to me both during my undergraduate studies and my thesis, thank you.

To the rest of Team Fitchett; Sam, Will and Nic. You were there when I began my masters and you are still there as I finish. You've answered every annoying question I ever asked, provided me with all the practical skills I needed to get through my thesis and kept the office feeling alive the whole way, so cheers, you guys are the best.

An extra thanks goes to all of the academic and technical staff within the chemistry department, in particular Dr's Marie Squire and Matt Polson for their extra help with Mass-Spec and NMR and X-ray Crystallography, along with Wayne Mackay and Rob McCregor for their invaluable skills.

Special thanks to all my friends and family outside of the chemistry department, particularly to Mark and Jodie Flowerday for always been there when I needed you guys, and especially to my brother Tim, for all the support, help and advice above and beyond your older brother obligation.

To Anki, you have a faith in me that never waivers and your patience and care for me has been amazing. Ich liebe dich.

Finally, Mum and Dad, you have created a drive in me to succeed that I will always be truly truly grateful for and my results are in no small part attributed to your hard work, so thank you.

Table of Contents

Acknowledgements.....	III
Table of Contents.....	IV
Abstract.....	V
Abbreviations.....	VI
Chapter One: Introduction.....	1
1.1 Introduction to Fluorescence and Fluorophores	2
1.2 The BODIPY Fluorophore.....	4
1.2.1 “BODIPY” Nomenclature.....	5
1.2.2 General BODIPY Syntheses.....	6
1.2.3 General BODIPY Syntheses.....	8
1.3 Effects of Modification to the “BODIPY Core”.....	11
1.3.1 Quantum Yield Trends.....	12
1.3.2 Bathochromic Shift in BODIPY Dyes.....	17
1.3.3 BODIPY: Creating Bathochromic Shift.....	18
1.4 Specially Modified BODIPY Derivatives.....	22
1.4.1 Photodynamic BODIPY Derivatives.....	23
1.4.2 Functionalized BODIPY Probes.....	26
1.4.3 Multiple Core BODIPY Derivatives.....	28
1.4.4 Large Aromatic Polycyclic BODIPY Derivatives.....	30
1.4.5 Metal Incorporation into BODIPY Frameworks.....	33
1.4.6 Cyclised BODIPY Derivative.....	35
Chapter Two: Development of HBC-Coupled BODIPY Derivatives.....	37

2.1 HBC-Coupled BODIPY's.....	38
2.2 Synthesis of HBC-type BODIPY 36.,.....	39
2.2.1 Synthesis of 5-Phenyl Dipyrromethane 41.....	41
2.2.2 Synthesis of <i>meso</i> -Phenyl BODIPY 5.....	45
2.2.3 Synthesis of 2,6-Dibromo BODIPY 38.....	48
2.2.3.1 Mass Spectrometry of BODIPY 38.....	49
2.2.4 The Sonogashira Reaction in BODIPY 39 Synthesis.....	51
2.3 Development of <i>Meso</i> -HBC-Coupled BODIPY 37.,.....	56
Chapter Three: Metal Incorporated BODIPY Structures.....	59
3.1 Metal Coordinating BODIPY's.....	60
3.1.1 Synthesis of BODIPY's 46 and 47.....	61
3.1.2 Development of BODIPY-Based Inorganic Frameworks.....	66
3.1.3 Attempted Complexation of BODIPY-Ligands 46 and 47.....	67
3.1.4 Metal Coordination Targeted Derivatisation of BODIPY 56.....	73
3.1.5 Metal Complexation of BODIPY 48.....	78
3.2 Synthesis of 2,4-Dimethylpyrrole.....	83
Chapter Four: Dual Core BODIPY Derivatives.....	85
4.1 Dual Core BODIPY Derivatives	86
4.2 Background to the Targeted Dual Core Functionalisation.....	86
4.3 Proposed Dual Core BODIPY Systems.....	89
4.4 Trialling the BF ₂ Core.....	92
Chapter Five: Conclusions and Future Work.....	94
5.1 Conclusions and Future Work.....	95
5.2 Dual Core Derivatives.....	95
5.3 Metal Coordinating BODIPY Derivatives.....	97
5.3.1 MOF-Targeted BODIPY Ligands.....	97
5.3.2 BODIPY Coordination Complexes.....	98
5.4 HBC-Coupled BODIPY Derivatives.....	100

5.4.1 2,6-Functionalized BODIPY Derivatives of 36.....	100
5.4.2 <i>Meso</i> -Phenyl Functionalized BODIPY Derivative 37.....	102
 Chapter Six: Experimental.....	 104
6.1 General Experimental.....	105
6.2 Compound Synthesis and Characterisation	107
References.....	120
Appendices.....	129

Abstract

This thesis provides insight into the chemistry of the BODIPY family of fluorophores. It describes the synthetic methods undertaken to attempt various structural modifications of the core BODIPY framework. Three different types of BODIPY themed molecules were targeted for synthesis; HBC-coupled BODIPY derivatives, metal coordinating ligand-type BODIPY molecules, and dual BF₂ core containing frameworks.

Chapter One, describes the background of BODIPY molecules, their chemistry and their large role within fluorescence based research and applications. This chapter also provides a short review of all relevant BODIPY derivatives and the related research. **Chapter Two** introduces the synthetic schemes investigated for forming HBC appended BODIPY derivatives and the results achieved here. **Chapter Three** presents the research into developing the relatively novel metal coordinating BODIPY molecules, and the promising syntheses carried out to form multiple BODIPY derivatives with metal interactive capability. **Chapter Four** outlines the research around creating BODIPY themed, dual BF₂ core systems, expanding on the fairly recent discovery of the BOPHY framework within the BODIPY research community. **Chapter Five** summarise the results and outlines the conclusions gained from the project along with the potential future direction of the research. **Chapter Six**, describes the experimental methodology of all adapted and newly formed syntheses of molecules formed throughout the thesis.

One novel derivative is described, with the full crystal structure and analytical characterisation, along with several new methods for synthesis and purification of established BODIPY compounds.

Abbreviations

General Abbreviations

^1H -NMR: Proton Nuclear Magnetic Resonance

^{13}C -NMR: Carbon Nuclear Magnetic Resonance

HSQC: Heteronuclear single quantum coherence spectroscopy

HMBC: Heteronuclear multiple-bond correlation spectroscopy

UV-Vis: Ultraviolet-Visible

ESI-MS: Electrospray Ionisation Mass Spectrometry

MP: Melting Point

IR: Infrared

NIR: Near Infrared

s: strong (IR)

m: medium (IR)

w: weak (IR)

br: broad (IR)

IUPAC: International Union of Pure and Applied Chemistry

Important Chemical Abbreviations

BF_3 -etherate/ $\text{BF}_3\cdot\text{OEt}_2$: Boron trifluoride diethyletherate

TFA: Trifluoro acetic acid

DDQ: 2,3-Dichloro-5,6-dicyano-1,4-benzoquinone

EDC: Ethylene dichloride = Dichloroethane

EG: Ethylene Glycol

THF: Tetrahydrofuran

DMF: Dimethylformamide

Chapter One

BODIPY: A Modern Fluorophore

1.1 An Introduction to Fluorescence and Fluorophores

Fluorescence is the emission of photons, as they relax via radiative progression from their excited state, formed through the absorption of light.¹⁻² The scientific observations of fluorescence began in the early 19th century, initially described by Edward D. Clarke in the form of a light glowing from within Fluorite rocks.³ These observations culminated in 1845 when Sir John Frederick William Herschel witnessed fluorescence from quinine.¹ This discovery catalysed the fluorescence era, with fluorophores being incorporated into multiple scientific applications, most notably as versatile imaging tools.⁴⁻⁶

Fluorophores can be described as a class of compounds which repeatedly undergo fluorescence.¹ They have capacity for absorption of light energy, giving rise to excitation, and subsequent emission, but also allow for the repetitive cycling of this process.¹ The synthesis of the most notable of the modern fluorophore's dates back over a century to the discovery of Fluorescein, synthesised in 1871 by Adolf von Baeyer [Fig. 1.1].⁷

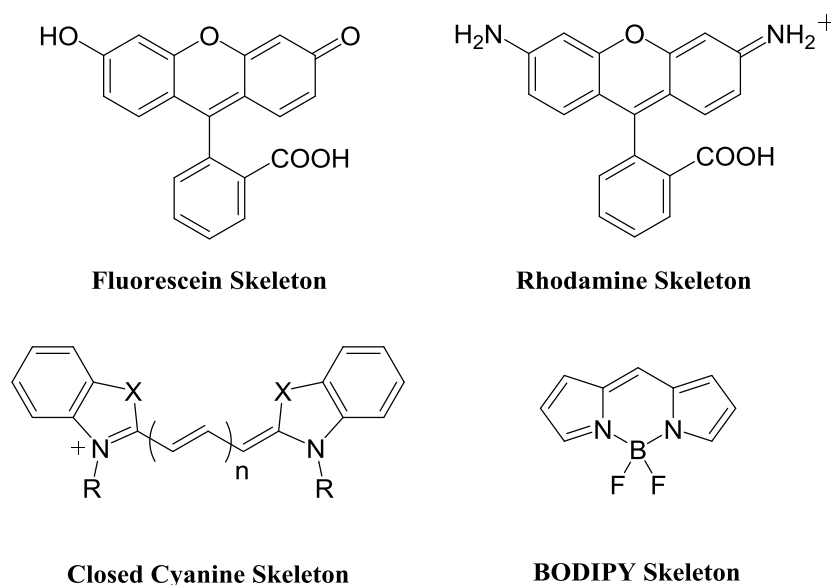


Figure 1.1. Organic Fluorophores.

It was several decades after its discovery until Fluorescein actually became established as a fluorescent dye, largely due to the lack of need for molecular labels at this point in time, and largely due to a lack of chemical knowledge of their powerful utility.⁸

Two other key classes of fluorophore were discovered during the 1900's, first was the Cyanine's [Fig. 1.1], which were first identified in 1856 through their clearly observed blue-green hue, witnessed when sitting idle in a bench-top solution.⁹ Later the Rhodamine family of dyes were discovered in 1905 [Fig. 1.1], via development to the fluorone skeleton, notable as the structural base of Fluorescein lead to their conception.¹⁰ Prior to realising the wide array of uses for such highly intense fluorescent compounds, Fluorescein lead the way as the first choice fluorophore for gathering chemical or biochemical information in both research and medicinal contexts. Both the Cyanine and Rhodamine dye families found many uses within the scientific community as well, with the Rhodamine dyes in particular becoming well noted as an early alternative to Fluorescein derivatives.^{4-5, 11}

Fluorescein isothiocyanate (FITC) found use as an imaging agent in fluorescence microscopy, wherein the fluorophore is tagged to a target molecule that is to be tracked, most likely after some form of molecular interaction or a reaction pathway.^{8, 12-13} Post reaction, the fluorophore is then excited through exposure to a light source of specific wavelength and the generated emission observed as fluorescence, which is detected and traced. Along with its application in fluorescence microscopy Fluorescein also found use as a topical and intravenous diagnostic tool in identification of medical conditions, primarily in the form of its sodium salt.¹⁴

The broad application of Fluorescein and early alternatives was restricted on the basis of safety reasons however. FITC is phototoxic and generates toxic compounds upon exposure to the energy associated with light absorption, whilst the sodium salt also generates its own safety issues primarily surrounding the pH differences between the natural cellular environment, and that of when it is exposed to sodium Fluorescein.¹⁵⁻¹⁷ Predictably due to their base structural similarities the Rhodamine dyes generally demonstrate considerable phototoxicity as well, whilst the Cyanine derivatives are known for being notoriously unstable.^{4, 15}

In the late 1900's fluorophores and fluorescence in general found extensive modern applications in an increasing range of scientific research areas. Different fluorescent compounds found further use in fluorescence microscopy, fluorescence imaging, as clinical diagnostic tools for medicine, molecular labelling agents and tracers, imaging

single molecule interactions in molecular biology and biochemistry along with applications in the environmental sciences for the tracking of trace elements and metal ions.¹⁸⁻²³ With the sudden growth of interest, the need for new fluorescent dyes that could challenge the power and versatility of Fluorescein and related compounds, whilst also improving upon their limitations, had been realised. This caused a large growth in research targeting the identification of new fluorophores, with significant interest also invested into the development of known fluorophores, whose potential as molecular labels and imaging agents were yet to be established.²⁴

Through this rapid expansion of interest in the area, multiple compounds were brought into the light, Green Fluorescent Protein (GFP) being one of these.²⁵ GFP was an already documented biological compound which found its name as an extremely powerful naturally occurring fluorescent tag in 1992, when Martin Chalfie who would later be awarded the Nobel prize for his research, demonstrated its use at tracking cells within *Caenorhabditis elegans* a species of transparent roundworm.^{24, 26} This came 30 years after its initial discovery in 1962, when it was isolated from a species of luminescent jellyfish. As a naturally occurring biologically active compound GFP found its own niche within the area of fluorescent dyes. Throughout the scientific community it was viewed as a trade-off between Fluorescein, because GFP exhibits a lower natural fluorescence, but is highly desirable for its extremely low general toxicity, and as a result of this property in particular, it has become the preferred fluorescent compound for imaging biological systems and living cell molecular interactions.^{15, 27-29}

1.2 The BODIPY Fluorophore

During the late 20th century as the interest in fluorescence rapidly grew, another family of fluorescent compounds with huge potential for application as fluorescent imaging agents were re-discovered, these being the difluoro bora-indacene (4,4-difluoro-4-bora-3a,4a-diaza-s-indacene hereafter abbreviated as BODIPY) family of dyes [Fig. 1.2].^{6, 30-33} BODIPY dyes are another series of intensely fluorescent organic molecules, based around a conjugated polycyclic system [Fig. 1.2].^{30-31, 34-38}

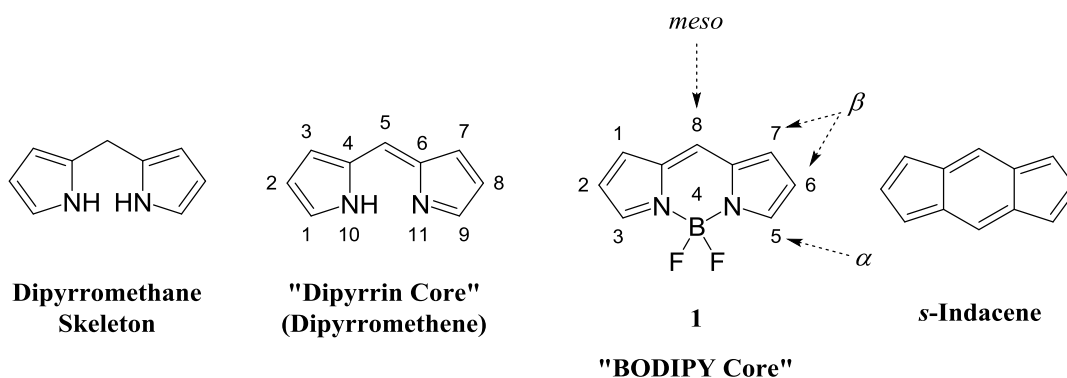


Figure 1.2. The “BODIPY Core” and related organic frameworks.

Since their discovery they have been extensively researched for application in the area of fluorescence imaging. The first of the BODIPY derivatives were synthesised in 1968 by Alfred Treibs and Franz-Heinrich Kreuzer.³⁹ This discovery followed the trend for most of the modern fluorophores in that it was not immediately recognized as a significant breakthrough in the field.

Several decades later between 1989 and 1992 the BODIPY framework was developed into commercially viable fluorescent dyes, the use of which catalysed an exponential increase in research solely targeting the development and structural progression of BODIPY dyes.^{33, 40} In 2009 the unsubstituted core **1** [Fig. 1.2] was finally synthesised and reported by three independent groups, this being initially hampered due to the high reactivity of the starting materials and the intermediate involved, resulting in significant synthetic difficulties.⁴¹⁻⁴³ After two decades of worldwide research targeting BODIPY dyes and the optimisation of both their photophysical and chemical properties, the range of commercially available BODIPY dyes has increased significantly, and the number of ways in which BODIPY dyes can be tailored for specific needs is unsurpassed in the field of fluorescence.^{30-31, 34-38}

1.2.1 “BODIPY” Nomenclature

The full name for BODIPY dyes in accordance with IUPAC guidelines is given as: 4,4-difluoro-4-bora-3a,4a-diaza-s-indacene, and modern research has thus led to an adapted abbreviation for BODIPY dyes, them often being specifically cited now in regards to

the boron substitution, with the di-fluorinated species indicated as *F*-BODIPY and alternatives having a different prefix letter dependent on the substituents attached [Fig. 1.2].³¹ This is a result of the increasing frequency of BODIPY dyes that are synthesised with phenyl and other groups, substituted in place of the fluorine atoms. In regards to the work described here however, as all relevant molecules are of the di-fluorinated type, the general abbreviation of BODIPY has been applied throughout.³⁰

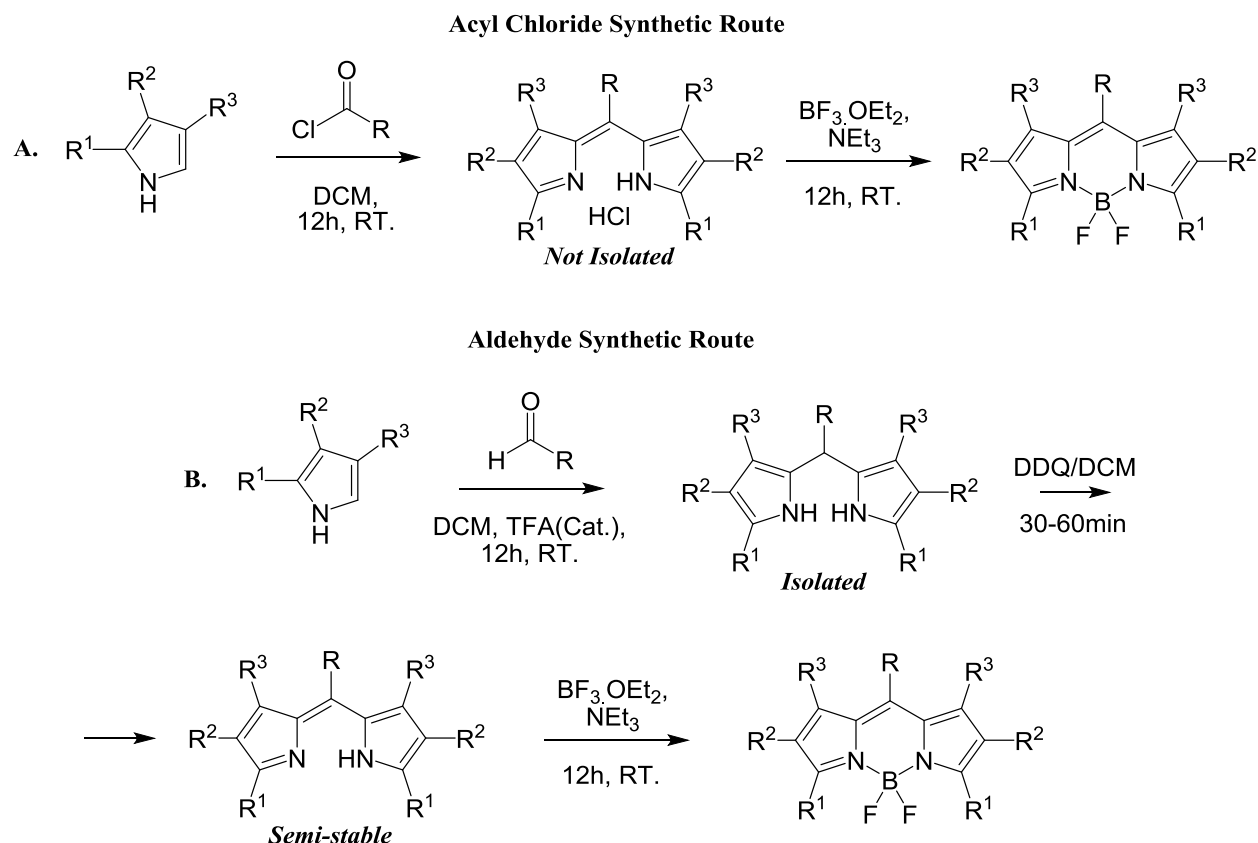
When applying the traditional IUPAC numbering system to BODIPY molecules, atom labels are consistent with the carbon polycyclic analogue of BODIPY, *s*-Indacene [Fig. 1.2]. This opposes the standard for the numbering of their precursor molecules, with both the dipyrins and dipyrromethanes following conventional numbering around heterocyclic systems and starting adjacent to the first heterocyclic atom [Fig. 1.2]. Given that the BODIPY molecules can still be regarded as analogous to the “dipyrin core” also, they still have the same *meso*, α and β labels for the respective ring positions however [Fig. 1.2].³⁰⁻³¹

1.2.2 General BODIPY Syntheses

Through considerable experimental work multiple synthetic routes have been discovered for the synthesis of BODIPY and BODIPY-type compounds.³⁰ Syntheses have been described using an α -formylated pyrrole derivative in a self-polymerisation reaction, through to the use of azapyrromethene precursors, to form aza-BODIPY derivatives, in which a nitrogen atom is substituted in place of the *meso* carbon atom.³⁰ The reactions all usually involve the use of a pyrrole derivative and the presence of some sort of electrophilic carbonyl group.^{31, 34-38}

In terms of the general routes for synthesising the BODIPY core however, there are considered two popular methods [Scheme 1.]. The first reaction uses pyrrole in combination with an acyl chloride, whilst the second replaces the highly reactive acyl chloride with the equivalent lower reactivity aldehyde functionality.^{31, 34-38} The substitution to the carbonyl reagent determines the functionality of the *meso* position, whilst the substitution to the pyrrole derivative gives rise to the peripheral groups in the 1-3 and 5-7 positions on the BODIPY framework [Scheme 1.]. Due to the highly

reactive nature of acyl chlorides they are best used for the formation of both peripherally and *meso*-substituted BODIPY's. The substitution to the acyl chloride itself, lowers its reactivity reducing the potential for side reactions, whilst using a substituted pyrrole removes the ability for self-polymerisation, this occurring readily via the mechanism of porphyrins synthesis.³⁰⁻³¹



Scheme 1. The two general synthetic routes **A.** and **B.** for forming the BODIPY core structure.

Note: "R" groups are generally Hydrogen, Methyl or Phenyl substituents for such molecules.

Formation of *meso*-substituted derivatives using the acyl chloride approach, proceeds via the formation of highly unstable dipyrromethene hydrochloride intermediates [Scheme 1.]. The reactivity of such intermediates can be reduced with increased C-substitution, and with it their stability increased, however usually isolation of these compounds is not attempted during these reactions.^{30, 35, 37} Route **A.** of Scheme 1 shows

the pathway for synthesis of the generic BODIPY molecule with the structure of the non-isolated intermediate dipyrin hydrochloride.

Route **B.** shows the alternative pathway when starting with an aldehyde instead as shown in Scheme 1. The intermediate dipyrromethane product can be isolated at this point, purification and characterisation can then be carried out. These isolated dipyrromethanes are stable for relatively long durations dependent on the level of substitution, however they do degrade slowly when exposed to harsh physiological conditions such as light, air or acid. In order to form the BODIPY framework from dipyrromethanes, they must be oxidised to their respective dipyrromethenes prior to addition of the Lewis acid and base, used for installing the BF_2 centre. These dipyrromethene intermediates are of similar instability to the hydrochloride salts and are usually not isolated at this stage. Oxidation usually proceeds via the addition of either DDQ or *p*-chloranil to a solution of the dipyrromethane in DCM. Both oxidants work, however they are chosen selectively based upon the dipyrromethane reactivity.^{30, 33, 35} DDQ is a much stronger oxidising agent and generally applied for syntheses using a more highly substituted and stable dipyrromethane, whereas *p*-chloranil is utilised when there are concerns of instability or chemical breakdown under harsh conditions.

The reactions are usually monitored closely via TLC, with this usually being sufficient to detect the presence of the respective dipyrromethene and in a one-pot type reaction, both the $\text{BF}_3\cdot\text{OEt}_2$ and NEt_3 are added to the same solution forming the BODIPY derivatives directly, with the bulk of the purification being left until the BF_2 complexation has occurred.

1.2.3 Chemical and Optical Properties of BODIPY

The fluorescent character of BODIPY is present as a result of the fully conjugated dipyrin system, containing the linking boron bridged nitrogen core.^{30-31, 35, 37} Many desirable photophysical properties arise from this unique framework, with BODIPY dyes commonly demonstrating quantum yields greater than 0.50, extinction coefficients frequently beyond $50,000 \text{ M}^{-1}\text{cm}^{-1}$, low levels of triplet-state formation and narrow

absorption and emission bands that occur around 500 nm, with small Stokes shifts, commonly around 15 nm.^{30-31, 34-38}

Figure 1.3 shows the commercially available BODIPY-FL, in action within the actin filament networks of bovine pulmonary artery endothelial cells.⁴⁴ The green fluorescent microtubules are imaged as a direct result of BODIPY-FL conjugation to the anti- β -tubulin mouse monoclonal antibody, which accumulates here during its metabolism [Fig. 1.3]. BODIPY-FL itself is a simple variant to the core structure, with three-chain alkyl linker at the 5-position connecting to a terminal carbonyl group which is commonly exploited for conjugation to other biomolecules or substitution for a functionality with fluorescent probe activity [Fig. 1.3].³³ As evidenced by the general optical properties shown in Figure 1.3, which will shall be elaborated later, BODIPY-FL is a very good example of the powerful photophysical characteristics commonly seen amongst this fluorophore family.

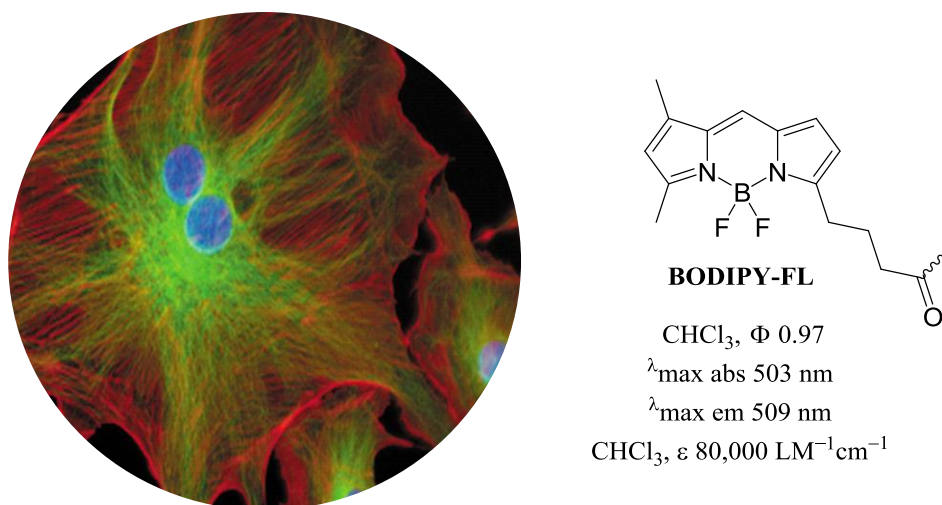


Figure 1.3. Left: Green fluorescence imaging from BODIPY-FL in action. Right: Generalised structure and optical properties of BODIPY-FL. *Note: The undefined wavy bond, depicts the usual site of bonding for molecular labelling applications.*

When considering the power of a fluorescent compound in sole respect to its optical properties, the three most commonly referenced data points are that of the absorption and emission maxima and the corresponding quantum yield. For absorption and

emission peaks of a compound utilised as a fluorescent tool, the 500 nm mark is considered a standard value for fluorophores, with fluorescein for example exhibiting absorption and emission maxima at 494 nm and 511 nm respectively.⁴⁵

With most applications for modern fluorophores being associated with biological contexts, it is most important that the dyes absorption and emission spectra are not shifted to higher energy's (lower wavelengths), as this creates the potential for cellular damage.^{2, 19-21} It is also considered generally favourable for fluorophores to have small Stokes shifts. A Stokes shift being the gap between the absorption and emission wavelengths, which when minimised allows excitation and emission to occur a much narrower excitation wavelength. BODIPY 1 has absorption and emission peaks of 497 nm and 504 nm, respectively, and given that it is a natural reference as the starting point for synthetic development of BODIPY dyes, they can be considered to have a more than acceptable fluorescence range [Fig. 1.2].⁴³ BODIPY-FL as an example of a commercially available fluorophore, absorbs at 503 nm, emitting at 509 nm [Fig. 1.3].⁴⁴ BODIPY-FL has experienced a large amount of success in the area of molecular labelling and fluorescence imaging since its conception. This success has driven significant attention to molecules that exhibit a similar spectral range and set of optical properties, greatly increasing their desirability within the scientific community.³³

The quantum yield of a compound is described as a ratio of the photons absorbed over the number of photons emitted and thus gives rise to a theoretical maximum of 1.0.² A fluorophore with a quantum yield measured at higher than 0.10 is generally considered a strongly fluorescent compound.³⁰ BODIPY dyes regularly exceed 0.50 and have been isolated with quantum yields as high as 0.98, BODIPY-FL again as an example, has a measured quantum yield of 0.97 [Fig. 1.3]. Given the commonly observed high quantum yields, BODIPY dyes are regarded as highly fluorescent and have significant potential as powerful imaging agents.³⁰

Along with the desirable photo-physical properties of the BODIPY framework, the skeleton itself has many other beneficial properties. It is; both chemically and photo chemically robust, exhibits stability to pH and temperature fluctuations, is relatively non-toxic and boasts a significant capacity for the fine-tuning of photophysical properties through modification of its peripheral functional groups.^{30-31, 34-38} Two of

these properties have of particular significance in the massive interest growth that BODIPY gained during the 1990's. These being the relative stability of BODIPY to photochemical exposure and the ease in which modifications can be made to the BODIPY framework. The photo stability of BODIPY dyes is extremely desirable as most of the alternative fluorophores like the rhodamine and fluorescein derivatives, as previously noted, are photo toxic due to their break down upon exposure to any high energy light waves.¹⁵⁻¹⁷ Reduced toxicity greatly increases the potential for BODIPY dyes to have medicinal and bio-imaging applications.

Due to the huge number of areas that fluorescence is utilised within the modern scientific community, there is no one fluorophore which is suitable for every application. Thus discovery of a single new fluorophore, whilst being potentially useful, is only significant in a broader sense if it has room for structural modification. This is why the BODIPY dyes are described with “unsurpassed versatility” throughout modern literature.³⁷ The capacity they hold for functionalisation is immense and the effect that even a small change to the periphery of the skeleton, can have on the overall photophysics of the BODIPY dye, can be very large, this allowing for tailoring to specific applications.

1.3 Effects of Modification to the “BODIPY Core”

As previously mentioned, the BODIPY framework holds an overwhelming potential for structural modification and fine tuning of its photophysical and chemical properties. Figure 1.4 is designed to highlight the power of small structural modifications to the BODIPY framework primarily in terms of their optical influence. It shows seven derivatives to the core molecule, three of which; BODIPY's **2**, **3**, and **4**, differ minimally from **1** in that they are di, tetra and hexa-methylated at the peripheral positions on the framework.^{43, 46-47} It also shows the corresponding *meso*-phenyl adducts of these derivatives, BODIPY's **5** – **8** [Fig. 1.4],⁴⁸⁻⁴⁹ which also exhibit vary different photophysical properties and help to elucidate certain phenomena commonly observed throughout BODIPY molecules described in the literature.

1.3.1 Quantum Yield Trends

There are multiple factors which play a role in deciding the fluorescent strength of a particular BODIPY dye, however there are two primary modifications which create the most significant bolstering and quenching effects to the quantum yield. Firstly would be the absence or presence of a group in the *meso* position and its steric freedom and electronic nature. Secondly would be the level and type of substitution around the BODIPY periphery, thus at positions 1-3 and 5-7 as a collective. The reason that *meso* substitution can be regarded as the first and most relevant quantum yield modification is witnessed through the comparison of **1** and **5** [Fig. 1.4]. The only difference between these two BODIPY's is the presence of a phenyl group in the *meso* position for **5**, yet the measured quantum yield of **5** is 0.05 as opposed to 0.95 [Fig. 1.4].

This is as a result of the non-planar nature created through the addition of the phenyl ring to the framework. As there is no steric restriction around rotation of this *meso*-phenyl group, it can rotate in and out of the plane of the BODIPY core.³⁰ This rotation allows for non-radiative emission to occur in the form of photo-induced electron transfer (PET) side reactions. In this sense an electronic reaction is occurring between the substituent and the BODIPY core, and therefore sometimes these systems are regarded separately, as a highly fluorescent group with an attached very non-fluorescent functionality. In the case of an electron transfer from the non-fluorescent component to the BODIPY core, the effect we see is the result of reductive PET or a-PET wherein the "a" stands for acceptor in regards to the electronic state of the fluorophore itself. If electron transfer occurs in the opposing direction, what we are seeing is the result of oxidative PET or d-PET for donor PET. This occurs when the electronic state of the fluorophore is such that the HOMO of the core itself can donate to the LUMO of the non-fluorescent substituent.^{2,30,50} Both a-PET and d-PET result in significant quenching as evidence by the massive quantum yield difference between **1** and **5** [Fig. 1.4]. These redox exchanges are not possible if the *meso* centres conformation is locked as the free rotation is what makes the process energetically favourable. With a 0.46 jump in quantum yield between **6** and **7** these two BODIPY derivatives are a good example of the effect of conformational restriction [Fig. 1.4].

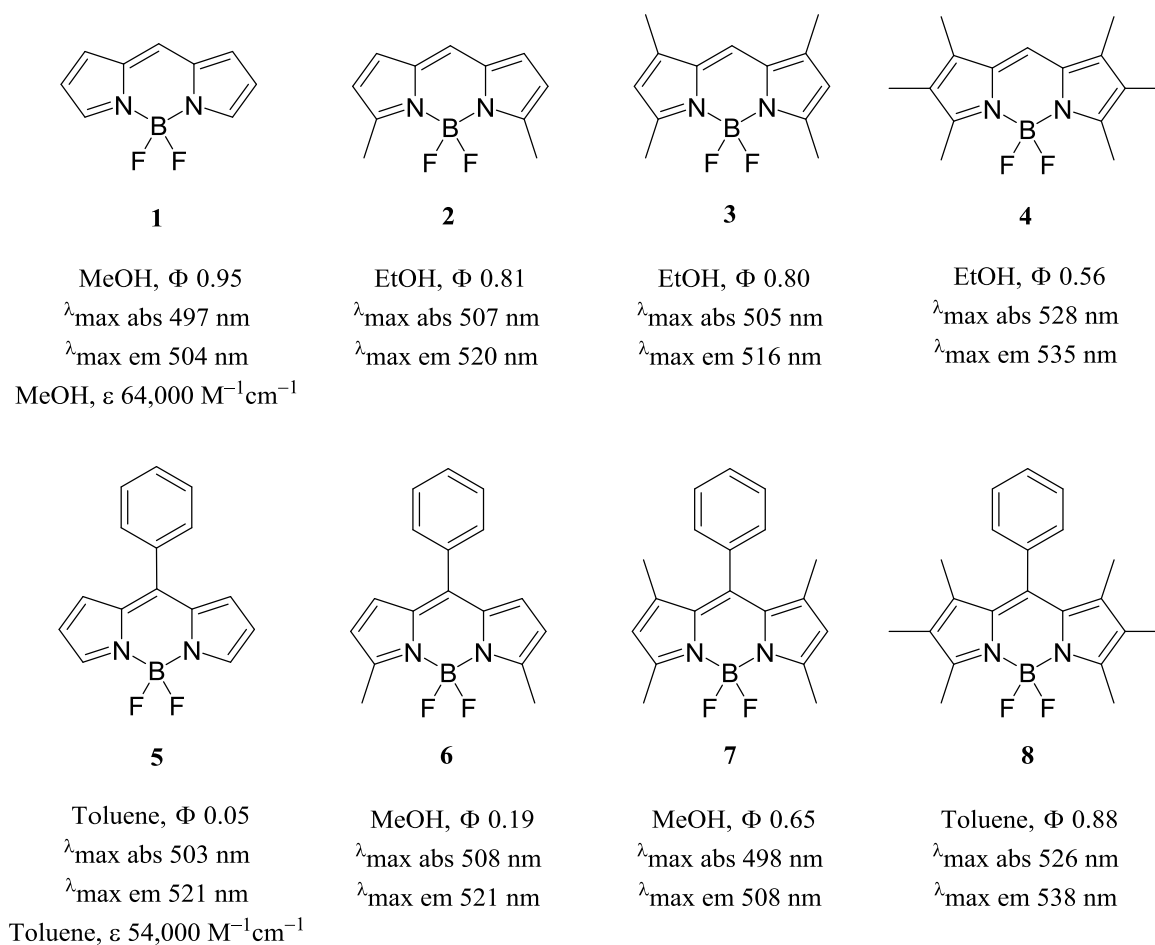


Figure 1.4. A selection of methylated “BODIPY core” derivatives, the equivalent *meso*-phenyl BODIPY’s and all relevant optical properties.

The methyl substitution to the 1, 7 positions creates a sterically hindered environment for the phenyl substituent, diminishing its ability to freely rotate and thus reducing the fluorescence quenching effect from the PET side reactions.^{30,50} Although not seen in Figure 1.4, it is also possible to control this effect through modification to the *meso* substituent rather than the core itself. The presence of any groups which limit the ability for free-rotation of the *meso* functionality will generate a similar result.

The decrease in quantum yield from molecules **1** through to **4** demonstrates the second trend observed for BODIPY dyes [Fig. 1.4]. This being that as the level of substitution increases around the periphery, the quantum yield is gradually lowered along with it. This is due to the conjugated nature of the BODIPY core which allows for delocalization of the electronic system through the attached substituents and thus

electron transfer to occur.^{30, 50-52} Similar to the effects observed for the *meso* substitution, this electron transfer then leads to a subsequent quenching of the quantum yield however given the size and position of the substituents the effect is not so pronounced. Increasing the size of the substituent and elongating further from the core has a more drastic quenching effect, if the conjugation is maintained through a series of double bonds or directly via ring fusion. If the conjugation is broken however, as the influence upon the electronic system is removed and the effect observed is minor in comparison.

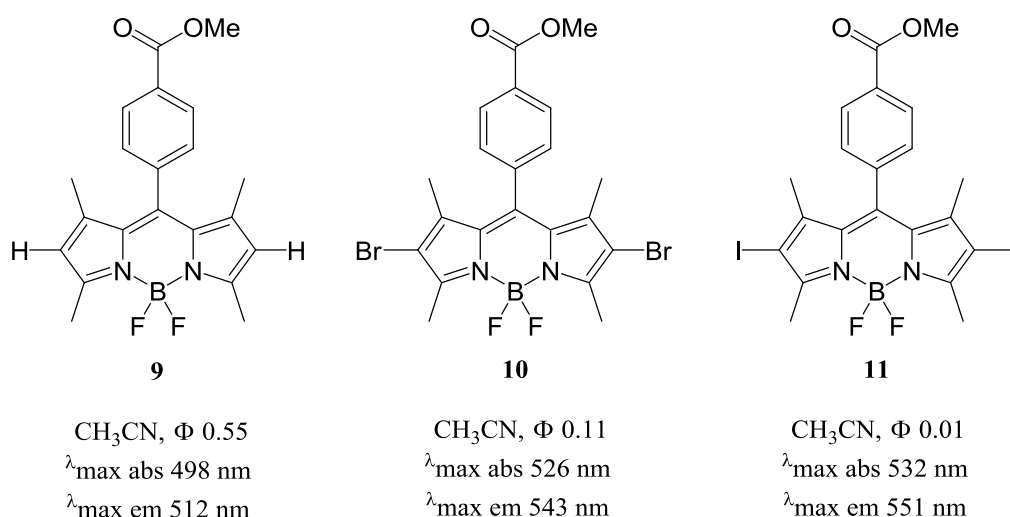


Figure 1.5. BODIPY derivative illustrating the heavy atom effect, a quantum yield quenching phenomenon.

Anomalies in this trend are evident when the BODIPY targeted is significantly *meso* substituted. This is clear when comparing **7** to **8** as the quantum yield actually increases by 0.23 when the framework is substituted at the 2 and 6 positions as well and from molecules **5** to **7** there is an upwards trend as well [Fig. 1.4]. Whilst these methyl substitutions do allow for further delocalization around the core, they also reduce the ability for PET side reactions via the *meso* substituent through the reduction of the HOMO energy level and as this is the dominant effect, increased substitution in the presence of a PET active *meso* group actually leads to a stabilising effect on the compounds quantum yield.⁴⁹⁻⁵¹

Molecules **9-11**⁵³ are an example of BODIPY derivatives which experience the heavy atom effect (HAE) [Fig. 1.5].⁵³⁻⁵⁶ This is an effect, created through the introduction of heavy atoms into the framework of a fluorophore. Fluorescence occurs through the excitation of an electron from the singlet ground state to the singlet excited state, and then a subsequent radiative emission back to the ground state.¹⁻² When the electron is present in the singlet excited state, it by nature has its spin still paired with the ground state. If, this spin is reversed however then an excited triplet state forms, wherein the spins are parallel rather than anti-parallel. When this transformation of excited states occurs nonradiatively and a singlet turns to a triplet or the reverse, this process is called intersystem crossing (ISC).^{53-54,56}

The primary causes of ISC are the presence of paramagnetic species in the presence of fluorescent molecules, and more commonly the presence of heavy atoms like the halogens, connected to the fluorophore.⁵³⁻⁵⁶ Heavy atoms promote ISC, and ISC results in a non-radiative loss of excited states. This meaning that rather than progressing via the radiative process of fluorescence back to the ground state, they instead return to the ground state via a non-radiative relaxation process. These photons are therefore not emitted, thus reducing the photon ratio and quantum yield and quenching the fluorescence observed from the fluorophore. This effect as a result of heavy atom presence, forms the HAE. Like most fluorophores, BODIPY's are thus subject to the effects of these heavy atoms being included in their framework. BODIPY **9** has a quantum yield of 0.55, this is the halogen unsubstituted derivative, however when the derivative is 2,6-dibrominated we observe HAE and the quantum yield drops 0.44 [Fig. 1.5].⁵³ Replacement of these bromine atoms with the much heavier iodine atoms, gives rise to a further quenching effect, with a measured quantum yield of 0.01.⁵³ At this stage, given BODIPY dyes general level of fluorescent character, this derivative can essentially be considered non-fluorescent.

Figure 1.6 and the derivatives shown, demonstrate multiple less frequently observed but clearly evident effects relating to quantum yields.^{30, 32, 57} These effects really suggest that despite there being patterns in the photophysical properties of BODIPY, there is a large level of unpredictability to the measured values we see. Electron withdrawing groups as opposed to electron donating groups have considerably different effects on the quantum yield when substituted into the conjugated system of a BODIPY

framework, this is evident when comparing the methoxy group of **12** as opposed to the fluorine atom of **13** [Fig. 1.6].^{30-31, 37} Halogens are in their nature electron withdrawing and deactivate aromatic systems via an inductive electron withdrawal effect due to their high electronegativity, they also contain lone pairs they are capable of resonance donation into the system and therefore have an activating effect simultaneously. Clearly what is more significant in terms of quantum yield, is the removal of electron density from the system itself rather than resonance contribution, with the highly electron donating methoxy group creates a BODIPY dye with double the quantum yield of **13** [Fig. 1.6]. This increased quantum yield likely due to its large electron contribution to the conjugated system, which acts to reduce the HOMO-LUMO energy gap and thus allows for faster relaxation of excited photons back to the ground state.

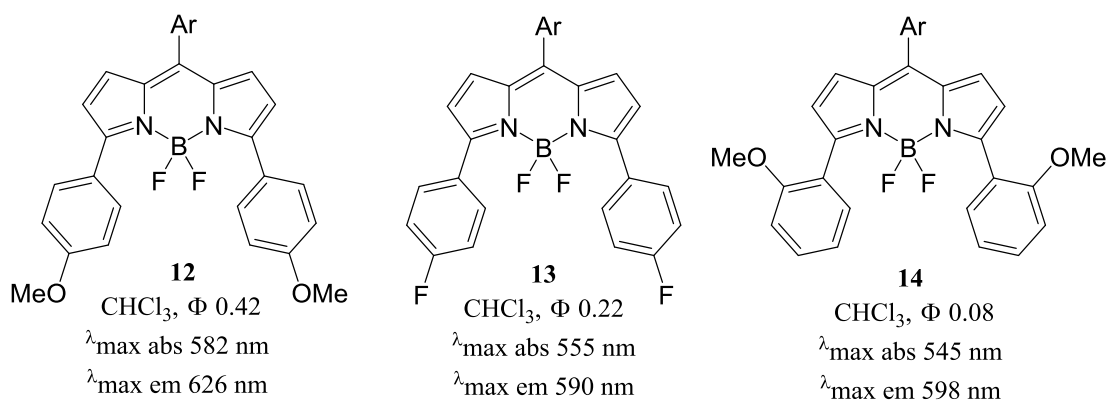


Figure 1.6. Three BODIPY derivatives that demonstrate common spectral shifting effects for BODIPY's. *Note: Ar = 4-iodo-phenyl.*

The position at which the group is placed when substitution, occurs clearly has a massive difference on the resultant quantum yield as well, as witnessed through the quenching of **14** as opposed to **12** [Fig. 1.6]. The electron directing effects of the substituents, given that they are all at least slightly donating, shows that for maximising quantum yield the system favours having electron density donated towards the carbon-carbon bond linking the group to the core itself. As both methoxy and fluorine groups are para directing, **12** and **13** are both directing towards this bond, whilst **14** is directing away, to the relative ortho and para positions [Fig. 1.6]. Given the strong directing

effect of methoxy groups, the evidence for preferential position can be seen between BODIPY's **12** and **14** [Fig. 1.6].

1.3.2 Bathochromic Shift in BODIPY Dyes

Development of the BODIPY's with the most significantly altered spectral shifts is primarily through conjugation extension at the pyrrole ring positions, however the principal theme revolves around extending the overall conjugation away from the core itself.^{30-31, 37-38, 51-52, 58-78} Whilst multiple structural motifs of BODIPY have an influence over the absorption and emission shifts observed, the movement is almost always towards the infrared, lower energy region of the electromagnetic spectrum. NIR shifts are generally the desired direction for tuning of the BODIPY core, as their low energy nature means that they can be utilised for a range more applications, particularly biological due to the lowered cellular damage associated.^{38, 60, 75, 79}

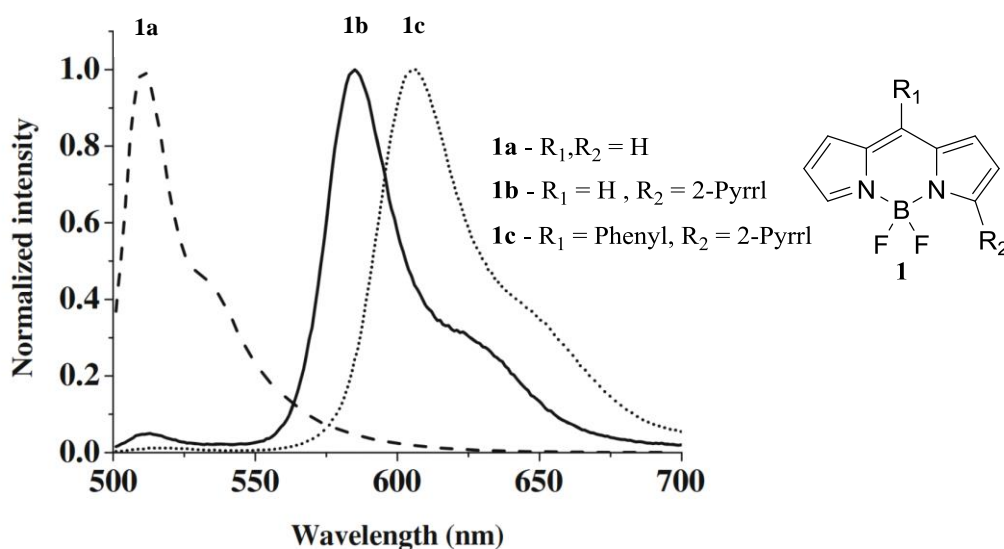


Figure 1.7. Normalized emission spectra overlay of three BODIPY derivatives.
 Note: $CHCl_3$, λ_{max} em 512, 586 and 608 nm, for **1a**, **1b**, and **1c** respectively.^[80]

The three derivatives from Figure 1.6 highlight extremely important characteristics of certain structural motifs relating to the absorption and emission trends as well as quantum yields.⁵⁶⁻⁵⁷ In BODIPY **12** we have the common para-methoxy phenyl rings substituted at the 3 and 5 positions. Comparisons of the photophysical properties of **12**

with each of compounds **13** and **14** shows that absorption and emission maxima for **12** are significantly higher than those of **13** and **14**, with over a 25 nm greater shift in each spectrum [Fig. 1.6]. This indicates that use of a strong electron donating substituent has a much more pronounced influence on bathochromic shift of BODIPY' than the highly electronegative halogen atoms like fluorine. Also it means that a methoxy group has a much larger effect when substituted in the para-position than when lying meta to the pyrrole ring. Figure 1.7 is included as an example of the types of spectral shifts that can easily be achieved and observed for BODIPY derivatives, both as a result of the pyrrolic substitution and inclusion of aryl functionality at the *meso* position.⁸⁰

Through the simple comparison of core BODIPY **1a** to derivatives **1b** and **1c**, the normalized intensity emission spectra can be clearly tracked towards the infrared region [Fig. 1.7]. Via the conjugation extension of the central framework a total red-shift of 96 nm in respect to the starting molecule is observed. The fact that these molecules all share the same core structure, but that relatively small external modifications can create such a huge spectral shifts is a testament to fine tuning capability of this dye family and a good way to introduce the potential of their structural modifications.

1.3.3 BODIPY: Creating Bathochromic Shift

To highlight the spectral modification potential of the BODIPY fluorophore, this section includes an array of derivatives as an example of the sheer amount of manipulation that can be performed around the framework of BODIPY **1**. Figure. 1.8 illustrates three BODIPY derivatives that show extensive conjugation of the core structure, coupled with the development of their photophysical properties.^{77, 81-82} BODIPY **15** exhibits significant red-shift with absorption at 667 nm and emission at 702 nm [Fig. 1.8].⁷⁷ This red-shift is strongly attributed to the combination of phenyl rings fused to the 1-2 and 6-7 positions that extend the central conjugation and the 4-methoxyphenyl groups in positions 3 and 5 that are maintained within the conjugated framework, activating it via the strong electron donating methoxy substituent. Published along with BODIPY **15** was a similar derivative with the iodine atoms exchanged for an ethynyl linker connecting an aryl functionality with the capacity to allow for extended

polymerization, this resulting in a further bathochromic shift significantly towards the NIR of giving 694 nm and 720 nm for absorption and emission, respectively.⁷⁷

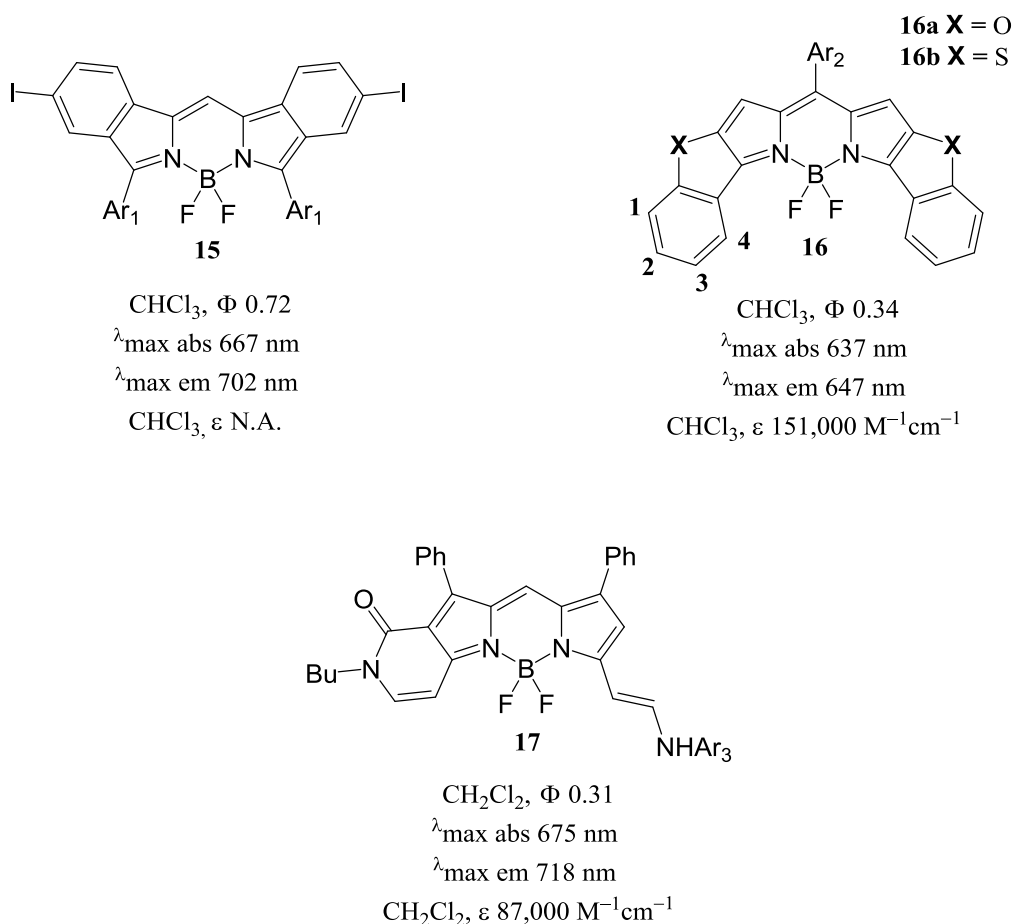


Figure 1.8. BODIPY dyes demonstrating the bathochromic effect of ring annulation to the core. Note: Ar₁: 4-methoxyphenyl, Ar₂: 4-iodophenyl, Ar₃: phenyl

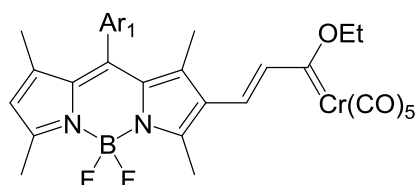
Ring annulation as observed in compound **15**, has become a common occurrence in the synthesis of spectrally shifted BODIPY's. [Fig. 1.8] Compound **16** is an example of another ring-annulated BODIPY dye that maximises conjugation extension, whilst maintaining aromaticity [Fig. 1.8].⁸² Respectively, absorption and emission wavelengths for the furan based **16a** are 637 and 647 nm, this compares to the benzothiophene fused derivative **16b**, published simultaneously within the same paper by Chen and co-workers, which exhibits values of 658 and 673 nm.⁸² Both bathochromic shifts are very large and highlight how direct conjugation extension significantly alters the electronic

state of the system such that it lowers the energy required for absorption and emission events to occur.

Using a ring annulated BODIPY similar to **16**, Boens and co-workers have established the preferred position for substitution of annulated ring moieties when aiming to generate red-shift [Fig. 1.8].⁸³ The paper demonstrated through the substitution of a methoxy group in each of the three positions **1**, **2** and **3** indicated in Figure 1.8, that the highest absorption and emission values observed of 646 and 676 nm, respectively, were witnessed when the substitution was at site '**3**'. When moved to carbon centre '**1**', there was a noticeable decrease in spectral shift of 12 and 19 nm for the respective spectra. The substitution of two methoxy groups onto the framework at positions **2** and **3** simultaneously, caused the spectra to shift 50 nm towards the higher energy region for both absorption and emission. Whilst substituting with methyl groups instead, at both positions **1** and **3**, created the second largest bathochromic shift towards the infrared. These results suggest in line with the previously discussed BODIPY trends, that BODIPY substitution is highly selective and the photophysical properties are subject to manipulation dependent not only on direct substitution to the framework, but also the electronic directing effects of all distant functional groups that either contribute to, or remove electron density from the conjugated system.^{30-31, 34-38} The presence of a simple group, even when distanced four or five carbon atoms from the core itself, can significantly influence the π -system such that it results in a large influence over spectral movement.

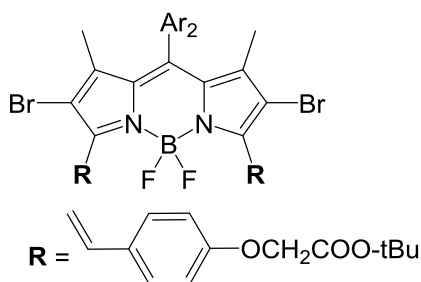
Molecule **17** is somewhat an extension of the annulation theme, made with a fused bispyridone motif that extends the core conjugation from positions 2 and 3 [Fig. 1.8].⁸¹ It exhibits an absorption wavelength of 675 nm and emission at 718 nm thus demonstrating a fairly large Stokes shift. Presence of 1, 7 phenyl rings plays a role in the large NIR absorption, as is evidenced in previous literature.³⁰ However, the massive jump towards the IR region has to be attributed to the fused bispyridone functionality, with 25 derivatives based on that motif all published within in the paper, and all having exhibiting beyond 650 nm red-shifts, the most extreme being a derivative that showed a massive 76 nm Stokes shift, from 682 to 758 nm.⁸¹ Cumulatively the absorption and emission spectra for compounds **15-17** [Fig. 1.8], are great examples of ring annulation and how it is viewed as an invaluable synthetic target, that opens up more carbon

centres for spectral fine tuning through clever substituent addition, that also simultaneously push the absorption and emission maxima towards the IR region.



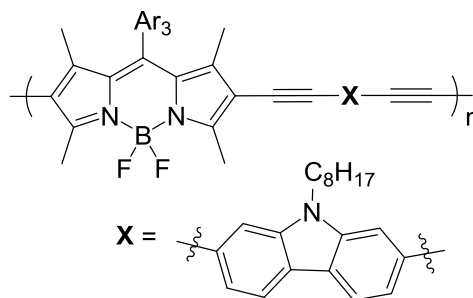
18

Hexane, Φ N.A.
 $\lambda_{\text{max abs}}$ 567 nm
 $\lambda_{\text{max em}}$ 542 nm
 Hexane, ϵ 31,000 M⁻¹cm⁻¹



19

Toluene, Φ 0.42
 $\lambda_{\text{max abs}}$ 657 nm
 $\lambda_{\text{max em}}$ 679 nm
 Toluene, ϵ 101,000 M⁻¹cm⁻¹



20

CHCl₃, Φ 0.12
 $\lambda_{\text{max abs}}$ 553 nm
 $\lambda_{\text{max em}}$ 638 nm
 CHCl₃, ϵ N.A.

Figure 1.9. BODIPY dyes with extended conjugation. Note: Ar₁: 4-methoxyphenyl, Ar₂: phenyl, Ar₃: 4-bromophenyl, **20**: Polymeric structure, “n” is undefined

Derivative **18** seen in Figure 1.9 is included as an example of large IR spectral movement coupled with generation of an anti-Stokes shift.⁷⁸ Inclusion of a Fischer Carbene at the 6-position was utilised to synthesise over 10 different derivatives that all exhibit considerable IR shifts to the around 550 nm, but which generate an anti-Stokes shift rather than the conventional high to high to low energy trend [Fig. 1.9]. An anti-stokes shift meaning that the photons absorbed by the BODIPY dyes were actually at a lower energy than the emitted photons. With the absorption for **18** measured at 567 nm, this corresponds to a 25 nm anti-stokes shift [Fig. 1.9].

BODIPY **19** is a simplified structure of one derivative published amongst a group of BODIPY's targeted for distyryl substitution [Fig. 1.9].⁸⁴ Three of the derivatives are the primary targets for comparison within the work. BODIPY **19** and one of the other dyes differ only through the presence or absence of a keto-ester functionality attached in the para position on the phenyl group, they have quantum yields of 0.42 and 0.44 respectively, with a difference in bathochromic shifts of only 11 nm in each absorption and emission [Fig. 1.9]. The third derivative has the keto ester also and replaces the 2,6-dibromo functionality with ethyl groups.⁸⁴ This substitution predictably leading to only a small shift in the spectra as well, exhibiting a 10 nm movement. All three derivatives thus range from 640 – 680 nm in both absorption and emission spectra putting them amongst the most significantly shifted of BODIPY derivatives. Once more demonstrating that elongating the conjugation away from the core can greatly disturb the photophysical properties.

Compound **20** was one of three compounds investigated for potential use as an ion probe [Fig. 1.9]. It was synthesised as a series of three derivatives, each derivative containing the same ethynyl based linkers, but with a different structurally modified spacing group in place of **X** [Fig. 1.9].^{59, 85} Near identical optical properties of large Stokes shifts and emissions around the 620-650 nm range were observed, however, as is common with such hyper conjugated systems the quantum yields were greatly reduced to values all below 0.2.³⁰⁻³¹ Despite the quenching of the quantum yields observed for the three BODIPY derivatives in Figure 1.9, the specific spectral shifts observed each differently conjugated molecule is highly interesting and re-introduces the largely unpredictable nature of BODIPY dyes. The scope of structures and the resultant range of properties that can be created through the extension of core conjugation is extremely large for this powerful family of fluorophores.

1.4 Specially Modified BODIPY Derivatives

Since BODIPY derivatives were brought to the forefront of scientific research in the 1990's, they have been extensively developed for specific applications utilizing their unique optical properties. Not only this, but multiple different framework designs have simply been synthesised with the sole purpose of examining their photophysical

properties, in the hope that new structural motifs with significant fluorescent imaging implications would be discovered. Outlined so far is the history of fluorescence and fluorophores as a group, leading into the concept of the BODIPY framework and many of the common trends that are observed in regards to the BODIPY core. This chapter will elucidate more detail around some of these specifically tailored derivatives and the chemistry behind their structural modifications, highlighting the areas that have been investigated most and the areas where functionalisation could potentially be expanded further.

1.4.1 Photodynamic BODIPY Derivatives

Photodynamic therapy (PDT) is a relatively new class of clinical therapy for the treatment of non-malignant tumours. In order to be an effective PDT agent these agents require a photosensitizing component coupled with light and oxygen exposure.⁸⁶ Through photochemical activation, a photosensitizer generates singlet oxygen ($^1\text{O}_2$) from triplet-triplet annihilation (TTA) with its own triplet excited states, and those of the triplet oxygen ($^3\text{O}_2$). TTA being the interaction of two separate triplet excited states, such that they lead to the formation of a lone singlet excited state, ‘annihilating’ both triplet states in the process. This also means that PDT derivatives must have high levels of ISC to promote formation of triplet states.

Once $^1\text{O}_2$ has been generated, due to its extreme reactivity, it causes intense damage to the surrounding environment, and thus the formation is targeted to occur within cancerous tissue leading to highly localized destruction of both malignant and non-malignant tumours in the immediate vicinity. Due to the extremely small half-life of $^1\text{O}_2$ the treatment is relatively controlled, as the species does not survive long enough to damage tissues outside of the location it is formed.

BODIPY derivatives have multiple properties which make them desirable targets for PDT derivatisation. The most prominent of these being their highly tuneable nature towards low fluorescence quantum yields but high triplet state quantum yields and their tendency to shift significantly towards the lower energy IR region of the

electromagnetic spectrum, whenever significant substitution occurs around the core moiety.^{30-31, 34, 38, 75}

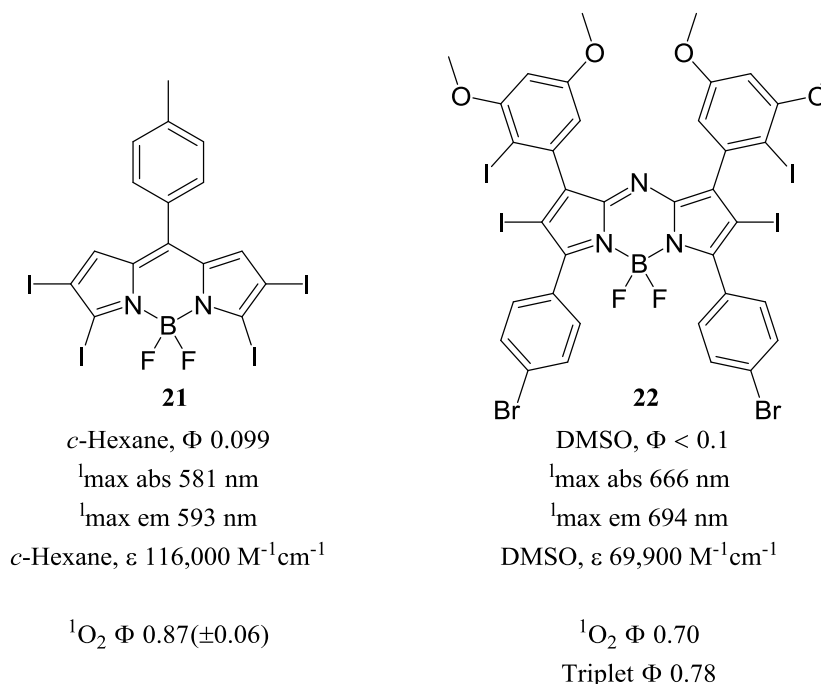


Figure 1.10. BODIPY PDT targeted derivatives with relevant optical properties. *Note: $^1\text{O}_2$ Φ and Triplet Φ are the respective quantum yields for singlet oxygen and triplet state generation, measured using O_2 free solvents.*

This is a highly desirable property, as a current limitation of many PDT derivatives is that they have shorter wavelengths for absorption and excitation, which means that they must be irradiated with higher energy to generate any detectable fluorescence. This is bad from a tissue damage perspective, as higher energy irradiation is obviously more harmful to the cellular environment, but what is more detrimental, is that such PDT derivatives with shorter wavelength spectra, can only be utilised for treatment of near surface tumour growth. This is because the higher energy near UV light, will not penetrate into deep tissues, and thus embedded tumour growths cannot be treated as the administered derivative cannot be excited into its triplet state, as it is buried within body tissue. Given that red-shifting coupled with ISC promotion are the two main criteria targeted for PDT derivative identification, Figure 1.10 contains two examples of BODIPY dyes that have been structurally modified to improve their PDT activity.

Molecule **21** contains the general base structure for BODIPY PDT derivatives, in that the core itself is polyhalogenated [Fig. 1.10].⁸⁷

As discussed earlier, halogen atoms quench the quantum yield of BODIPY dyes through the heavy atom effect.⁵⁶ This occurs directly as a result of ISC, with ISC promoting triplet state formation and subsequently through the interactions of these triplet states, $^1\text{O}_2$ is generated. BODIPY **21** has a measured $^1\text{O}_2$ quantum yield ($^1\text{O}_2 \Phi$) of 0.87, this number being representative of quantum yield similar to that of the fluorescence quantum yields, in which it is a ratio representing the amount of singlet oxygen species generated per triplet state formed and thus with a maximum value of 1.0, 0.87 is a highly efficient level of generation [Fig. 1.10].⁸⁷ As you would expect the actual fluorescence of **21** is almost completely quenched, however this is the desired sign of a potential PDT derivative, as it is indicative of full conversion of singlet excited states via ISC, as none are being allowed to progress via radiative emission back to the ground state.

Molecule **22** was synthesised as part of a series of PDT active BODIPY derivatives of the ‘aza’ type [Fig. 1.10].⁸⁸ Aza-BODIPY’s have the *meso* carbon centre substituted with a nitrogen atom, and are similarly potent fluorophores to that of the core BODIPY dyes. These particular aza-BODIPY derivatives have substantial arylation around the core framework, with reduced direct halogenation, and target greater spectral shifts coupled with maximised $^1\text{O}_2$ quantum yields. BODIPY **22** has a ‘Triplet Φ ’ figure quoted, of 0.77 which is again similar to the fluorescence quantum yields, in that it is a ratio, this time of the number of triplet excited states generated per singlet excited state formed. Essentially meaning that 77 percent of the singlet excited states formed for BODIPY **22** undergo ISC to form triplet excited states.

Despite the lower $^1\text{O}_2 \Phi$ of 0.70 in **22** compared to the 0.87 observed for **21**, derivative **22** is a more realistic example of a PDT agent, as the absorption band is in a much more favourable position at 666 nm, as opposed to the 581 nm absorption observed for **21** [Fig. 1.10].⁸⁷⁻⁸⁸ These more highly conjugated, larger BODIPY systems that are still electronically altered enough to promote ISC appear to be the way forwards for PDT active BODIPY development.

1.4.2 Functionalized BODIPY Probes

Fluorescence based probes for biological imaging and ion, pH and gas detection have become increasingly encountered within the scientific literature over the past decade. All manners of different organic based fluorophores have been investigated for their potential as one of these invaluable tools.⁷⁵ The BODIPY family of fluorophores has not escaped this area of investigation either with an expanse of literature relating to BODIPY probe development, exploding into the scientific databases in the recent years, and multiple reviews summarising the key developments being published to assist in research efforts.^{23, 38, 58, 79, 89-92}

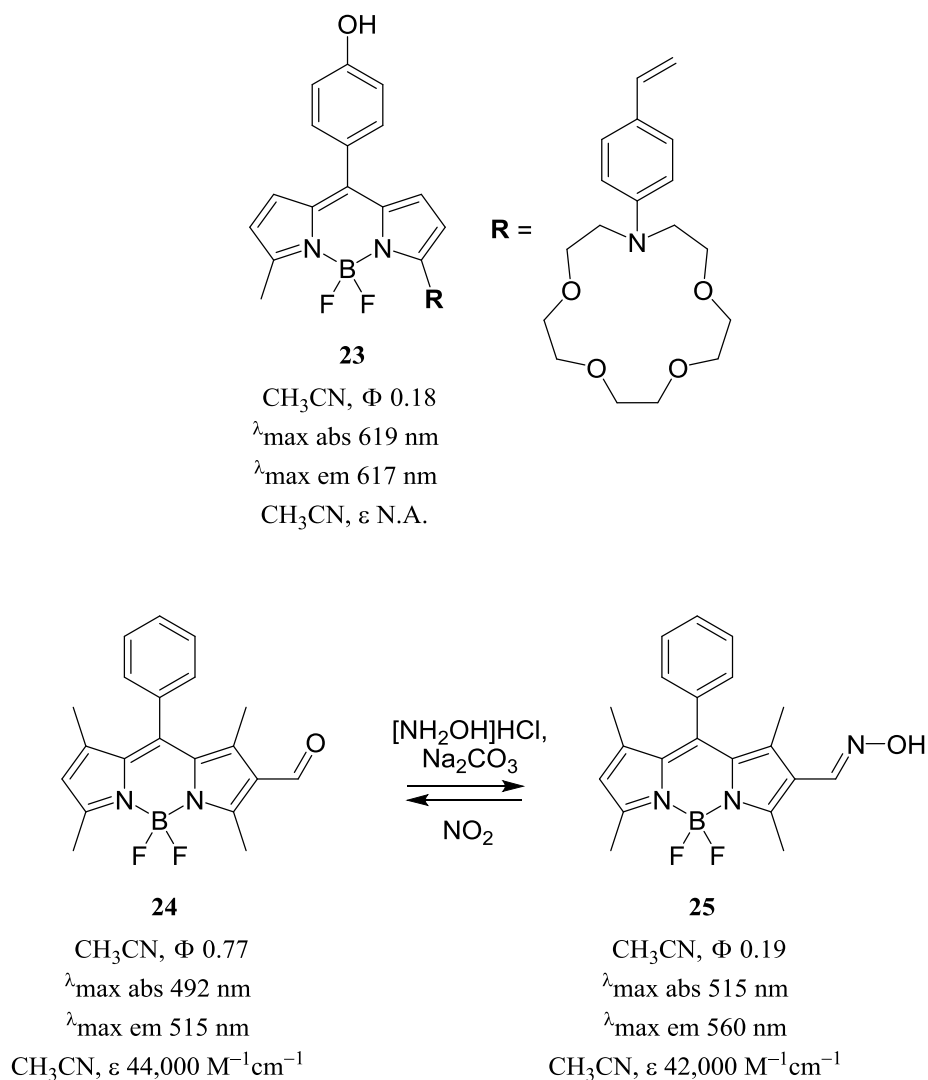


Figure 1.11. BODIPY derivatives designed for analytical probe applications.

Two types of probes designed for very different purposes and very different modes of activity are BODIPY's **23** and **25**, both shown in Figure 1.11, along with the precursor **24**.^{58, 90} BODIPY **23** is a probe designed around the principle of host-guest interactions, with the large aza-crown functionality attached at the terminal end of a conjugated link able to interact with an array of ions [Fig. 1.11]. These aza-crown moieties have large cavities within their ring-like structure wherein they can bind cationic metals often selectively, and given the vacancy within the ring and the presence of lone pairs around the oxygen atoms, this process is usually highly favourable with dependency on the particular metal ion being targeted.⁵⁸ The hydrophobic nature of the aza-crown exterior directs the water soluble metal ions into the ring structure where they can be bound and isolated, in essence a very simple probe mechanism is taking place, which allows these BODIPY derivatives to be used for enhanced ion detection and sequestration [Fig. 1.11].^{58, 79}

Derivative **24** is the synthetic precursor to the NO₂ air detection BODIPY based probe – **25** [Fig. 1.11]. Using a combination of hydrochloric acid and hydroxylamine with sodium carbonate, the precursor can be easily converted into **25** which contains the highly sensitive hydroxylamine functional group at the 2-position on the BODIPY core. Through straightforward NO₂ gas exposure, the probe readily converts back into **24** and can then be synthetically converted back into probe form. The defined mechanism of the reaction occurring to allow for the interconversion of the probe between **24** and **25** is currently unknown, with either product simply being isolated each side of the process. Given the highly fluorescent nature of **24** compared to **25**, the presence of NO₂ in the air can thus be detected through any technique that can measure relative quantum yields of a compound, which is only necessary if the change isn't noticeable enough through basic observation of the solution. This type of switching mechanism is an extremely common probe design for BODIPY dyes, due to their ready functionalization around the core periphery.^{30-31, 90, 92} Almost any sensitizing group can be appended to the core and given conjugation is maintained, as demonstrated in chapter one, almost any perturbation to the BODIPY core will be detectable in terms of fluorescence diminution or enhancement.

1.4.3 Multiple Core BODIPY Derivatives

Some groups researching BODIPY functionalization have developed several different types of multiple cored derivatives.^{48, 71, 76, 93-95} Shown in Figure 1.12 are examples of two these such derivatives. Molecule **26** is an example of a dimeric derivative, which can be viewed as two individual BODIPY monomers that have been conjugated with spacer or linker groups.⁷⁶ In this case the linkers are a 2-2 dithiophene moiety [Fig. 1.12]. This structure is amongst an array of BODIPY dimers which have been synthesised using sulfur containing moieties like thiophene as bridging components.^{71, 93} They consistently exhibit very low quantum yields, with **26** almost fully quenched at only 0.06 for measured fluorescence quantum yield [Fig. 1.12].

A theory to explain this phenomenon was postulated by a group that have analysed similar derivatives to **26**.⁵⁴ The hypothesis being that as sulphur has access to the d-orbitals and a larger number of low energy unoccupied orbitals, it has potential to readily accept electron donation from the BODIPY core. If this was to occur from the excited state HOMO then it would be an oxidative PET reaction and would reduce fluorescence significantly and as these sulfur atoms are often maintained at very close proximity to the BODIPY core within these dimers, the distance for this PET side reaction to broach is often minimal.

Despite the extreme quenching effect that is observed for these sulfur containing dyes they continue to be targeted for research.^{63, 67, 96} The reason for this is evident in the optical properties of **26** [Fig. 1.12]. There is an extreme red-shifting effect observed, significantly beyond the standard level of spectral movement witnessed in this highly tuneable family of dyes. With an emission band above 800 nm this is considered amongst the perfect range for imaging applications, whilst the absorbance is much lower at 706 nm and thus a significant Stokes shift is evident. If the specific reason behind the observed quenching in their quantum yields could be discovered and resolved, these sulfur based BODIPY dyes could have serious imaging applications with their large spectral shifts and is likely why they continue to be of high interest within the scientific community.

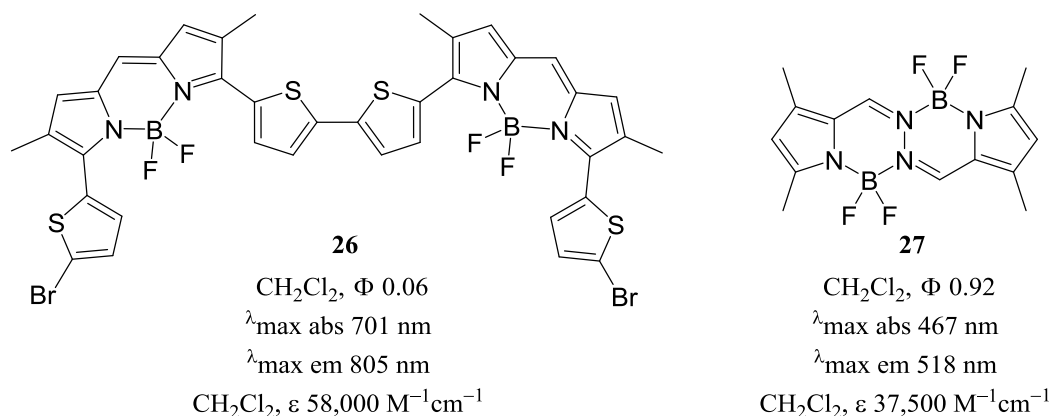


Figure 1.12. The chemical structure and optical properties of two fluorescent dyes incorporating dual BODIPY cores into the framework.

The dual core fluorophore **27** is an example of a much less common technique for the inclusion of two cores into the BODIPY framework [Fig. 1.12]. BODIPY **27** cannot be considered two linked monomers, with the evidence of its connectivity and communication beyond that of two distinct monomer, shown through calculations within the paper itself.⁹⁵ It is a standalone dual core derivative, wherein the two cores are synthesised within the same single heterocyclic precursor.⁹⁵ This molecule abbreviated to BOPHY in a similar manner to BODIPY itself, can also not be considered a true BODIPY molecule as there is no inclusion of the classic dipyrroin based skeleton, just the installation of the same core functionality. It does however exhibit extreme fluorescence intensity with a quantum yield of 0.92, which is well in accordance with true BODIPY molecules like its core equivalent **3**, that has a quantum yield of 0.80 [Fig. 1.4]. The emission maximum is also similar to **3**, which emits at 516 nm, however the absorbance differs greatly with a blue shift apparent, as it has moved from the 505 nm observed in the tetra methylated core BODIPY framework, down to only 444 nm in **27** [Fig. 1.12].

A series of new BOPHY derivatives expanded the framework with extended aryl substitution that built on the conjugation and had the effect of pushing a similar Stokes shift into more favourable NIR region whilst maintaining quantum yields around 0.4, thus indicating they have potential imaging applications as well.⁹⁷ What has potentially the most interest in these particular systems however, is the cyclic voltammetry experiments carried out by Ziegler and co-workers which suggested communication

between the different cores within the framework. This result, despite BODIPY **27** exhibiting two absorption and emission spectra's that suggest multiple isolated cores, does lead to a significant number of questions to investigate within these unique BODIPY-type structures.

1.4.4 Large Aromatic Polycyclic BODIPY Derivatives

Extending the conjugated framework has been discussed previously, with these groups allowing for increased photon absorption in the form of larger extinction coefficients and more electron transfer across a greater π -system. However this phenomenon was studied, both computationally and quantitatively, wherein the photophysical properties of multiple similarly structured fluorophores were measured and the results compared based upon the level of conjugation.⁹⁸ It was determined that for a large number of highly conjugated systems, particularly those with rod-shaped substituents, for instance in the shape of a diphenylacetylene molecule, the rate at which a fluorophore progresses from the singlet excited state, back to the ground state, actually increases as the level of conjugation grows. Whilst simultaneously, there was a strong correlation to a slower rate for radiationless relaxation processes occurring, also as the level of conjugation extended further.⁹⁸

As a result of the conjugating effects, multiple BODIPY derivatives have been synthesised that have large polycyclic moieties attached through the peripheral and *meso* positions of the core. The inclusion of such large aromatic groups acts as a development to the simple conjugation extended derivatives. Rather than individual substituted phenyl rings, attached directly to the core or via conjugated linking bonds. Large polycyclic groups attached in a similar fashion, either terminally or directly, have an increased effect on the singlet lifetimes and the elimination of non-radiative processes.

BODIPY **28** is an example of a derivative which has been conjugated with anthracene via a simple carbon-carbon bond in **28a**, an ethynl linking bond, as in **28b**, or in the case of **28c**, via a phenylacetylene spacing group [Fig. 1.13].⁹⁹ These derivatives were designed as a series of 'cassettes' for energy transfer processes.

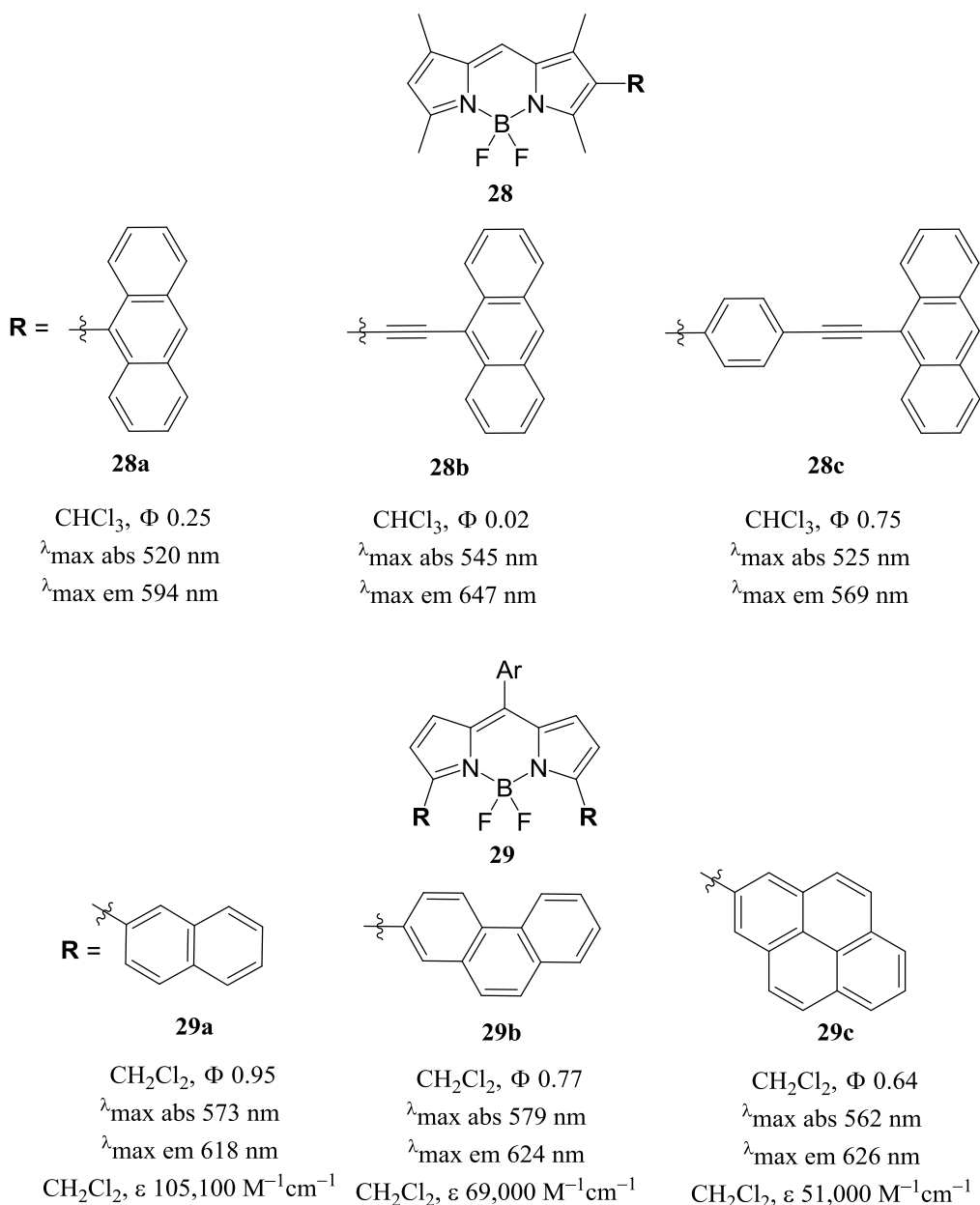


Figure 1.13. Large polycyclic substituted BODIPY dyes.

Note: Ar = 2,4,6-(trimethyl)phenyl.

The targeted outcome being the generation of a photon absorbing donor substituent, that is capable of through-bond energy transfer to the acceptor group, in this the case the BODIPY core. These through bond energy transfers can be considered a Dexter type energy transfer. Dexter energy transfers are a short range fluorescence quenching mechanism, wherein excited electrons are non-radiatively passed from a donor molecule to a second acceptor molecule over a distance no greater than around 10Å. They differ

from the PET reactions described in chapter one, in that they are not solely photo induced, and the electrons somewhat cycle through the two substituents. An electron from the singlet excited state, or LUMO of the donor group, is transferred through bonds to the singlet excited state of the acceptor group. Simultaneously a ground state electron is transferred from the acceptor to the donor and this allows the acceptors singlet excited state electron to radiatively emit back to the ground state

The advantage of managing this type of electron transfer process is that as the donor group does not emit itself, its absorption can be tuned to a different wavelength to that of the core acceptor moiety. Thus allowing the donor group to be excited at one wavelength and create a completely different emission from the acceptor, essentially creating large Stokes shifts. As seen through the optical properties quoted for **28b** [Fig. 1.13], this cassette clearly has generated the largest amount of energy transfer between donor and acceptor functionalities, suggesting that the ethynyl linkers are far superior for electron transfer than interspersing aromatic groups.

BODIPY **28b** has a Stokes shift of over 100 nm, coupled with a very low quantum yield of only 0.02, as is the expected result from the generation of an increased amount of non-radiative side processes via these electron transfers [Fig. 1.13]. Undoubtedly these derivatives that can be excited almost peripherally to the core, will have applications in the field of bioimaging, where conventional probes can't be used in particular areas as the exciting wavelength may be harmful, these compounds will be a valid alternative providing an isolated excitation option.

Derivative **29a-c** also seen in Figure 1.13, are similar examples to those of **28**. They have not been designed with a cassette type activity in mind however, but more simply as an investigation into the effects of substitution with such large aromatic polycyclic moieties, specifically at the 3 and 5 positions [Fig. 1.13].⁶⁵ What is interesting about the three derivatives, is that as the size of the functionality increases, the optical enhancement actually decreases in respect to the fluorescence intensity. The quantum yield, and molar absorptivity both shrink as the aromatic ring number goes from 2 to 3 to 4, in **29a-c**, respectively [Fig. 1.13]. Similar derivatives to **29a** but which have only a singular aromatic ring substituted at the 3, 5 positions exhibit lesser optical enhancement properties also, thus indicating that there is somewhat of a sweet spot for

these derivatives.³⁰ Despite this strange trend, the photophysical properties for **29a** are extremely powerful for application into the fluorescence imaging area given that it has significant red-shifting, a quantum yield above 0.9 and an extinction coefficient larger than 100,000 M⁻¹ cm⁻¹.

1.4.5 Metal Incorporation into BODIPY Frameworks

So far within the scientific community, BODIPY dyes have not been extensively researched for their metal binding properties. Research has targeted the development of derivatives that have more obvious imaging applications and potentially metals could have a complicating effect in this goal. Derivatives like **30** however, are amongst a not uncommonly seen structural motif within the BODIPY literature, with the coordinating effect of the dipyrromethene functionality often being explored and this being combined with the highly fluorescent nature of the BODIPY core.¹⁰⁰

Dipyrromethene appended derivatives target a predominantly unsubstituted core framework, to remove the possibility for steric clashing and complexation hindrance. Most focus on the commonly exploited coordination metals like platinum, palladium and ruthenium.¹⁰¹ As seen in Figure 1.14, the optical properties for **30** are fairly unflattering with almost full quenching, minimally sifted absorption and emission spectra, and in BODIPY standards a low molar absorptivity value also. Given the large number of *d*-orbitals available for electronic interaction with such metal species, it is not surprising that they exhibit a fluorescence quenching similar to that sulfur bridged species, due to the increased PET reactions allowed. Given the diminished fluorescence intensity, the potential for these particular derivatives is clearly yet to be established.

Ligand **31** as it can be named, is a BODIPY derivative targeted in the novel Metal-organic framework (MOF) area of BODIPY research [Fig. 1.14].¹⁰² Structure **32** shows the type of structure created through classic MOF synthetic conditions, and is one simple structure amongst an array formed using similar BODIPY-MOF ligands.

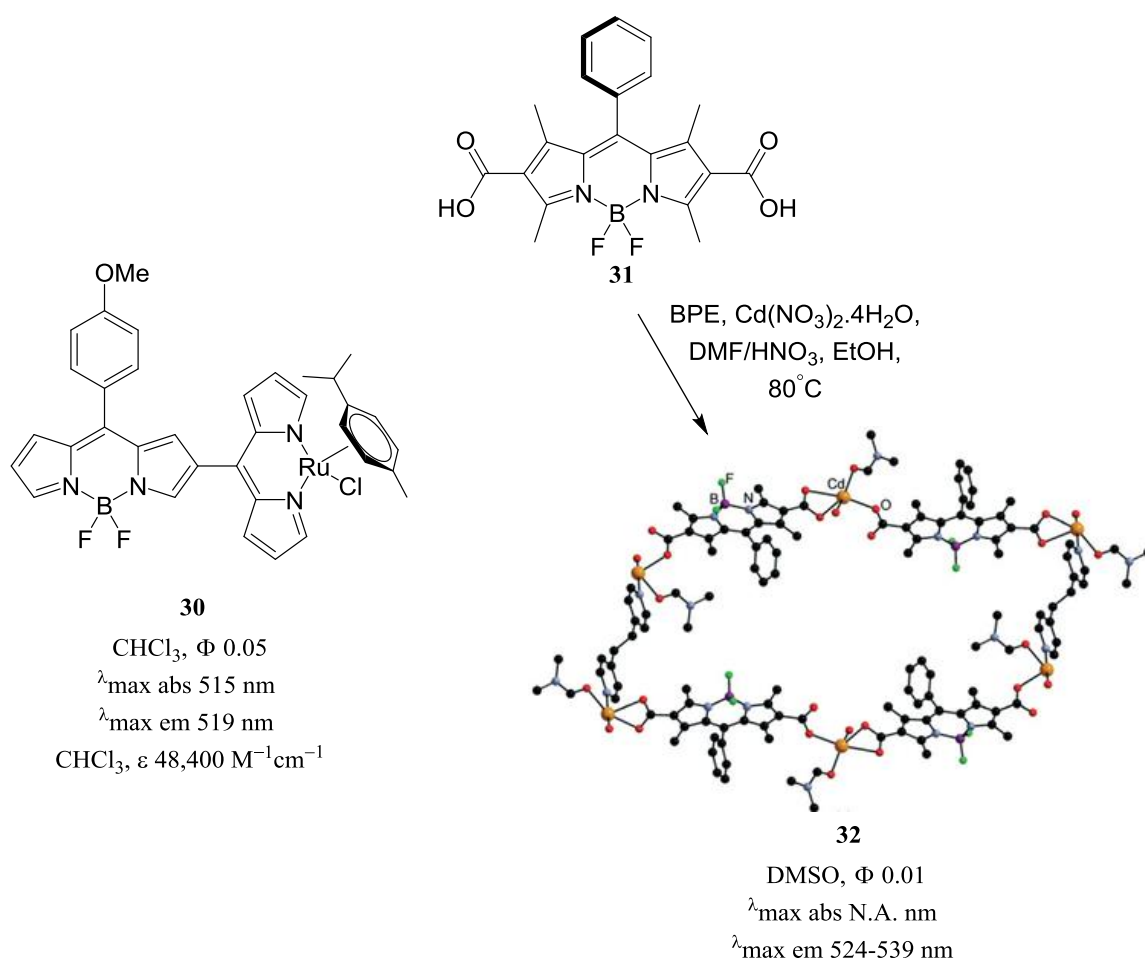


Figure 1.14. Left: Dipyrin appended metal coordinating BODIPY derivative. Right: One of multiple BODIPY-MOF's recently designed.

Recently multiple BODIPY based MOF's were published which exploit a large range of the classic MOF architectures that have been extensively researched over the recent decades.¹⁰³⁻¹⁰⁸ Whilst this research was synthetically focused, there were some optical measurements taken for the developed MOF structures, with **32** amongst a group of five MOF's all formed using BODIPY **31** as the bridging ligand [Fig. 1.14].¹⁰² These five MOF's all demonstrated very low fluorescence intensities with minimally shifted spectra but there is a seemingly infinite number of framework combinations that can be pursued and thus these BODIPY-MOF's are of high interest.

1.4.6 Cyclised BODIPY Derivative

Annulation of the BODIPY core has not had much interest within the scientific community, despite the vast array of structural modifications been carried out on BODIPY derivatives by researchers around the world. This is potentially due to the preference for ring-attenuated species or the fused derivatives, as a result of the often complicated syntheses involved with cyclisation reactions. It can be considered much simpler for the formation of BODIPY derivatives to just start with a ring fused pyrrole of the desired type, and then simply carry out the BODIPY formation using this precursor. This does have its limitations however as the extension to which pyrrole can be functionalized, prior to BODIPY formation does have its limits. Some BODIPY derivatives have been synthesised using cyclisation reactions with interesting results however. BODIPY **33** is an example of one such derivative which would be extremely hard to develop via the substituted pyrrole method and essentially has two phenanthrene molecules attached directly to the core, via the 2-3 and 5-6 positions [Fig. 1.15].¹⁰⁹

Molecule **33** was created by the cyclisation of a biphenyl group, with the two bonds formed in this step indicated in bold. BODIPY **33** compares well with **29b** as both have phenanthrene moieties included in their electronic system, but the phenanthrene is attached in two different methods for each, either fused directly to the core or linked via conjugation through a carbon-carbon bond [Fig. 1.13] [Fig. 1.15]. The rest of the frameworks do differ slightly, with the absence of *meso* substitution in **29b** and a non-methylated framework in **33** but the significant difference is the means of phenanthrene connection. Derivative **33** exhibits molar absorptivity double that of **29b** with 140,000 $\text{M}^{-1} \text{cm}^{-1}$ compared to the respective 69,000 $\text{M}^{-1} \text{cm}^{-1}$. It is also massively shifted towards the IR in comparison, but exhibits a significant fluorescence intensity drop in terms of measured quantum yield [Fig. 1.15].¹⁰⁹

In opposition to **33**, the cyclised derivative **35** exhibits a noticeable blue shift in absorption and emission wavelengths, coupled with the maximisation of its fluorescence efficiency, with a quoted quantum yield of 0.99 [Fig. 1.15].¹¹⁰ The quoted molar absorptivity is also inconsistent with **33**, being relatively low at 44,800 $\text{M}^{-1} \text{cm}^{-1}$ however this is only a small decrease from precursor **34** [Fig. 1.15].¹¹⁰

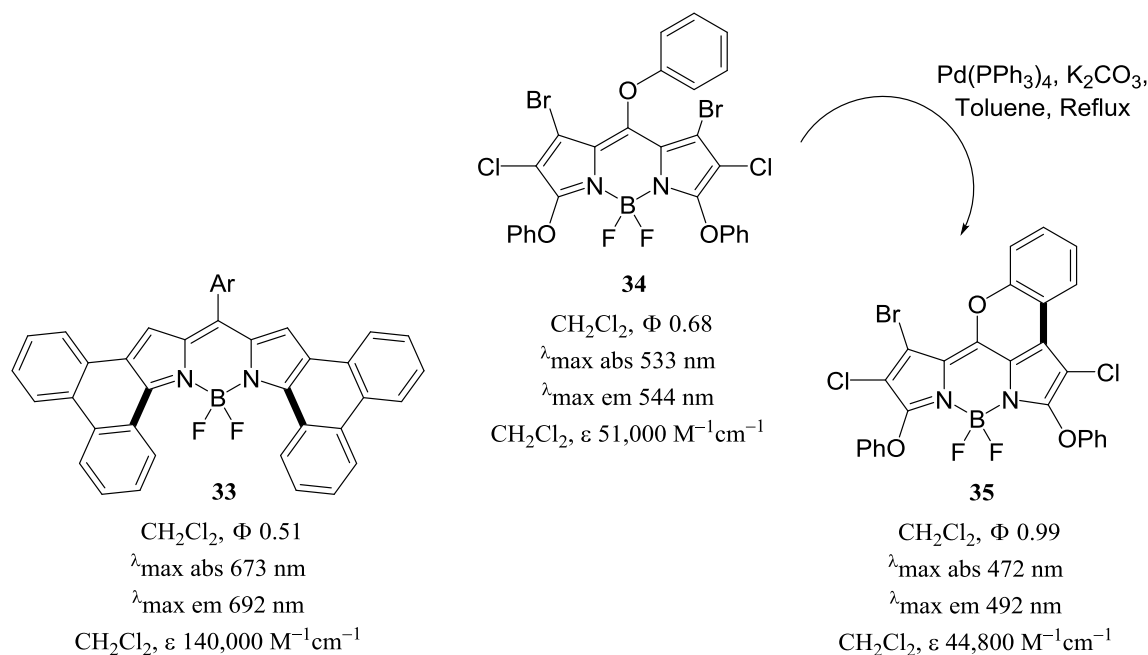


Figure 1.15. Cyclised BODIPY derivatives.

Using a palladium catalysed reaction, the bond shown in bold has been formed between the core itself and the *meso*-phenoxy group. Clearly these *meso*-phenoxy groups have a quantum yield stabilising effect. This is indicated through the maintained fluorescence intensity of **34**, evident despite its tetra-halogenated framework, but it seems that directly cyclising this group to the core has resulted in an even increased stabilising effect given the jump up to 0.99 in **35** [Fig. 1.15].¹¹⁰ Along with this observed quantum yield stabilisation, **35** was isolated in a crystalline state, wherein the BODIPY framework has an almost fully planar *meso* group due to the cyclisation restricting any rotation and thus allowing for a staggered π - π stacking arrangement of these *meso*-phenyl groups, wherein one molecule is on top of the next with all of the *meso*-phenyl substituents in line. Given the drastic photophysical differences between **33** and **35** there is clearly a high level of unpredictability associated with these cyclised derivatives but given the extreme molar absorptivity and red shift measured for **33**, and the fluorescence intensity recorded from **35**, these derivatives have clear potential applications in fluorescence imaging techniques [Fig. 1.15].^{31, 37, 110}

Chapter Two

Development of HBC-Coupled BODIPY Derivatives

2.1 HBC-Coupled BODIPY's

Hexa-*peri*-hexabenzocoronene (HBC) is a large aromatic polycycle of the Coronene family. Essentially it is a Coronene molecule with six benzene rings fused into each junction of the periphery, it is commonly formed via the cyclisation of the corresponding hexaphenylbenzene derivative [Fig. 2.1]. Due to its colossal aromatic character and resulting huge conjugated π -system, HBC exhibits interesting photophysical and electronic effects. As described in depth in Chapter One, such large aromatic functionality has a significant effect when linked to the BODIPY core, with the size of the effect dependent on both location and type of conjugate linkage.

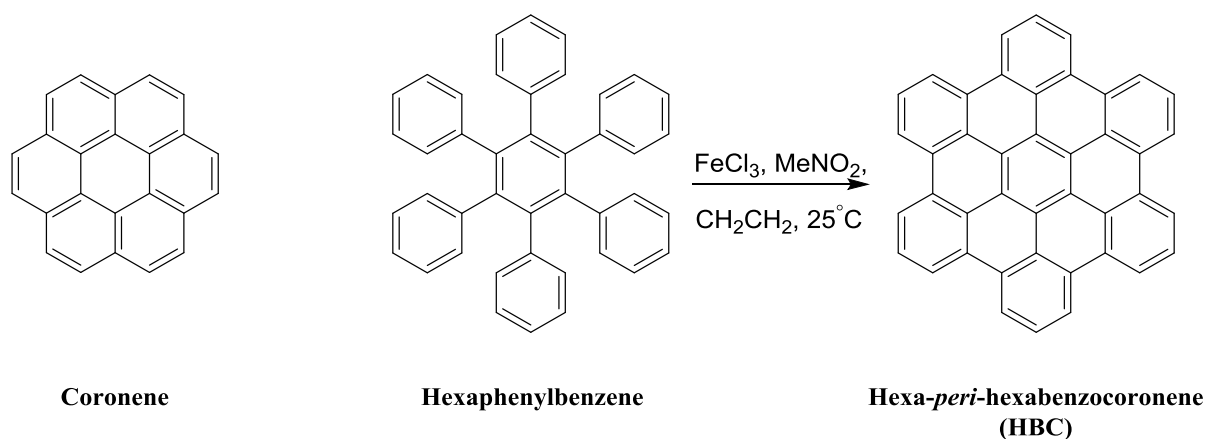


Figure 2.1. Left is Coronene, with Hexaphenylbenzene and HBC, illustrating the cyclisation.

BODIPY dyes with HBC substitution are currently unprecedented within BODIPY literature and given the size and extent of the aromatic character within HBC, it can be assumed that connection to a BODIPY framework would result in the development of some intense optical properties, potentially beyond those observed for lesser aromatically substituted BODIPYs like derivatives **28a-c** and **29a-c** discussed from Figure 1.13. Given the potential for these derivatives, BODIPY **36** was conceived as one potential synthetic target for the project.

Beyond the simple conjugate linkage of HBC to the *meso* or peripheral positions of the core, there are other options for inclusion of the HBC structural motif into a BODIPY framework. What could be considered a more novel synthetic approach to this, would be development of a BODIPY derivative that has potential for cyclisation with an HBC moiety. BODIPY **33** also discussed in Chapter One [Fig. 1.15], as one of the only cyclised BODIPY derivatives already created, exhibited extreme red-shifting and a phenomenally high molar absorptivity in comparison to most conjugated systems, thus suggesting that the direct cyclisation to create core-fused derivatives has much more potentially for optical enhancement. This lead to the design of derivative **37**, which is dual-HBC functionalized, through direct cyclisation to the core.

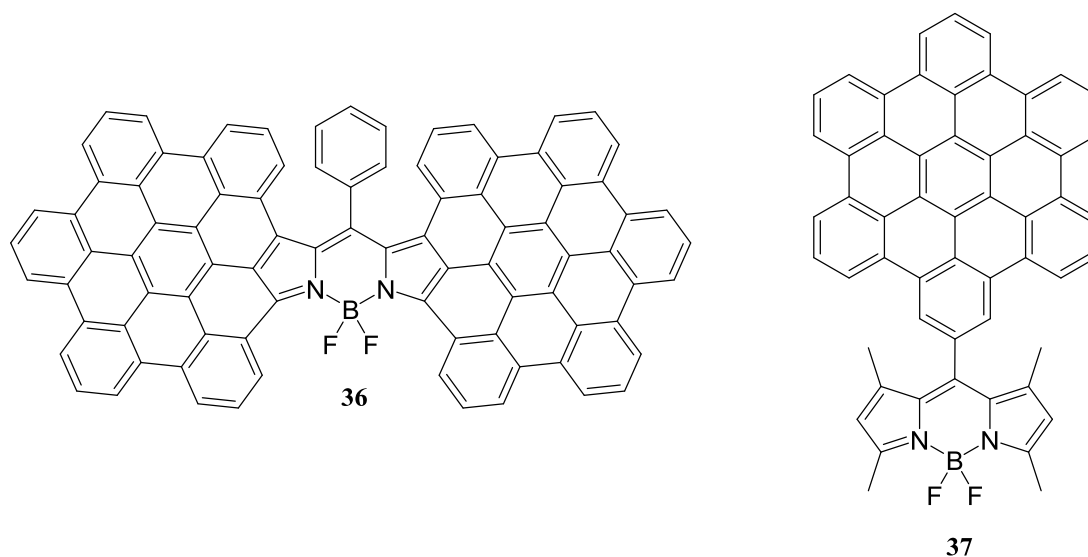
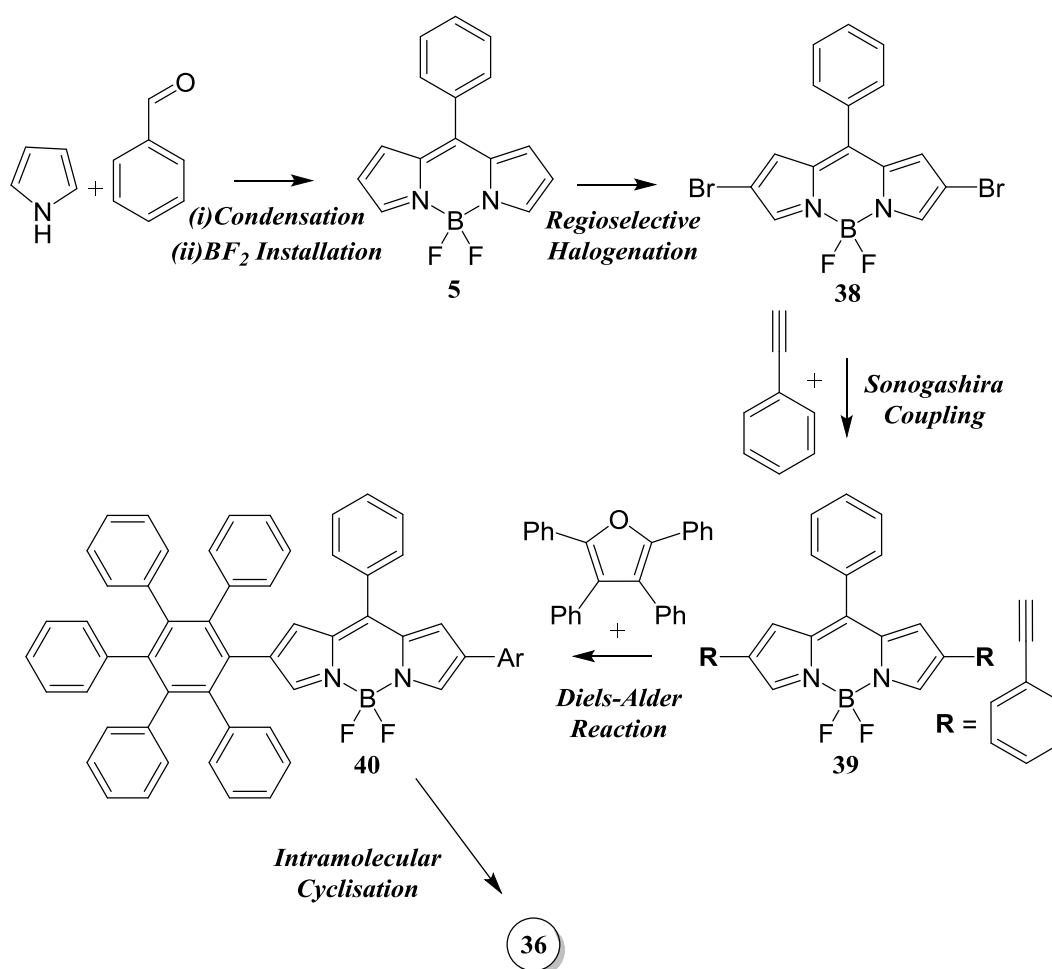


Figure 2.2. The two synthetic targets, for large polycyclic aromatic appended BODIPY derivatives.

2.2 Synthesis of HBC-Coupled BODIPY **36**

The synthesis of derivative **36** [Fig. 2.2], requires a peripherally unsubstituted base BODIPY derivative like **5** [Fig. 1.4]. This will allow room for the cyclisation to the core. Scheme 2 highlights the general pathway proposed for the synthesis of **36**, beginning with the development of this *meso*-phenyl BODIPY and omitting all of the specific reaction conditions as these shall be discussed later. Compound **5** undergoes

regioselective bromination to form the dibrominated species **38**. This molecule then undergoes a palladium catalysed Sonogashira coupling to attach the 2,6 phenylacetylene moieties shown [Scheme 2.]. After this point, the synthesis proceeds using the same methods developed for HBC synthesis, with a Diels-Alder reaction forming the polyphenylated derivative **40**, followed by intramolecular cyclisation of the phenyl rings to give rise to **36**.



Scheme 2. Proposed pathway for synthesising derivative **37**. Note: Ar = Other pentaphenyl benzene substituent (not shown due to spacing).

2.2.1 Synthesis of 5-Phenyl Dipyrromethane **41**

Synthesis of almost all BODIPY molecules, typically results in reactions yielding less than half of the theoretical. This unwanted effect is amplified for unsubstituted

BODIPY frameworks like **5**. This is for two reasons, the primary one being the associated susceptible electronic state of its precursor, with literature quoted yields commonly seen at lower than 10% and 20 percent being considered a highly yielding reaction. This however is dependent on whether α - β substituted pyrroles are used as the starting material, as improved yields can be much more easily achieved when pyrrolic substitution increases. The selectivity can be attributed to multiple reasons, the first being that the intermediates formed in BODIPY syntheses, the dipyrromethenes and their salt forms for the aldehyde and acyl chloride synthetic pathways respectively, are notoriously unstable as noted in Chapter One. They degrade at varying rates, and are highly susceptible to side reactions. They are however stabilised by increasing the level of substitution present likely a result of the combined effect from hyper conjugation and blocking of reaction sites.

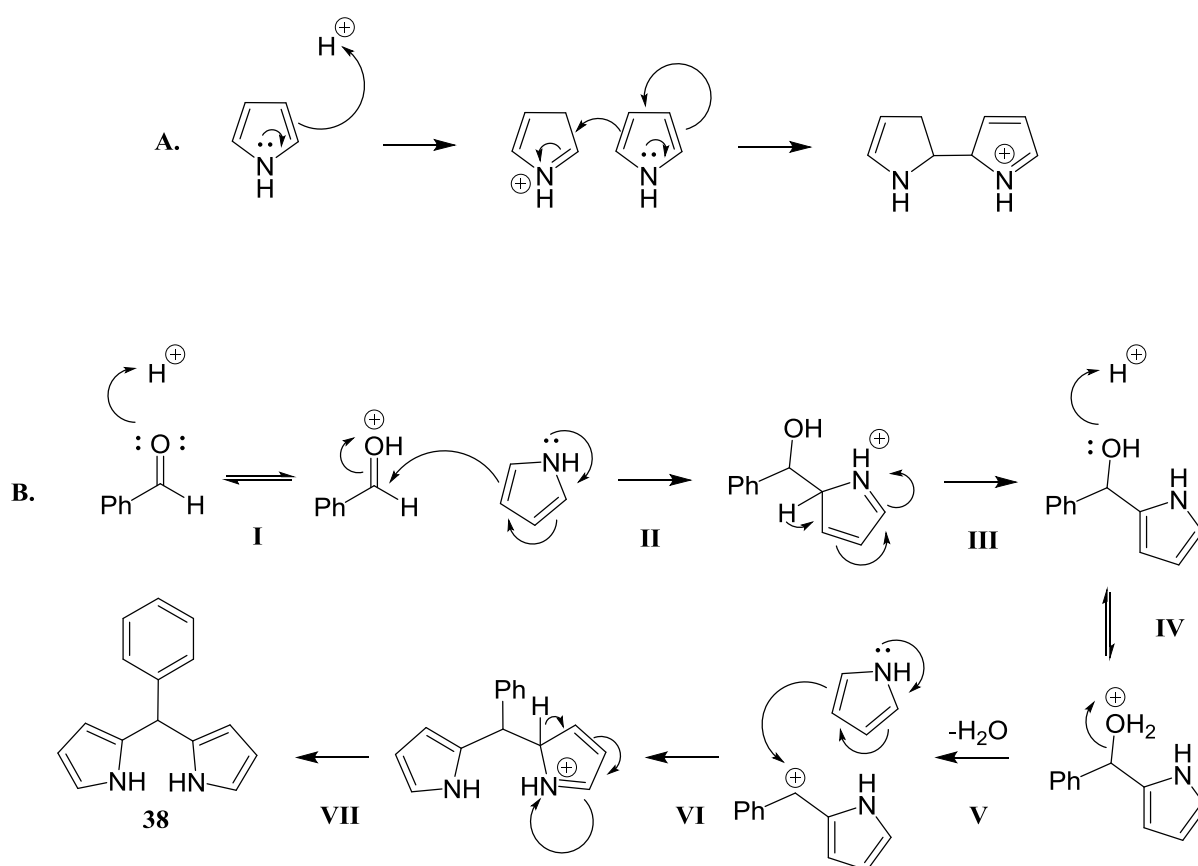


Figure 2.3. **A.** The mode of pyrrole polymerisation. **B.** Basic reaction mechanism for dipyrromethane and porphyrin synthesis.

Due to the reactivity of pyrrole and the strongly nucleophilic character present as a result of its π -excessive electronic system, pyrrole molecules have a tendency to react with one another in a polymerisation reaction [Fig 2.3 **A.**]. This polymerisation is increased under the reaction conditions used for BODIPY formations, as the presence of mild acid is a catalytic reagent in this process, along with the reactions forming both porphyrins and pyrromethanes [Fig. 2.3 **B.**]. Substituting the pyrrole starting material acts to inhibit this as a direct result of steric restraint, rather than any particular electronic effect. By occupying the α - β positions around the pyrrole framework it removes the access for nucleophilic attack from another pyrrole molecule and prevents the formation of porphyrin ring adducts or pyrrole based polymers [Fig. 2.3]. Both of these side reactions leading to quenching of the reaction yields by removing a starting material from the reaction. The formation of porphyrin adducts occurs via the substitution of a further equivalent, as is seen in 'B' of Figure 2.3. Similar to step **VI** of this pathway another pyrrole molecule can attack the dipyrromethane framework in a similar fashion to subsequently form the tripyrromethane adduct and with one more cycle, the tetraphenyl porphyrin.

These side reactions can be minimised by performing the reaction in a large excess of pyrrole. With it acting as a solvent, the molar excess reduces the loss of any pyrrole to unwanted side reactions. This technique was adapted for the synthesis of **5**, initially using a four mole excess for synthesising the intermediate in the prior step [Figure 2.4]. Having an excess of pyrrole in the reaction mixture does somewhat complicate the purification of the intermediate dipyrromethanes however. The crude material is flooded with pyrrole based impurities which are not easy to remove. Common methods rely on vacuum distillation to evaporate pyrrole impurities from the mixture or a novel method developed within the department, utilises centrifugation to separate them out based on their high polymeric molecular weights. However both are dependent on the specific reaction conditions utilised.

Figure 2.4 shows the two sets of reaction conditions that were used for the synthesis of 5-phenyl dipyrromethane (**41**). These are the conventional methods described for the vast majority of BODIPY derivatives throughout the literature and were trialled throughout the project [Fig 2.4]. Six equivalents of pyrrole and one equivalent of benzaldehyde were dissolved in DCM and the condensation reaction was initiated with

the addition of a catalytic volume of TFA [Fig. 2.4 A.]. TLC monitoring was used to detect the formation of brown light sensitive compound, with the TLC spots rapidly changing colour when exposed to the UV-Vis lamp.

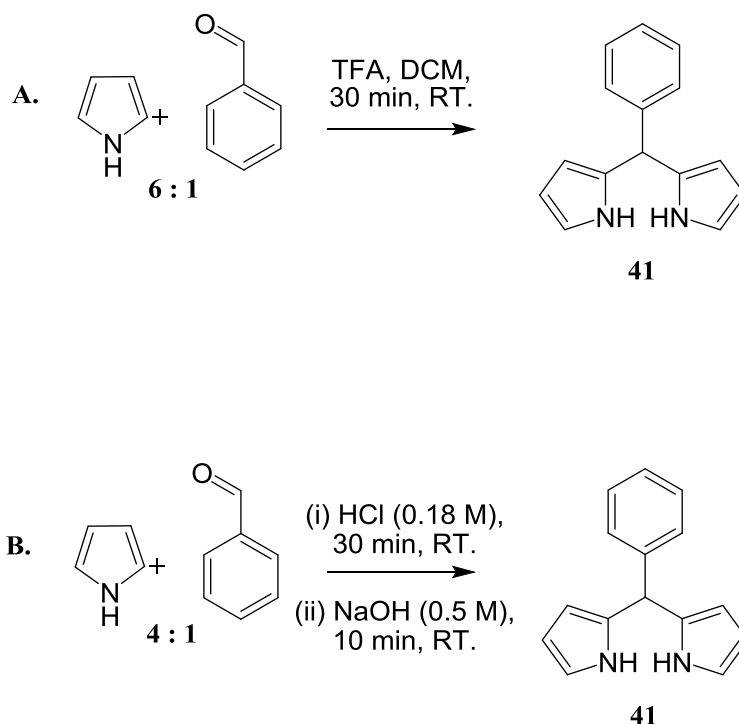


Figure 2.4. **A.** First set of reaction conditions attempted for dipyrromethane synthesis. **B.** Second set of reaction conditions used.

^1H -NMR of the crude product obtained post-work up, quickly confirmed the successful synthesis of **41** via comparison to the literature values.¹¹¹ Issues arose when purification of **41** was attempted, despite literature methods being closely followed and TLC analysis being conducted to determine the correct solvent system. Multiple columns were run on several crude reaction mixtures, testing a series of different solvent systems based around DCM/methanol combinations. These solvent systems were unsuccessful due to the high level of smearing. Increased polarity through higher percentages of methanol tended to give greater separation under TLC analysis, however the use of methanol concentrations above 20 percent is limited due to the degrading effect this has on the silica.

The difficulty in purifying the compound was likely a result of the previously discussed reactivity issues for these intermediates. Even when kept in the fridge overnight both light protected and air sealed, the product ^1H -NMR peaks rapidly disappeared under subsequent NMR repeats and were replaced by what appeared to be a peaks characteristic of a pyrrole adduct. NMR peaks of the impurity corresponding with the integration values for pyrrole however with a different chemical shift. TLC analysis coupled with ^1H -NMR also indicated a large amount of unidentified material in the crude product, which was expected given previously noted complications of BODIPY syntheses. However, given the insight gained through further experimentation, these reactions were potentially complicated further through the use of such highly reactive acid source.

The discovery of a novel green method for the synthesis of aryldipyrromethanes allowed for the synthesis of large amounts of crude compound **41**, whilst simultaneously requiring a less pyrrole [Fig. 2.4].¹¹² The method described by Dehaen and co-workers utilized an aqueous solvent system as the medium for the reaction, with 0.18 molar concentration of hydrochloric acid as the catalytic H^+ in place of TFA [Fig. 2.4 **B.**]. This extremely mild acid source provides a much lower reactivity environment for the dipyrromethane synthesis to occur, minimising the formation of porphyrin adducts. The acid dipyrromethane framework decreases in reactivity as each pyrrole molecule is substituted, and when the available catalytic H^+ ions are limited due to the extremely weak acid source, this makes the further addition of the extra pyrrole molecules that form the porphyrin, much less likely [Fig. 2.3]. Given that the polypyrrole formation seen in Figure 2.3 is similarly acid activated, the amount of formed pyrrole polymers formed is also reduced when the concentration of H^+ is decreased.

As described in the paper, a highly viscous red precipitate that hampered stirring was formed shortly after the combined addition of pyrrole and benzaldehyde to the acidic solution. A large magnetic stir bar set at full velocity was required to maintain any stirring and even then the reaction was always ceased after 30 minutes due to the viscosity of the product. In later repeated synthesis of **41**, base addition was carried out after much shorter reaction durations. Immediately giving rise to a colour change from red to yellow in the crude solid.

The synthetic method published by Dehaens group did not describe this addition of sodium hydroxide, it was added after the repetition of the synthesis still failed to improve upon the highly impure product mixture. Given the known reactivity of dipyrromethanes with acid, a base quench to neutralise the acid was hypothesised to aid in reducing the side reactions further. Work-up for this green method simply involved decanting of the aqueous solution from the solid. The decanted liquid quickly turning a deep green colour upon standing, likely due to pyrrole adduct formation. The solid was then washed with copious water followed by Pet. Ether, and then placed *in vacuo* to slow degradation and further dry the material. Using this method approximate yields of 50 percent were achieved and the reaction was easily carried out on high scales beyond 10 g. Yields remain approximated as the crude material was never purified, ¹H NMR showed clear evidence of the desired product within the crude mixture and thus it was deemed an unnecessary step given the difficulty involved. Attempts to chromatographically separate the dipyrromethane never gave rise to any solid material once dissolved in any solvent system. Small amounts of **41** were obtained pure through repeated crystallisation attempts however never in quantities to be of any synthetic use. Thus the dipyrromethane was used crude at a concentration of approximately 50 percent based on ¹H-NMR peak integrations.

2.2.2 Synthesis of *meso*-Phenyl BODIPY **5**

Figure 2.5 outlines the reaction method used for the formation of *meso*-phenyl BODIPY **5**, with the reagents not varying from the classic synthesis. The synthetic difficulties described thus far in the chapter, solely relate to the formation of pyrrolic unsubstituted dipyrromethanes. The instability of these intermediates as discussed previously, does strongly dictate the high yield quenching observed for BODIPY syntheses. But, there are more broadly applicable synthetic difficulties that apply to almost all BODIPY derivatives and the synthesis of **5** was not exempt from these.

Both of the key reagents responsible for formation of the core moiety are sensitive to chemical breakdown themselves. The boron supply comes in the form of the Lewis acid BF₃-etherate, which readily reacts with water and thus the moisture in the air, to liberate the highly toxic hydrogen fluoride gas. Triethylamine, the other primary reagent for

synthesis of the BF₂, also readily degrades, with this reaction being catalysed by light exposure, the triethylamine breaking down into the dimethylamine alongside N-oxide or nitroso amine impurities.¹¹³ These issues mean that extensive the reaction shown in Figure 2.5 must be tightly regulated to ensure maximum yields. Thus installation of the BF₂ core was carried out using a carefully developed set of reaction conditions adapted from several literature preparations, to ensure that the reagents were exposed to the minimum amount of water and air. These specific conditions were formed through repeated attempts at the synthetic method described within the BODIPY literature, and over a period of several months limiting factors were identified and eliminated.

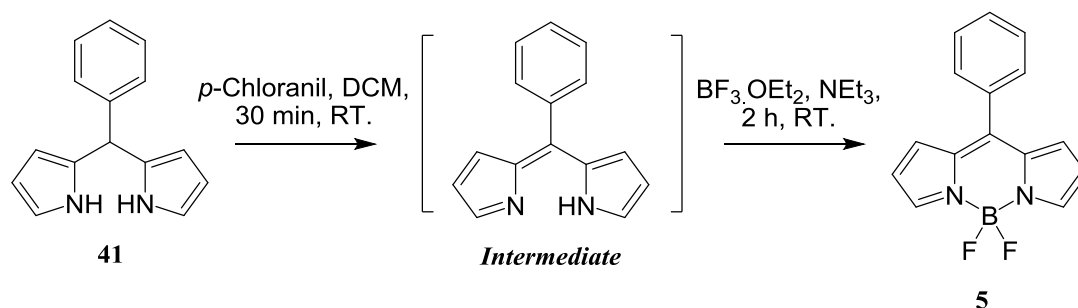


Figure 2.5. Reaction conditions for *meso*-Phenyl BODIPY synthesis.

The first apparent issue was the choice of oxidant. The initial selection of DDQ was based on the need for a stronger reagent to fully oxidise the dipyrromethane. Whilst oxidation of the dipyrromethane seemed to go to completion as indicated by TLC, DDQ was swapped for the milder oxidising *p*-chloranil after the reaction failed to yield any BODIPY after several attempts. The hope being that the DDQ was simply too strong and that having it present in the reaction mixture for the entire process was creating unwanted side reactions that could be remedied by the less potent oxidant *p*-chloranil. Coupled with the issue of which oxidant to use, was the correct method for maintaining an inert atmosphere for the entire duration of the reaction. Literature reaction methods stated addition of the oxidising agent, dissolved into a solution of DCM and injected into the vessel. DDQ and *p*-chloranil however both proved largely insoluble in DCM and thus addition without compromising the reaction was difficult as insoluble oxidant would clog the syringe needles and remain within syringe chamber itself, making

addition of the correct mass uncertain. This was overcome through the inclusion of the powdered *p*-chloranil into the Schlenk flask, prior to being placed under high vacuum in preparation for the reaction. This meant that the vacuum line could be simply switched to a gas flow and dry DCM could be added directly into the vessel without any risk of exposure.

Initial issues were also had with the use of impure boron BF₃-etherate and triethylamine samples. Fresh BF₃-etherate was purchased from Sigmaaldrich and came sealed with a Suba-type seal to ensure maximum control over exposure to the atmosphere. Triethylamine was set-up drying over calcium hydride, and distilled prior to every reaction. Due to the extreme liberation of hydrogen fluoride gas created upon introduction of the BF₃-etherate, a strong flow of nitrogen gas was established as a required component for the reaction also, in order to limit the hazardous exposure to the gas, but to also remove unwanted species from the reaction atmosphere as fast as possible.

The most complicating factor was in regards to the starting materials. Due to the inability to purify **38** [Fig. 2.4], the reaction was utilising an impure dipyrromethane as the starting point for the BODIPY framework, and along with this, the intermediate dipyrromethenes formed during the oxidation step, are significantly more reactive than the already unstable dipyrromethane. These challenges were the hardest to overcome as purification of the dipyrromethane was too time consuming and inconsistent to commit to as a viable option and the reactivity of the dipyrin intermediate cannot be altered without altering the chemistry of the resultant BODIPY also. These factors lead to a massive amount of adduct formation and collection within the crude reaction mixture. Over 50 g of dry product obtained from a reaction, which was only carried out on a 12 g scale. All TLC analysis of crude products indicate a highly fluorescent orange spot representative of **5**, however this spot was mostly hidden beneath a long band of colours and significant smearing from an unknown black impurity.

The extreme volumes of crude product obtained from the reactions limited the potential for chromatographic purification at this stage. An alternative method of purification was discovered however, utilising the unique solubility of the **5** in Pet. Ether. The crude product was dried onto silica powder using the dry-loading technique, carried out

commonly for a flash column when the product is not soluble in the solvent system chosen. Once fully impregnated onto the silica, the resultant solid was dried *in vacuo*, and any lumps removed via through grinding. The consistently fine powder was then loaded into a 25 by 88 mm extraction thimble and a Soxhlet extraction in Pet. Ether was carried out. The warm Pet. Ether selectively extracted semi-pure, BODIPY **5** with only small scale impurities evident in both ^1H -NMR and TLC analysis. This method lead to the reliable isolation of gram scale quantities of *meso*-phenyl BODIPY.

2.2.3 Synthesis of 2,6-Dibromo BODIPY **38**

In order to form the phenylacetylene substituted derivative **39** [Scheme 2.], the *meso*-phenyl BODIPY framework must first be halogenated to create a site for the cross-coupling reaction to occur. This reaction was very high yielding and extremely easy to perform [Fig. 2.6.]. The two bromine equivalents are simply dissolved in DCM and added to a DCM solution of **5**, dropwise over the course of an hour, and then stirred for a further two hours minimum [Fig 2.6.]. The addition rate must be carefully monitored to ensure no errant excess volumes of bromine are added, as these will saturate the system briefly and lead to increasingly halogenated derivatives. NMR confirmed significant product formation after the first reaction, however what also was observed and quickly became a pattern was the formation of small quantities of mono and tetra brominated species also, due to the very fine difference in equivalents required to generate the different species. Despite what the literature stated, anything less than two equivalents gave rise to mono adducts, and anything greater than two, gave rise to some tetra halogenated adducts.¹¹⁴ In particular if the reaction conditions were relaxed then moisture quenching of the bromine solution took place and very significant quantities of mono-brominated BODIPY appeared in the ^1H NMR.

Obtaining 100 percent pure 2,6-dibromo BODIPY (**38**) proved difficult for similar reasons to other compounds synthesised, in that chromatographic attempts to isolate **38** were hindered. This time as a result of the extremely similar chemical properties of the dibromo species compared to the tetra and mono adducts alike. Their similar polarity making chromatographic separation very challenging, with TLC spots running generally under each other on the plate. Given the high yields obtained and the reasonably large

scale of the reactions, crystallization was attempted with Pet. Ether giving rise to a reduction in impurities. By repeating the recrystallization multiple times, **38** was attained at approximately 95 percent purity, with only a small amount of the tetra brominated species present also.

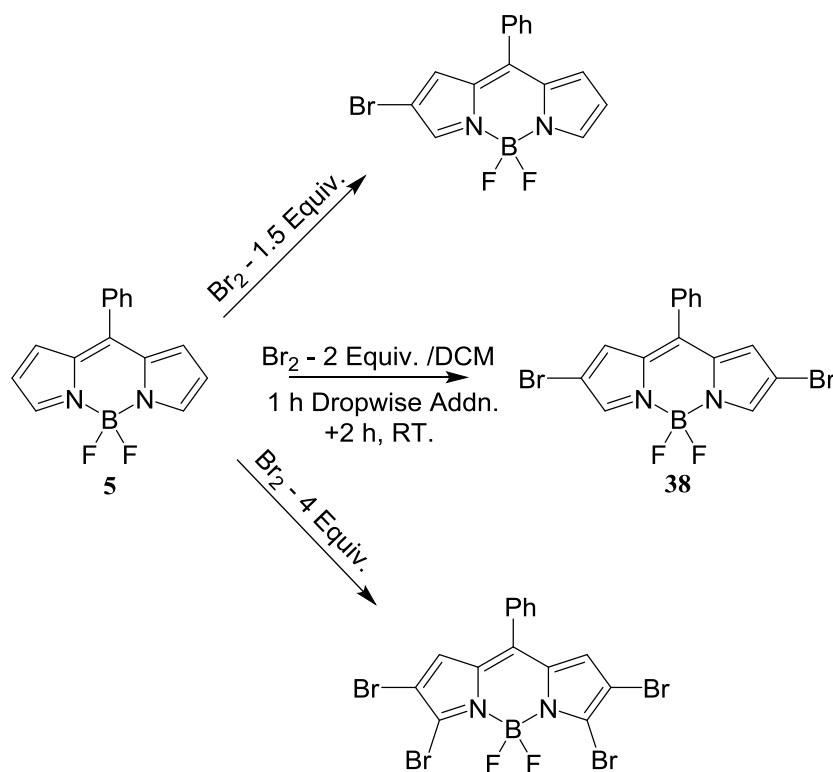


Figure 2.6. Regioselective Bromination of BODIPY **5**.

2.2.3.1 Mass Spectrometry of BODIPY **38**

Mass spectrometry of the BODIPY compounds during this project proved to be considerably difficult for a series of reasons. To begin with, boron has both ^{10}B and ^{11}B isotopes, creating a possible extra set of peaks for each BODIPY derivative. Simultaneously, whilst the BF_2 complexation is generally considered a permanent process due to the high stability of BODIPY dyes, due to the extreme ionisation processes involved in Mass spectrometry, there is observed fragmentation of this core moiety, which forms complicating peaks around the likely target area of the spectra.

Along with this, BODIPY's **38** and **39** in particular, both have bromine atoms and therefore isotope splitting due to these as well, with both ^{79}Br and ^{81}Br evident within spectra. The effect of bromine splitting combined with the two potential boron isotopes, leads to easily viable formation of five peaks, with the potential for more dependent on the isotope combinations. These effects confused and distorted the mass spectra of BODIPY **38** to such a level that getting a definitive peak of this compound was not possible. From observations of post-work up spectra of the attempted Sonogashira reactions to form BODIPY **39**, it was evident that the presence of bromine in these reactions was also having a considerable confusing effect. Having the characteristic splitting pattern of bromine evident within a sample can be useful, as it tells you that that sample is still functionalized with this halogen atom, but when in combination with unknown hydrogen atom ionisation and the boron isotopes, it lead to interpretation issues for Mass spectrometry data.

Despite the spectral complications described, it was still presumed a spectra would be ascertained for BODIPY **38**, given the confirmation of its successful synthesis through both ^{13}C and ^1H -NMR spectra consistency with literature values. However even with attempted caesium doping, no spectra peaks could be matched to any potential isomeric structures of **38**. A paper by Volmer and research associates provided insight into why the Mass spectrometry may be incoherent, beyond even the initially understood reasons of isotopic influences.¹¹⁵ Using CID experimentation to ionise a series of BODIPY dyes into analysable fragments, they determined the most common fragmentation patterns and dissociated ion species for their selection of derivatives. Given the wide range of relatively simple derivatives used within this research, their results can be extrapolated to give a fairly representative example of what Mass spectrometry results be expected for a considerable number of commonly observed BODIPY frameworks. Through their research they identified that the most common almost universal dissociation, was that of HF loss. Occurring in a similar but slightly lower frequency was the loss of $\bullet\text{CH}_3$ radicals as well, with the resultant BODIPY fragments commonly observed. They stated that these methyl radical losses occur regularly alongside H^+ ionisation as well, and that H^+ radical cation loss is also observed, this being one of the most confusing elements of the Mass spectrometry data obtained from such BODIPY dyes. Essentially the findings summarised that combinations of methyl group and hydrogen ion loss, along with their

respective radicals and the dissociation of HF as well, all act to hinder interpretation of the mass signals for BODIPY derivatives.¹¹⁵ This conclusion was a revelation explaining the difficulty within this project in using mass spectra to analyse derivatives, and why analysis of **38** and **39** were so difficult. Interestingly though, the derivatives of least difficulty in terms of Mass spectrometry identification, were those of the tetramethylated frameworks, despite the potential confusion that obviously could have been evident from the methyl group radical ionisation.

2.2.4 The Sonogashira Reaction in BODIPY **39** Synthesis

Cross-coupling reactions have an extreme level of diversity and given the right catalyst system selection, the range of derivatives that can be formed is immense. Sonogashira couplings are utilised the coupling of aryl halides with terminal alkynes. They are generally considered fairly reliable and robust reactions in terms of cross-couplings, with known syntheses usually occurring readily at moderate temperatures and reaction times below 24 hours, without the need for harsh solvent and base combinations. There are certain limitations and sensitivities evident for Sonogashira reactions however, as there is with all cross coupling reaction types.

BODIPY **39** is an unknown compound, with no records evident in the literature and a minimal amount of derivatives published that share close structural similarities. Thus a tetra-methylated BODIPY framework had to be chosen as the most effective reference point, despite how largely altered the core electronic system can be affected by methyl substitution. The reference derivative was also synthesised using a 2,6-iodinated precursor rather the brominated species as is the case here. Multiple reaction conditions were experimented with and a focus was always placed on the maintenance of a maximally inert environment in order to lower the risk of any side reactions.

Table 1 outlines all of the reaction conditions tried for developing the diphenylacetylene coupled BODIPY derivative **39**. For this particular Sonogashira reaction, palladium(0) tetrakis(triphenyl phosphine) was utilized as the catalyst, as per the literature preparations.¹¹⁶ This palladium catalyst is amongst the most frequently encountered within the literature with an abundance of evidence associated to its broadly applicable

reactivity and increased stability as opposed to other palladium salts [Table 1.]. Given that palladium is most stable in the II oxidation state, the oxidative quenching of the metal during the reaction is a serious issue as it is active when in the zero oxidation state. Multiple palladium catalysts are introduced into the reaction systems for cross-couplings, in the form of an inactive 2^+ complex, and reduced *in situ* to the desired oxidation state through chemical activation.

Given that our palladium source was beginning in the zero oxidation state however any exposure to air, particularly in the presence of heat, leads to the formation of palladium oxide and a loss reaction yields. Prolonged oxygen exposure is enough to completely quench a cross-coupling system, given the loading of the catalyst being used is always very low. Hence control of the reaction system is extremely important with both water and air exposure being potent sources of palladium reactive components. In order to ensure the palladium source being used was pure, it was recrystallized from ethanol immediately prior to each coupling, and then dried for a minimum of two hours on a high vacuum line.

As evident in Table 1, the solvent and base system used for reactions was varied multiple times, with the most common conditions being adapted from the literature, which detailed a combination of DMF and triethylamine. This system initially showed promise from the creation of strong pink to deep purple colour changes, consistent with those quoted in the literature for the reference BODIPY structure.¹¹⁶ These colour changes appearing in tandem with the presence of BODIPY indicative peaks in the ^1H -NMR, consistent with what could be expected for **39**, and a clear loss of starting material simultaneously observed both in the NMR and via TLC analysis.

Repetitive washing with solutions of increasing ratios of water to brine, was required to slowly extract the DMF from the post-reaction mixture, leaving the the crude product available for *in vacuo* drying. Solid crude purple-black materials obtained, were isolated using this method, and showed multiple fluorescent products through UV irradiation of TLC plates. Column chromatography was successful in isolating these fractions however ^1H -NMR, and HSQC of products, combined with mass spectrometry results, could not elucidate a definitive structure. There were no mass spectrometry peaks

correlating to any derivatives with phenyl acetylene substitution of either the mono, di or tetra alternatives to this structure.

Solvent	Base (Excess)	Catalyst	Phenyl-acetylene (Mole Equiv.)	Co- Catalyst	Temp (°C)	Time (Hours)
DMF	NEt ₃	Pd(PPh ₃) ₄ (10 mol%)	4	CuI (5 mol%)	65	6
DMF	NEt ₃	Pd(PPh ₃) ₄ (10 mol%)	4	None	65	8
DMF	NEt ₃	Pd(PPh ₃) ₄ (5 mol%)	4	CuI (5 mol%)	65	72
NEt ₃	NEt ₃	Pd(PPh ₃) ₄ (5 mol%)	4	CuI (5 mol%)	65	24
Toluene	DIPA	Pd(PPh ₃) ₄ (5 mol%)	8	CuI (1.25 mol%)	70	48
Toluene	DIPEA	Pd(PPh ₃) ₄ (5 mol%)	8	CuI (1.25 mol%)	80	48
NEt ₃	NEt ₃	Pd(PPh ₃) ₄ (5 mol%)	4	CuI (1.25 mol%)	110	48
NEt ₃	NEt ₃	Pd(PPh ₃) ₄ (5 mol%)	2.5	CuI (1.25 mol%)	50	8
THF	NEt ₃	Pd(PPh ₃) ₄ (10 mol%)	2.5	CuI (10 mol%)	65	24
THF	DIPA	Pd(PPh ₃) ₄ (10 mol%)	2.5	CuI (10 mol%)	65	24

Table 1. Sonogashira Coupling Conditions

However peaks were within the range of the expected molecular weights for such compounds, but without any exact matches, indicating that there was most likely the formation of an unidentified and unexpected BODIPY coupled derivative, potentially with some structural loss due to the ionisation involved when using an electrospray based Mass spectrometer, despite its relatively mild ionisation level in comparison with other Mass spectrometers. Multiple mass spectra peaks were also identified as belonging to a boron containing molecule fragment, due to the specific splitting patterns

observed. One peak was identified to a specific splitting pattern of both a boron and bromine containing species, however it still did not correlate to any matched masses, compared individually, based on any potential adduct formations that could have taken place.

Given the unsuccessful nature of the literature method being followed, the reaction conditions were carried as per Table 1. Low and high temperature reaction conditions were tested, with varying reaction times implemented and reformed volumes of phenylacetylene trialled. These factors were varied systematically to help elucidate what was the most likely source error for the unsuccessful attempts. The hypothesis from the best interpretation of the spectroscopic data available, was that the resultant product material most likely contained a mono-coupled adduct of **39** shown in Figure 2.7 as molecule '**39x**'.

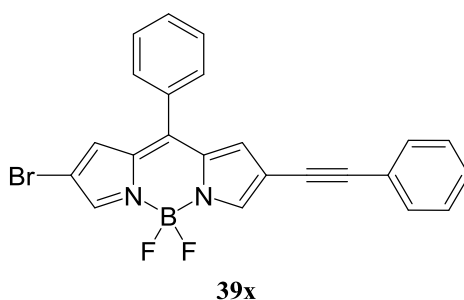


Figure 2.7. Hypothesised mono-coupled adduct of BODIPY **39**.

This molecule maintains the presence of one bromine atom on the structure as per the mass spectrometry data, but also has a phenylacetylene group coupled in place of the second bromine atom [Fig. 2.7]. The reason theorised for this incomplete reaction is the possible quenching of the palladium source as discussed, previously, however every precaution was taken to avoid this and the reaction environment was tightly regulated from any atmospheric exposure making this an unlikely source for the error.

As per most Sonogashira reactions, a copper-co-catalyst was used initially to assist in activation of the acetylene functionality which it is hypothesised to do so through the formation of a terminal pi-alkyne complex. This copper co-catalyst was however not included in every repetition of the reaction, as can be seen in Table 1. Like the temperature and time modifications, the presence of copper was adjusted in order to

elucidate if this was the source of the reaction issues. The initial inclusion of copper was not on the basis of the literature preparation being followed, but rather based on the larger combined Sonogashira literature. Published materials regularly recommending the inclusion of copper in order to maximise yields and minimise reaction run-times due to its activating effect on the alkyne derivatives.

However, it is well documented that copper has a homo-coupling effect on the activated phenylacetylene molecules, coupling two of these together rather than with the halide source. This homo-coupling was theorised to be one of the most significant issues of this specific reaction in particular, due to the presence of large phenyl peaks present in the post-reaction ^1H -NMR. These peaks however only matching the aromatic ring peaks of phenylacetylene, with the ethynyl proton absent from the spectra, when compared to a phenylacetylene standard. This suggesting the two phenylacetylene had homo-coupled giving rise to the observed spectra.

The phenylacetylene homo-coupling was reduced by the use of a large phenylacetylene excess for many of the reactions. This excess allowing for the loss of some phenylacetylene to side reactions, whilst still maintaining enough for the decoupling of **38**. This was further complicated however due to the use of slightly impure dibromo precursor. As described previously, successive recrystallization of **38** lead to the formation of a highly pure solid being isolated, however this was still tainted with some tetra brominated species, with the mono adduct appearing absent from NMR. The use of this slightly impure species lead to the need for a further excess of phenylacetylene and is likely a large contributor to the complicated spectroscopic analysis involved post-reaction, as potentially multiple different poly-coupled or mono-coupled derivatives were being observed on tetra, or di brominated BODIPY structures. Ultimately significant effort went into the synthesis of **39** and spectroscopic analysis was indicative of coupling activity. No pure compound was however definitively isolated and identified as **39** and given the extensive number of attempts at the synthesis and the fact that no core unsubstituted peripherally coupled BODIPY derivative exists as of yet, there is potential that the methylation of the core is required to sufficiently reduce the highly reactive nature and allow for unhindered 2,6 diphenylacetylene coupling.

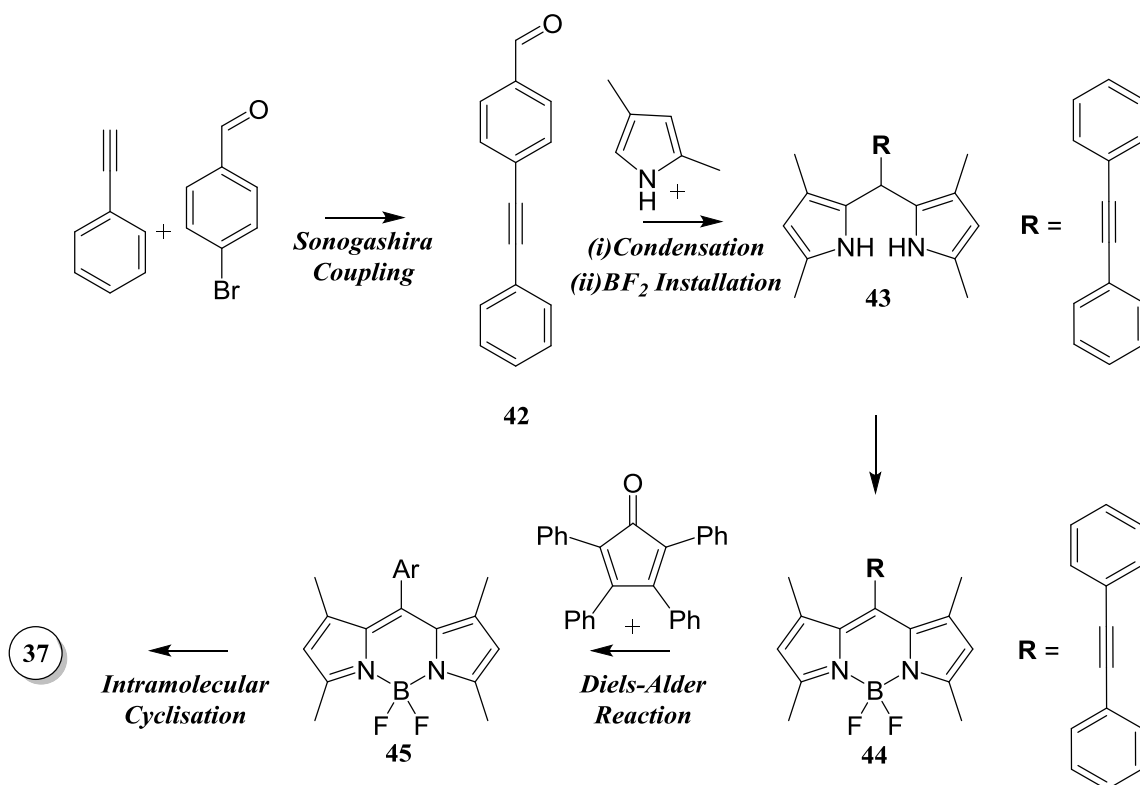
2.3 Development of *Meso*-HBC-Coupled BODIPY **37**

Shown in Scheme 3 is the synthetic pathway for development of the *meso* HBC-coupled BODIPY derivative (**37**) [Fig. 2.2]. The synthesis of this derivative was viewed as a more reliable alternative to the formation of **36**, given the limited success when attempting the palladium catalysed cross-coupling of the dibrominated species. By carrying out the Sonogashira coupling of 4-bromobenzaldehyde with phenylacetylene at the start of the synthetic scheme, arguably the most challenging reaction in the pathway is completed first. It was also hypothesised to be much higher yielding for the diels-alder and intramolecular cyclisation steps, and generate far less side adducts along the way, given the increased stability of the core structure with the presence of 1, 3, 5 and 7 position methyl groups. These methyl groups present through the use of 2,4-dimethyl, pyrrole rather than unsubstituted ‘free’ pyrrole. The use of a substituted pyrrole in itself makes the synthesis of the core structure much simpler, removing any chance of porphyrin formation due to steric hindrance and removing the ability for the self-condensation side reaction of pyrrole also.

The initial Sonogashira coupling step was carried out using palladium(II)dichloride-bis(triphenylphosphine). This meaning as indicated, that the palladium source is introduced in the inactive 2^+ state and is subsequently activated through a ligand interaction with triphenyl phosphine to form the active palladium(0)-tetrakis(triphenyl phosphine) *in situ*. This made the reaction less sensitive to moisture and oxygen exposure as the palladium remained stable during the reaction set-up, although tight control was still required to ensure that the palladium(0) was not quenched through oxidation as it was formed. This reaction went to completion readily and gave good yields of compound **42**, as indicated by both ^1H -NMR and mass spectrometry [Scheme 3.].

As hypothesised, formation of the tetra-methyl substituted dipyrromethane **43** [Scheme 3.], was far simpler than the corresponding peripherally unsubstituted BODIPY derivatives. It was formed readily utilising literature methods once again described by Cohen and co-workers in the same paper.¹¹⁷ Formation of **43** was confirmed by ^1H NMR, however shortly after the synthesis of **43**, it was discovered that the 2,6 diethyl substituted version of BODIPY **37**, the target molecule for this avenue of research had

been synthesised, along with an array of other similar HBC coupled BODIPY molecules. This led to a decreased interest in the immediate completion of Scheme 3, with the research project focus being that of developing “novel” BODIPY molecules and novel direction in this pathway being hindered by the difficulties encountered in the Sonogashira reaction step of Scheme 2.



Scheme 3. Proposed pathway for synthesising derivative 36.
Note: Ar = Pentaphenyl benzene

Given the time constraints within the project and a need to limit distractions from the now primary goal of developing some BODIPY-based MOF's, research towards 43 was put on hold entirely. Upon subsequent ^1H NMR analysis of the crude product at a later date several months after synthesis, the crude material showed complete degradation to phenylacetylene, highly characteristic of the dipyrromethane frameworks. All peaks evident as for molecule 42, minus the indicative aldehyde peak at a chemical shift of 10 ppm. These results suggesting that despite the increased stability and ease of formation

evident for such methylated frameworks, complete stabilisation from chemical degradation is still not attained and the species will still degrade at an appreciable rate, especially if not maintained in the appropriately controlled environment, with minimum air, moisture and light exposure.

Chapter Three

Metal Incorporated BODIPY Structures

3.1 Metal Coordinating BODIPY's

Shown below in Figure 3.1, are the three BODIPY derivatives targeted for synthesis due to their potential interactions with metal ions. BODIPY **46** was synthesised previously by Pradhan and co-workers, however, this was isolated only as an intermediate in the formation of an extended synthetic target [Fig. 3.1].¹¹⁸ The framework of **47** is based around a mono-carboxylate derivative also previously reported, but is targeted in this project for both metal complexation itself and also for peripheral functionalization, with possible substitutions at the 2 and 6-positions of the framework to generate another site for simultaneous coordination of multiple metal ions. Both **46** and a peripherally substituted **47**, are of interest for their potential applications and for forming MOF type structures, exploiting the classic Isophthalic acid type binding mode of **46**, with the theoretical 'corner' themed binding mode of a peripherally substituted derivative of **47**. The clear bridging potential of these theorised structures should enable them to act as linking ligands within a MOF.

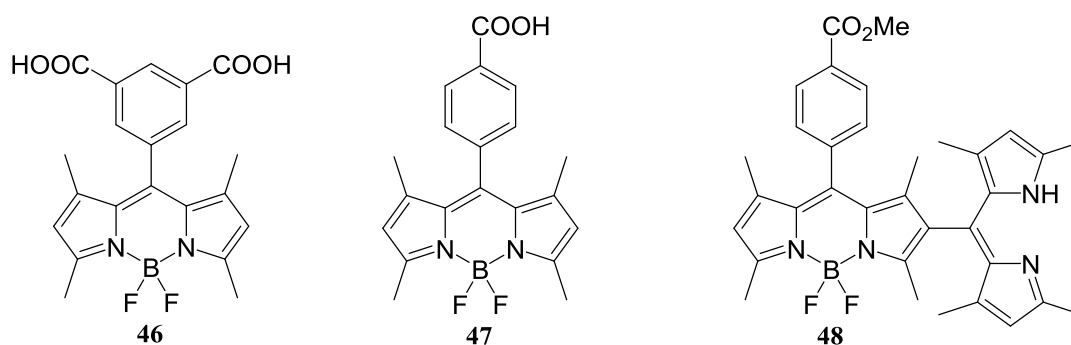


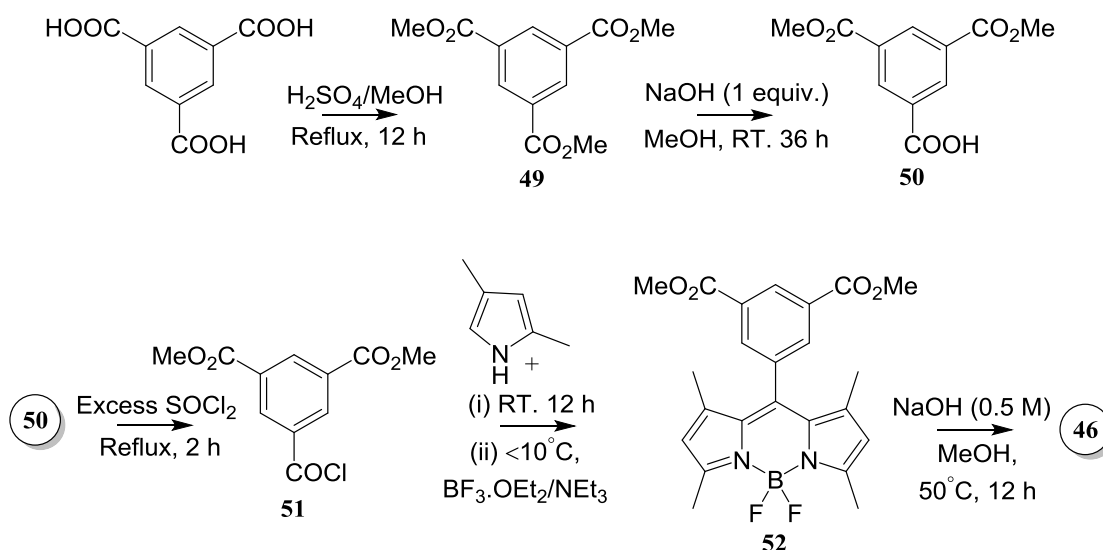
Figure 3.1. Three targeted potential metal coordinating BODIPY derivatives.

Compound **48** is a novel alternative BODIPY structure, designed for its metal complexation potential rather than its MOF capability, although if the phenyl ester functionality was hydrolysed it would have potential as a corner type binding motif as well [Fig. 3.1]. The dipyrromethane moiety in the 2-position of the BODIPY framework is a commonly exploited structural motif within inorganic chemistry.¹¹⁹ By converting a dipyrromethane to its respective dipyrin, complexation is readily achieved and this has

been witnessed in some different BODIPY derivatives in the past. For a BODIPY molecule, the relatively uncommon phenomenon of electronic communication between the BF₂-core and a metal centre may be observed.⁹⁵

3.1.1 Synthesis of BODIPY's 46 and 47

Throughout this chapter, the reaction pathways adapted for the synthesis of **46**, **47** and **48** shall be discussed, along with precursors and derivatives of these structures formed during their synthesis.

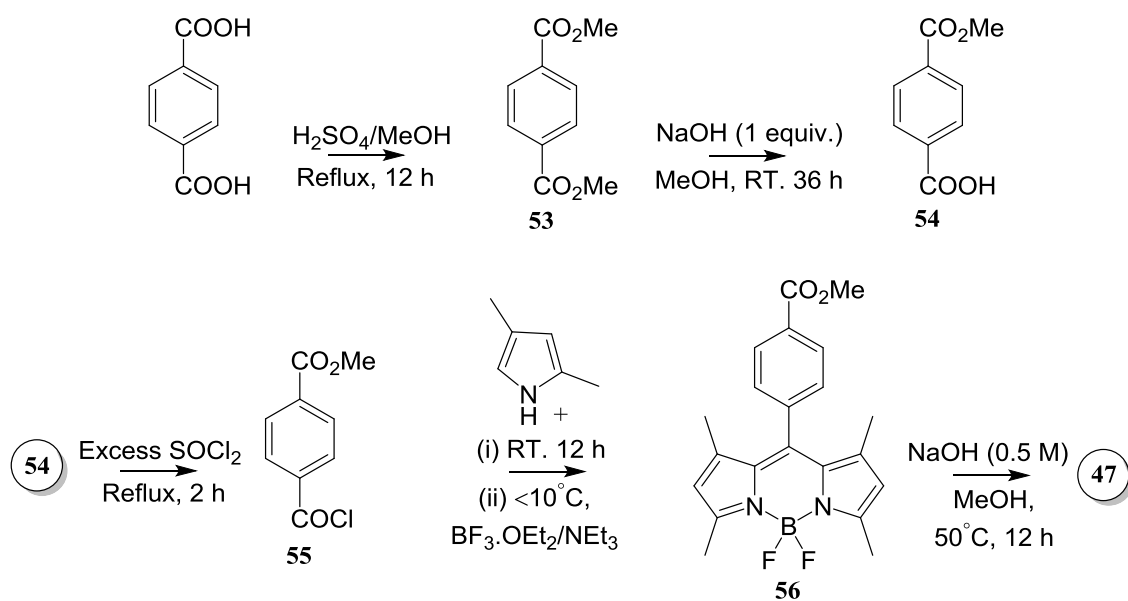


Scheme 4. Synthetic pathway for MOF-BODIPY **46**.

The basic synthetic pathways for both **46** and **47** largely involve the same reactions, given the close similarities between the two structures. Scheme 4 outlines the multiple steps involved in development of **46**, this being the simpler of the two derivatives to synthesise due to lack of any peripheral substitution post core-formation. Whilst Scheme 5 shows the almost identical synthetic pathway utilising the corresponding di-substituted benzyl derivatives, for formation of **47** instead.

Compared to the previously sensitive and challenging BODIPY syntheses described in Chapter Two for the formation of the HBC-coupled derivatives, the chemistry utilised

for the formation of molecules **46** and **47** was initially straight forward. Using standard esterification conditions, concentrated sulfuric acid was added to a solution of Trimesic acid or Teraphthalic acid in methanol, with refluxing overnight forming the corresponding esters **49** and **53**, respectively. These reactions proceeded in high yields and were carried out on a large scale with no discernible impurities evident in the ^1H -NMR spectra and no purification steps necessary.



Scheme 5. Synthetic pathway for MOF-BODIPY **47**.

The second step of the reaction pathway was more complicated, with strict control of the sodium hydroxide stoichiometry required, in order to ensure that only one methyl ester was hydrolysed to form the mono-carboxylate derivatives **50** and **54**. When addition of the sodium hydroxide was regulated to a slow enough rate and used in a small mole deficiency this reaction also proceeded without any issues, with a small volume of the starting material re-isolated after each repetition of this reaction, along with considerable quantities of product. By allowing the reaction to run for 36 hours, all mole equivalents of the base were reacted, with the more reactive fully esterified benzenes reacting preferentially over already hydrolysed products due to the deactivating effect of the carboxylic acid functionality. No side products were detected in the post-reaction analysis with double hydrolysis evident. Given the highly selective

nature of the reaction, work-up consisted of a simple filtration to collect the unreacted starting material and then precipitation of the mono-acid products from solution through pH manipulation.

Common literature methods were once again closely followed for the formation of the acyl chloride derivatives, 2,4-dimethoxycarbonyl benzoyl chloride, (**51**) and 4-methoxycarbonyl benzoyl chloride, (**55**). Care was taken to maintain a moisture free environment and minimise atmospheric exposure to the highly reactive thionyl chloride. Only oven dried glassware was used, and complete saturation of the reaction system with Argon gas was maintained throughout, to reduce the possibility of moisture entering in with any air. Despite distillation of the thionyl chloride prior to the synthesis, this step appeared to introduce the highest level of impurity into the products, with ^1H -NMR indicative of side-reactions forming some unknown species, however these were minimal quantities when considered relatively. Given the highly reactive nature of the resultant acyl chlorides, purification was not attempted and the products were never kept longer than overnight. They were stored at reduced temperatures, under an inert Argon gas blanket.

At this stage the acyl chlorides were generally dried rapidly using a high vacuum over a period of several hours, with the specific times dependent on the sample. Immediately after drying they were converted into the corresponding dipyrromethene hydrochloride salt. Due to the increased reactivity of acyl derivatives as opposed to the previously utilised aldehydes, no acid activation is necessary with HCl, TFA, or otherwise. With maintained stirring, molecules **51** and **55** were combined with 2,4-dimethylpyrrole in dichloromethane under and argon gas atmosphere, then left overnight until TLC analysis showed clear indication of a new species within the reaction mixture and the loss of the characteristic pyrrole smear. A specific TLC smear made by pyrrole derivatives is very characteristic of their presence, as they undergo a rapid photo-catalysed reaction through UV exposure to produce obvious brown stains.

The bypassing of any dipyrromethane formation results in formation of the highly reactive dipyrin salt intermediates. Their reactivity in comparison to the respective dipyrromethene alternatives is extremely high, and thus specifically for BF_2 installation of these acyl chloride synthesised BODIPY's, addition of the BF_3 -etherate and

triethylamine has to be carried out in a dropwise fashion with the presence of an ice-bath to maintain the reaction temperatures below 10°C. Cooling acts to limit the reactivity of any species present such that the reaction is more controlled.

Despite controlling the addition of these highly reactive reagents and the use of an appropriately substituted pyrrole, the formation of a considerable amount of side product impurities, was still evident from these reactions. Alongside this, a massive excess of the highly reactive BF₃-etherate is always used in BODIPY formation, ensuring saturation of the installation site. These factors, coupled with the inability to purify the acyl chloride precursor, or the intermediate dipyrin framework either, means that there is a large source for impurities even with maximum precaution taken to minimise such unwanted side reactions.

With the presence of a large quantity of impurities, the difficulty of purification for these BODIPY compounds is once more significant. The most reliable option of flash chromatography is hampered by the sheer volume of crude product isolated. Several attempts were made on different crude product samples isolated in repeat reactions to form **52** and **56**, and the best purification procedure discovered utilised a combination of Pet. Ether trituration/extraction as the first step. After adding Pet. Ether to the crude dry solid materials isolated *in vacuo*, the resultant mixture was agitated whilst set to 50°C, such that the bulk of the soluble phenyl-ester BODIPY's were dissolved into the Pet. Ether. This was repeated multiple times, leaving a fluorescent liquid phase containing the majority of BODIPY's **52** and **56**, along with an insoluble solid phase containing the majority of the insoluble organic materials and a small volume of remnant BODIPY.

With the large percentage of crude impurities removed from the resultant extract, these products were viable for chromatographic separation to attain pure BODIPY **52** and **56**, using solvent systems of 80:20 and 70:30 dichloromethane to Pet. Ether for each, respectively, with the products eluting as the second components in each mixture and each demonstrating an intense bright orange colour and moderate fluorescence intensity under TLC analysis. The first component eluted during these columns also exhibited strong fluorescence under TLC analysis and was most likely the BODIPY compound with BF₂ absent frameworks [Schemes 4, 5]. This was suggested by both ¹H-NMR, which exhibited peaks with the same integrations but slightly different shifts for the

meso-phenyl group, and large shifts in the methyl protons, as would be expected for a core absent structure as these are the most directly influenced, coupled with mass spectrometry results. The exact reason for the source of these core-absent adducts is unknown, but there is potential that the reactions were incomplete or that at some point during the work-up procedure the BODIPY core was disturbed and the nitrogen-boron bonds weakened or broken.

Despite the large presence of side-adducts, BODIPY's **52** and **56** were isolated from the column in several hundred milligram scales, but in relatively low yields with 11 and 15 percent being the highest yields obtained for each, respectively. These yields can be considered very low from a general reaction perspective, however as mentioned in Chapter One, BODIPY reaction yields commonly fall below the 20 percent margin, with the methylated frameworks more able to achieve appreciable yields with, but still being far from desirable. To complete the synthesis of the metal coordinating BODIPY prospects, **46** and **47**, the ester groups on BODIPY's **52** and **56** had to first be hydrolysed into their carboxylic acid form. Whilst this hydrolysis reaction can be carried out *in situ* during MOF formation, in general it is carried out prior to any attempted complexation and the acid derivative isolated to remove a step and any potential complicating factors associated with the hydrolysis, such as the partial-hydrolysis products that could be formed from BODIPY **46** specifically.

Whilst there is a vast array of reaction conditions utilised for hydrolysing ester groups, two that are commonly observed for such hydrolysis reactions are those of sodium hydroxide in water and/or an alcohol, or the more organic friendly conditions where solubility is more of an issue, which generally combine potassium hydroxide with tetrahydrofuran. For the synthesis of **46** and **47** the initial reaction conditions used utilised a low concentration of sodium hydroxide in methanol. The reason for choosing these particular conditions was two-fold, firstly; the large majority of the previous reactions along the two synthetic pathways had also used methanol as the primary solvent and second, the previously reported synthesis of the dimethyl ester BODIPY **46** had been carried out also using a combination of sodium hydroxide and methanol as opposed to any other common hydrolysis reagents. The low base concentration approach was chosen as a precaution to potential instability of the ester or acid BODIPY derivatives, as despite the generally accepted robustness of the BODIPY

scaffold, in lab research and post-reaction analysis throughout the project had suggested that in particular BF_2 core loss is a possible unwanted side event of BODIPY chemistry.

Complications arose during repeated attempts at the hydrolysis reaction under the chosen conditions. Selective precipitation of the two derivatives **42** and **46** from their respective crude solutions was easily performed via acidification down to a pH of one. The initial crude precipitate isolated during the filtration step of the work-up procedure was extremely difficult to work with, as it was significantly hygroscopic and the associated water proved difficult to remove, leading to smearing of the product around the inside of the glass frit used for filtration. Initial attempts to dissolve the product from the frit to minimise the amount of crude material left being aggregated to the glass also proved difficult due to the highly insoluble nature of the two BODIPY molecules, a result of the carboxylic acid functionalities now present. Due to the required addition of hydrochloric acid for precipitation of the BODIPY's from solution, coupled with the hygroscopic nature of the solids, the products remained very acidic and addition of methanol in order to dissolve them off of the frit appeared to catalyse the re-esterification of the carboxylic acids back to their respective esters **52** and **56**. This was evident from the NMR analysis of some products isolated from the reactions, which showed development of peaks highly characteristic of such BODIPY esters, at the expected value of 3.96 ppm.

Pure samples of **46** and **47** were eventually isolated from hydrolysis carried out using the sodium hydroxide and methanol combination, by precipitating the BODIPY's once again with hydrochloric acid addition, then filtrating slowly over a grade five frit and washing through slowly with ethyl acetate, with both of the BODIPY's exhibiting low solubility in the solvent. The ethyl acetate was then evaporated and the resulting red powders dried once *in vacuo*, gave rise to both of the carboxylic acid derivatives as pure samples, ready for metal coordination formation.

3.1.2 Development of BODIPY-Based Inorganic Frameworks

Over the last two decades the volume of MOF literature grown exponentially. MOF's have followed a similar pattern as that experienced by fluorophores several decades ago,

when they exploded into the forefront of modern research, as discussed in Chapter One. A vast number of applications for MOF's have been suggested, such as molecular storage or transport devices, along with their use as various types of molecular tool, such as switches and sensors. It is now well-known that MOF's are both extremely powerful and highly unpredictable. It often appears to be somewhat serendipitous in the way certain MOF's have simply self-assembled themselves when the right set of conditions has either been meticulously selected or randomly arrived at. The general understanding is that discovering the correct set of conditions to form a particular MOF can take; significant time, vast experience, lots of trial and error, luck, and usually a combination of all of these factors.

With this knowledge, both carboxyl derivatives **46** and **47** were subjected to a range of reaction conditions adapted from research highlighted in particular by Baudron and co-workers, who developed a series of luminescent MOF's utilising BODIPY frameworks as ligands within the structures. Insight was however also taken from the expanse of MOF literature to help elucidate the best conditions and techniques to use. Whilst molecule **47** itself, does not actually have potential to form MOF's due to its singular coordinating functional group, it was subjected to a series of equivalent conditions to those established for **46**, due to its potential to form discrete metal complexes.

3.1.3 Attempted Complexation of BODIPY-Ligands 46 and 47

Table 2 shows the series of reaction conditions that were attempted for the synthesis of MOF's from BODIPY **46**, and Table 3 shows the smaller selection of conditions trialled for complexation of **47**. For the trialling of MOF forming conditions, focus was kept on keeping them both simple and highly systematic in terms of the organisation and preparation. As such, multiple aspects of the reaction conditions were kept fairly consistent to minimise variability. Given that the two ligand BODIPY's being used are both carboxylic acid derivatives, the general scheme followed for choosing reagents followed the well described method of combining a metal salt with an appropriate mole equivalent of the ligand, in a suitable solvent, under the presence of some base to allow for deprotonation of the acid functionalities to their coordination active carboxylate ion forms.

Only two different metals were used, both the copper and zinc nitrate salts and similarly only two different mole ratios of ligand to metal were used, these being the standard 1:1 and 2:1 ratios. Along with this the time and temperature were kept to only three different possibilities each, the temperatures tested, being that of 50, 100 and 150°C, whilst the temperatures were maintained for either 36, 48 or 72 hours, dependent on the level on solid material evident within the reaction vials. The primary reaction conditions that were significantly varied were that of the solvent selection and ratios, and the presence, volume and type of any additional acid and/or base.

A

Metal Salt (Nitrate)	Ligand:Metal Ratio	Solvent 1 (Abbreviations)	Solvent 2 (Abbreviations)	Base/Acid	Temp (°C)	Time (Hours)
Zn ^a	1:1	DMF (1 mL)	N.A.	N.A.	100	36
Zn ^a	2:1	DMF (1 mL)	N.A.	N.A.	100	36
Zn ^a	1:1	DMF (1 mL)	N.A.	HNO ₃ (2 Drops)	100	36
Zn ^a	2:1	DMF (1 mL)	N.A.	HNO ₃ (2 Drops)	100	36
Zn	1:1	DMF (10 mL)	N.A.	N.A.	100	48
Zn	2:1	DMF (10 mL)	N.A.	N.A.	100	48
Cu	1:1	DMF (10 mL)	N.A.	N.A.	100	48
Cu	2:1	DMF (10 mL)	N.A.	N.A.	100	48
Zn	1:1	EG (9 mL)	DMF (1 mL)	N.A.	150	72
Zn	1:1	DMF (10 mL)	N.A.	HNO ₃ (2 Drops)	50	72
Zn	1:1	EtOH (5 mL)	DMF (5 mL)	N.A.	50	72
Zn	1:1	EtOH (10 mL)	N.A.	NaOH	100	72
Zn	1:1	EtOH (10 mL)	DMF (Cat.)	N.A.	100	72
Zn	2:1	EtOH (10 mL)	DMF (Cat.)	N.A.	100	72
Zn	1:1	DMF (10 mL)	N.A.	N.A.	150	72
Zn	1:1	EtOH (10 mL)	DMF (1 mL)	HNO ₃ (2 Drops)	100	72
Cu	1:1	EG (9 mL)	DMF (1 mL)	N.A.	150	72
Cu	1:1	DMF (10 mL)	N.A.	HNO ₃ (2 Drops)	50	72
Cu	1:1	EtOH (5 mL)	DMF (5 mL)	N.A.	50	72
Cu	1:1	EtOH (10 mL)	N.A.	NaOH	100	72
Cu	1:1	EtOH (10 mL)	DMF (Cat.)	N.A.	100	72
Cu	2:1	EtOH (10 mL)	DMF (Cat.)	N.A.	100	72
Cu	1:1	DMF (10 mL)	N.A.	N.A.	150	72
Cu	1:1	EtOH (10 mL)	DMF (1 mL)	HNO ₃ (2 Drops)	100	72

B

Metal Salt (Nitrate)	Ligand:Metal Ratio	Solvent 1 (Abbreviations)	Solvent 2 (Abbreviations)	Base/Acid	Temp (°C)	Time (Hours)
Zn ^a	1:1	DMF (1 mL)	N.A.	N.A.	100	36
Zn ^a	2:1	DMF (1 mL)	N.A.	N.A.	100	36
Zn ^a	1:1	DMF (1 mL)	N.A.	HNO ₃ (2 Drops)	100	36
Zn ^a	2:1	DMF (1 mL)	N.A.	HNO ₃ (2 Drops)	100	36
Zn	1:1	DMF (10 mL)	N.A.	N.A.	100	48
Zn	2:1	DMF (10 mL)	N.A.	N.A.	100	48
Cu	1:1	DMF (10 mL)	N.A.	N.A.	100	48
Cu	2:1	DMF (10 mL)	N.A.	N.A.	100	48
Zn	1:1	EG (9 mL)	DMF (1 mL)	N.A.	150	72
Zn	1:1	DMF (10 mL)	N.A.	HNO ₃ (2 Drops)	50	72
Zn	1:1	EtOH (5 mL)	DMF (5 mL)	N.A.	50	72
Zn	1:1	EtOH (10 mL)	DMF (Cat.)	N.A.	100	72
Zn	2:1	EtOH (10 mL)	DMF (Cat.)	N.A.	100	72
Cu	1:1	EG (9 mL)	DMF (1 mL)	N.A.	150	72
Cu	1:1	DMF (10 mL)	N.A.	HNO ₃ (2 Drops)	50	72
Cu	1:1	EtOH (5 mL)	DMF (5 mL)	HNO ₃ (2 Drops)	50	72
Cu	1:1	EtOH (10 mL)	DMF (Cat.)	N.A.	100	72
Cu	2:1	EtOH (10 mL)	DMF (Cat.)	N.A.	100	72

Table 2. **A** = reaction conditions attempted for forming MOF's around BODIPY **46** and **B** = conditions for forming coordination complexes of **47**. *Note: Total volumes for each vial were 10 mL, Superscript 'a' = total volume of 1 mL.*

The reactions were done in small glass vials, sealed post-preparation with plastic caps and then air tight via insulation taping around the cap to glass join. Vials were then placed in heating basins and covered up to the lids with sand, with the heating basins set upon elements to maintain the desired temperatures. Thermometers were maintained within the heat basins at all times to give a constant thermal reading. Given the slightly different size and shapes of the heating basins, coupled with the varying efficiencies of the heating elements used, small temperature variations between plates were evident, noticeable to around 5°C shifts, particularly when increasing heating to 150°C. Given the trial nature of these complexations however, this variation was not considered irrelevant, but rather acceptable. With the initial target being identification of a general

set of conditions that would promote crystallisation, rather than identifying the ‘perfect’ set immediately.

The first 8 complex reactions attempted, were maintained at approximately 100°C, and used a total volume of only 1 mL, comprised entirely of DMF, with this acting as both the solvent and base for the systems. Four were prepared for each of the ligands **46** and **47**, zinc nitrate was used as the metal salt due to its success in the previously published BODIPY MOFs, and was in both 1:1 and 1:2 mole ratios to the ligands. Two of the complexation reactions were tested utilising the addition of a small volume of nitric acid, and two without. This nitric acid was added following similar methods to previous BODIPY-MOF research.¹⁰² The acid is hypothesised to slow down the rate of deprotonation by limiting the presence of base and thus hindering the decomposition of DMF to its respective amine precursor, dimethylamine, and thus possibly allows the crystallisation process and formation of the MOF frameworks to occur in slower and more favourable manor in terms of the product quality. A potential issue with this theory being that the nitric acid may simply just quench any deprotonation from occurring at all, until it has being fully consumed, at which point the deprotonation would actually occur all at once rather than slowly as was hoped, and so could instead have a detrimental effect.

After the 36 hours these eight complexation reactions of the BODIPY ligands showed clear presence of a precipitate, in small aggregated clumps. The vessels containing ligand **46**, had more brown aggregated precipitate, whilst the reactions of **47** had a fine purple precipitate present. Also, for both sets of ligand reactions, the volume of insoluble material formed appeared to be double in the solutions that started with a 2:1 mole ratio of ligand to metal, likely meaning that the ratio had not affected the type of structure formed, but rather just the mass formed.

UV irradiation detected the presence of some fluorescent materials in the solutions, but the solid precipitates appeared non fluorescent and were extremely insoluble. Solutions of hot DMSO, usually considered the highest solubility solvent system, could not solubilize any of the product materials. This result suggesting that some sort of polymeric species had formed, but likely at a rate too fast to allow for crystallisation. Any further analysis to elucidate the particular structure of the solids was limited, due to

their incredibly insoluble nature. ^1H -NMR of the decanted reaction solutions gave rise to small peaks corresponding to the starting BODIPY molecules, however no other characteristic peaks were observed.

Given the inability to dissolve the formed solids, and due to the time constraints of the project, attempts at carrying out any further analysis on the materials were ceased and more reaction conditions were trialled instead. The total solvent volume was raised to 10 mL and a series of eight more reactions were tested, this time with no acid addition to any of the reactions, but instead making half of the reactions up with the zinc nitrate as the metal salt and half with copper nitrate instead. This set of complexation reactions was left for an additional 12 hours as opposed to the first set, while the rest of the reaction conditions were maintained constant. These complex reactions gave rise to identical solid formations as per the previous reactions, with the slight exception of the copper nitrate systems, in which they exhibited product formation still, but with slightly paler colourations than that of their zinc counterparts.

Up until this point, only DMF had been utilised as both the solvent and base present in any reaction systems, thus as per Table 2, a wide array of solvent combinations and reaction conditions were trialled next. In total another 30 reactions were set-up, 12 more for the mono-carboxylate BODIPY **47** and 18 more for ligand **46**. Each ligand was tested in a solution of 9:1 ethylene glycol to DMF set at 150°C, this chosen due to the high solubility of ethylene glycol towards more insoluble organic materials generally, along with the high boiling point which allows for sealing of the reaction vials without excessive risk of pressure build up and explosion. More reactions were tried once again utilising DMF as the sole solvent and base, but also at the higher 150°C temperature, with the theory that higher temperatures do increase the solubility of compounds and thus may make the insoluble product materials, soluble for longer, and allow them to slowly crystallise instead of crashing out.

Given the use of ethanol also in the formation of the published BODIPY MOF's, this solvent was also utilised at both 50°C and 100°C attempted both with and without any DMF, nitric acid and trialled also with low concentration sodium hydroxide added as an alternative base to DMF as well. The low temperature reactions were trialled on the principle that heat hastens the rate of reactions and thus lowering the temperature will

slow them down, again potentially giving the solids more time to crystallise rather than precipitate crudely. From comparisons of solid appearance between the first and second sets of complexation reactions, it appeared that the alternate failed to generate any compounds different to that of those already formed and isolated, with both the observed colour and solubility levels being the same.

Certain trends in the favourability of the ligands towards particular reaction conditions were evident however, despite the lack of any successful crystallization. Firstly, whilst the previous two sets of complexations produced product materials when set at the 100°C mark, none of the higher temperature reactions, set at 150°C, showed any appreciable solid formation. Solids were also only present in one of the lower 50°C reaction conditions that utilised the higher 50% ratio of DMF to ethanol [Table 1.], but solids were present in all of the 100°C ethanol based reactions tried. This strongly suggesting a preference toward 100°C reaction temperatures, with higher temperatures potentially creating thermal break down of the BODIPY ligands, and lower temperatures requiring a significantly larger base presence in the form of the DMF preferably, with this excess likely necessary to promote the deprotonation when thermal catalysis is absent.

None of the conditions tried with complete absence of DMF showed any appreciable solid formation either, with even the catalytic volumes of DMF being enough to result in some precipitate evident. Along with this, the ligands tended to show no preference for either metal salt, with each giving rise to seemingly equivalent volumes of product materials, nevertheless with slightly different colourations evident, as would be expected. They were also unaffected by the presence of the nitric acid, with reactions both with and without any acid presence, both giving rise to solids. Similarly the duration left heated appeared irrelevant to complexation, with no observed changes occurring in any reactions past the 36 hour point, despite being left for double that time.

Thus despite the lack of definitive results from these complex reaction trials, and the inability to form any identifiable MOF's, there is an expanse of useful data that can be pulled from these attempts. Simultaneously there is evidence from these reactions, given the immediate formation of some highly insoluble compounds, that there have been multiple polymeric structures formed. It is just too hard to definitively say what they

may be without investing considerably more time into their analysis given their insolubility, by or managing to generate some that are in a more suitable state for analysis.

3.1.4 Metal Coordination Targeted Derivatisation of BODIPY 56

BODIPY **56** was synthesised for complexation itself, however also as a target for peripheral functionalization, as mentioned earlier in the chapter. A method frequently observed within the BODIPY literature for such peripheral substitutions, is that of β -formylation via a Vilsmeier-Haack reaction. This method is versatile, particularly for BODIPY derivatives, and there have been examples of both di and mono-formylated derivatives synthesised.¹²⁰⁻¹²² Furthermore the resultant aldehyde functionality can be reacted to form a variety of different functional groups.¹²⁰⁻¹²²

The method uses the highly reactive phosphoryl chloride, along with DMF, with the solvent being that of ethylene dichloride (EDC). Careful control of the temperature is important during the initial steps of the reaction, as the combination of DMF and phosphoryl chloride can generate a significant volume of gas. To begin with, the reaction must be maintained below 10°C for the first five minutes, then given another 30 minutes at room temperature to finish the activation step, prior to any further reagent addition. After this, a solution of BODIPY **56** dissolved in EDC, is added and the reaction mixture is heated to a moderate temperature around 50°C for a period of two hours.

Other than the small difficulty of having three different temperatures to regulate during the reaction, this method readily gave rise to the mono-formylated BODIPY **57**, as seen in Figure 3.2. The highly characteristic aldehyde proton peak was witnessed on the ¹H NMR spectra at 10 ppm as expected through comparison to NMR data obtained from similarly formyl substituted derivatives published within the literature.¹²² BODIPY **57** is the first novel compound to be synthesised during the project, with no previous reports of this specific formylated BODIPY derivative published in any of the recognised chemistry databases. Given the unprecedented nature of the compound, it was fully characterised via ¹H-NMR, ¹³C-NMR, UV Vis spectroscopy, IR spectroscopy, melting

point and mass spectrometry. Crystals of **57** were obtained through slow evaporation of the crude reaction mixture from DMF, post-work up procedure. This allowed for X-ray crystallographic analysis of the BODIPY molecule as well, with the crystal structure obtained matching BODIPY **57** to an R factor value of 0.041, with the structure obtained shown in Figure 3.2.

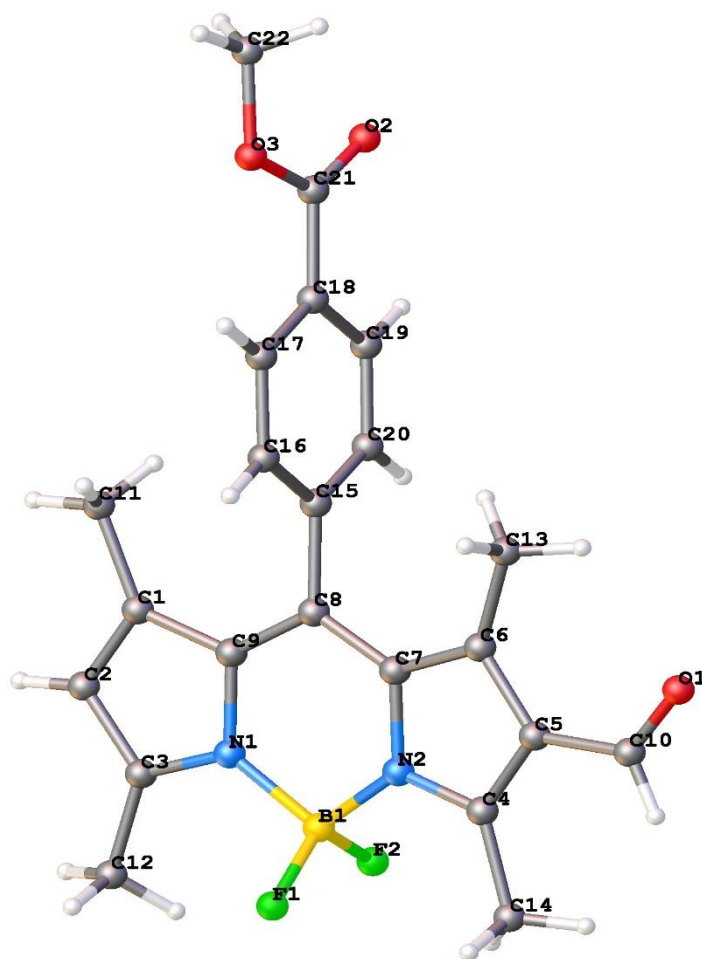


Figure 3.2. View of BODIPY **57**, highlighting the perpendicular alignment of the *meso*-phenyl group. *Note: Hydrogen atoms are included, but numbering is assigned only for Carbon and Oxygen atoms for maximum structural clarity.*

The crystal structure of **57** was very typical of BODIPY dyes [Figure 3.2]. The unit cell contained two molecules of **57**, slightly off-set in a head-head fashion with the ester functionalities pointing towards one another. A $92.53(1)^\circ$ torsion angle ($C_8-C_9-C_{15}-C_{20}$)

of the phenyl ring, created a conformational locking effect in regards to the position of the ester group relative to the plane of the core framework. The ester group lying only slightly out of the plane of the phenyl ring with only a $6.02(1)^\circ$ rotation, relative to the $C_{21}-O_3$ double bond, with the phenyl group positioned perpendicular to the rest of the structure. The newly introduced aldehyde functionality at C_{10} , lies in the plane of core aromatic system however, with only $0.47(1)^\circ$ of torsion ($C_6-C_5-C_{10}-O_1$). Bond angles were very routine throughout the framework, with the carbon-carbon bonds within pyrrole rings all displaying similar bond lengths around 1.40 \AA , consistent with an aromatic system. The same was observed for the phenyl group carbon-carbon bonds with the lowest bond length being $1.385(2) \text{ \AA}$ ($C_{15}-C_{20}$) and the highest $1.40(2) \text{ \AA}$ ($C_{16}-C_{17}$). Boron to nitrogen bonds were typical at $1.548(2) \text{ \AA}$ (B_1-N_1) compared to literature values of other BODIPY derivatives,⁴²⁻⁴³ as were all carbon-carbon bonds of methyl substituents. The bond length of the C_8-C_{15} bond was much longer at $1.49(2) \text{ \AA}$ in line with the phenyl ring rotation, supporting a loss of conjugation and aromaticity through the perpendicular nature of the phenyl ring, relative to the BODIPY core.

Given the previous reactions that have been carried out within the project and the experience gained around both dippyromethane and carboxylic acid formation, these two functionality's were considered to be the suitable candidates for formation at the periphery of **57**, from reaction of the aldehyde. It has been well known for many years that aldehyde groups can be further oxidised, and will readily form their respective carboxylic acid derivatives under the right conditions, these oxidation processes forming the basis of the now renowned and the often taught 'Silver Mirror Test' wherein they react with Tollens reagent.¹²³⁻¹²⁴ Given the well documented chemistry of aldehyde oxidations,¹²⁵⁻¹²⁶ it was hypothesised that the aldehyde group formed via the formylation at the 2-position, should similarly undergo an oxidation to the corresponding carboxylic acid.

The hypothesised reaction conditions indicated for the formation of derivative **58** are seen in Figure 3.3, as most likely the dichromate or permanganate ions, which are both popular aldehyde oxidants. These ions coupled with an organic solvent, in this case listed as DCM, due to its affinity for most BODIPY dyes. Given the strong oxidants present for such reactions, it was also theorised that the oxidation may act to simultaneously convert the phenyl ester to the carboxylic acid also. This however is not

a requirement as the ester can just be hydrolysed using the previously described methods utilised for BODIPY's **52** and **56**, however it occurred that the ester may simply be hydrolysed in a side reaction.

Unfortunately only one attempt at oxidising **57** to form **58** was possible due to time constraints, and this was unsuccessful, with no oxidation observed for the aldehyde functionality and no any ester hydrolysis evident. This attempt used KMnO_4 as the oxidant, with a small amount of base present in the form of sodium hydroxide. The likely reason the reaction didn't go to completion is the large amount of steric crowding around this peripheral position, due to the adjacent methyl groups on either side. Possibly an alternative oxidant would be more able to gain access to the carbon centre and thus catalyse the oxidation process.

Given the large number of dipyrromethane syntheses already carried out in the project, the method of synthesis for BODIPY **48a**. Two equivalents of 2,4-dimethylpyrrole were added to a solution of **56** in dichloromethane and a catalytic amount of several drops of TFA were added. Within 30 minutes TLC analysis of the reaction mixture showed the loss of all starting material and the development of two new fluorescent compounds.

$^1\text{H-NMR}$ of the post-work up reaction mixture indicated a series of peaks corresponding to those expected for the targeted compound, both in terms of integration and chemical shift. Strangely however there was a large pyrrole-based impurity evident within the NMR spectra also, with the peaks indicative of the methyl substituents on that of 2,4-dimethyl pyrrole, however lacking the associated aromatic hydrogen peaks. Along with this the aromatic peaks of the expected derivative demonstrated excessive integration values and some showed splitting, too distant to be associated to the same molecule. This lead to a hypothesis in line with the TLC analysis, that two different products had resulted from the peripheral dipyrromethane synthesis, these being the 2-monopyrrolyl adduct **48b** and the 2-or dipyrromethane adduct **48a**. This hypothesis was confirmed by mass spectrometry, with the resultant spectra clearly indicating distinct compound peaks, matching the calculated masses for both the monopyrrolyl and dipyrrolyl substituted derivatives.

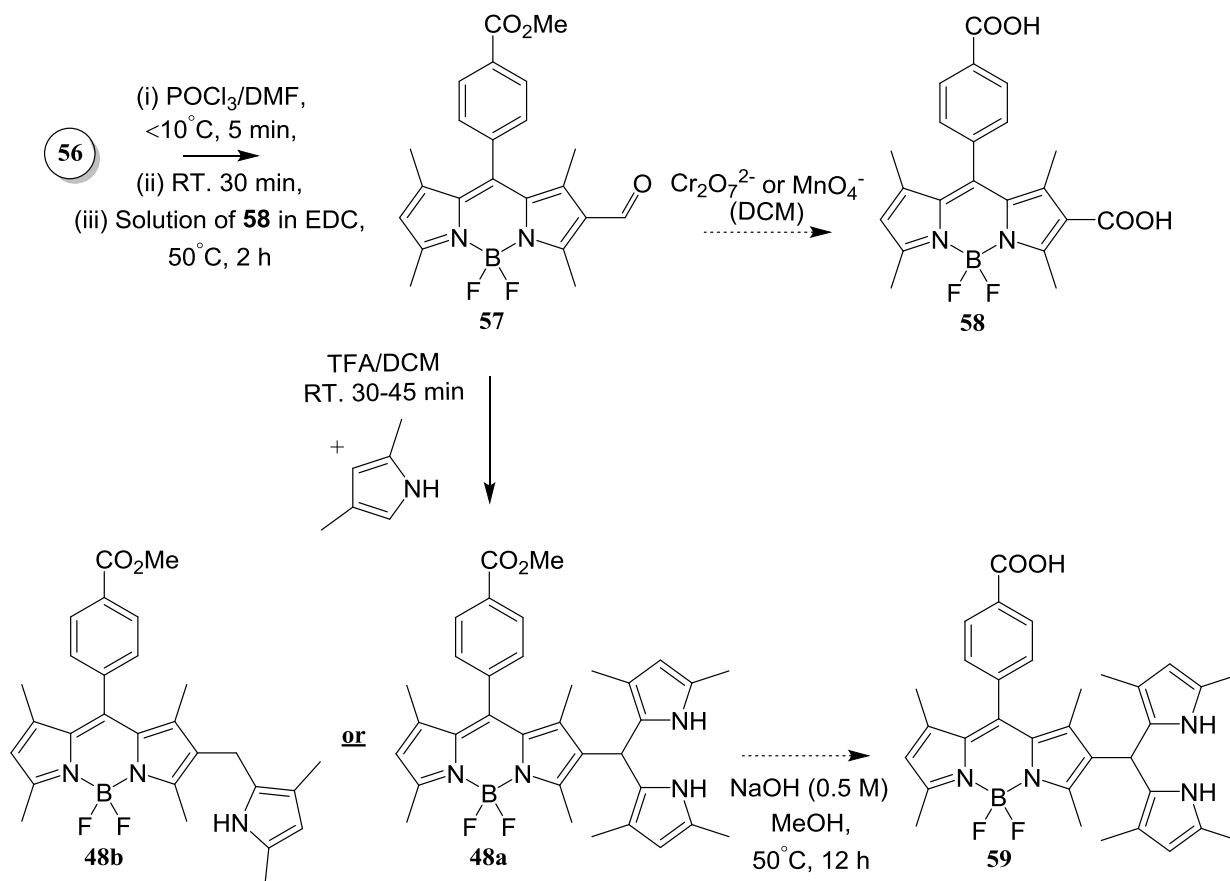


Figure 3.3. BODIPY derivatives of **56**, proposed synthesis shown, targeting peripheral functionalization via β -formylation.

Potentially due to the interactions between silica and the pyrrole units on **48a** and **48b**, there was significant difficulty in isolating a pure sample via column chromatography. Using a solvent system of 3:1 DCM to Pet. Ether, BODIPY **48a** ran with a retention factor of 0.83 under TLC analysis, as opposed to the elucidated impurity which ran with a retardation factor of 0.15, with minimal smearing evident for either spot. Despite the massive difference in retention factors and the observed clear separation however, **48b** still baselined through the entire column carried out in the same solvent system. Thus creating the hypothesis of an interaction between the pyrrole groups, particularly the hydrogen and nitrogen atoms becoming involved in hydrogen bonding. This is a not unheard of phenomenon within chromatographic analysis and is often avoided through the addition of a small volume of weak a base such as triethylamine, which acts to deprotonate the pyrrole moieties and thus remove the possibility for any interaction.

Due to time constraints however, BODIPY **48a** was unable to be isolated from the monopyrrolyl impurity however, limiting the ability to fully characterise it as a novel synthetic compound, with only the ^1H -NMR and mass spectrometry data gathered of the impure crude sample, and also limiting the ability to synthesise **59** as seen in Figure 3.3, through hydrolysis of the phenyl ester functionality to create another potential ligand for MOF incorporation.

3.1.5 Metal Complexation of BODIPY 48

Despite the inability to isolate a pure fraction of molecule **48a**, with the goal of identifying its metal coordinating ability, it was reacted in its crude form with the impurity **48b** still present. This was hypothesised on minimal synthetic concern for formation of any complexes however, as the monopyrrolyl derivative would not coordinate the metal centres in a mono-dentate mode with only the one pyrrole group available, thus **48a** would still have preferential reactivity given its bidentate coordinative dipyrromethane group. The real inconvenience of having the impurity present comes when calculating molecular ratios for the reactions, as the percentage of impurity can only be roughly estimated based on integration of the ^1H -NMR spectra for the crude material, with the mass spectrometry spectra being unreliable for analysis in this way as different compounds fly within the mass spectrometer at different efficiency's, thus a compound shown to be in high abundance within the sample may just ionise and move within the mass spectrometer much better than any other samples, but actually be in a lower quantity. This inaccurate measure of the relative mass percentage for **48a** relative to **48b**, means that it is impossible to accurately measure the required masses of reagents needed for the complexations.

However, several complexation reactions were attempted using the crude sample of **48**, the first of these was the attempted reaction with the dihydro ruthenium dichloride diphenanthroline complex ($[\text{RuCl}_2(\text{Phen})_2] \cdot 2\text{H}_2\text{O}$) to form molecule **60**. Two methods were considered for this reaction, the first being a slower more gentle method, utilising a combination of base and ethanol as the reaction system and requiring refluxing for a minimum of six hours.^[100] This method and similar methods, are witnessed within the literature commonly for ruthenium reactions, with the relatively long reaction time a

result of the general stability of ruthenium complexes and the difficulty of displacing ligands compared to many other transition metals. The other primary method is a much more aggressive approach using a microwave reaction method and several two minute cycles of extreme thermal and atmospheric pressures, through 500 W microwave irradiation. This method the result of work carried out by a doctoral student within the group, for ruthenium complexation to N-heterocyclic carbene's containing compounds.

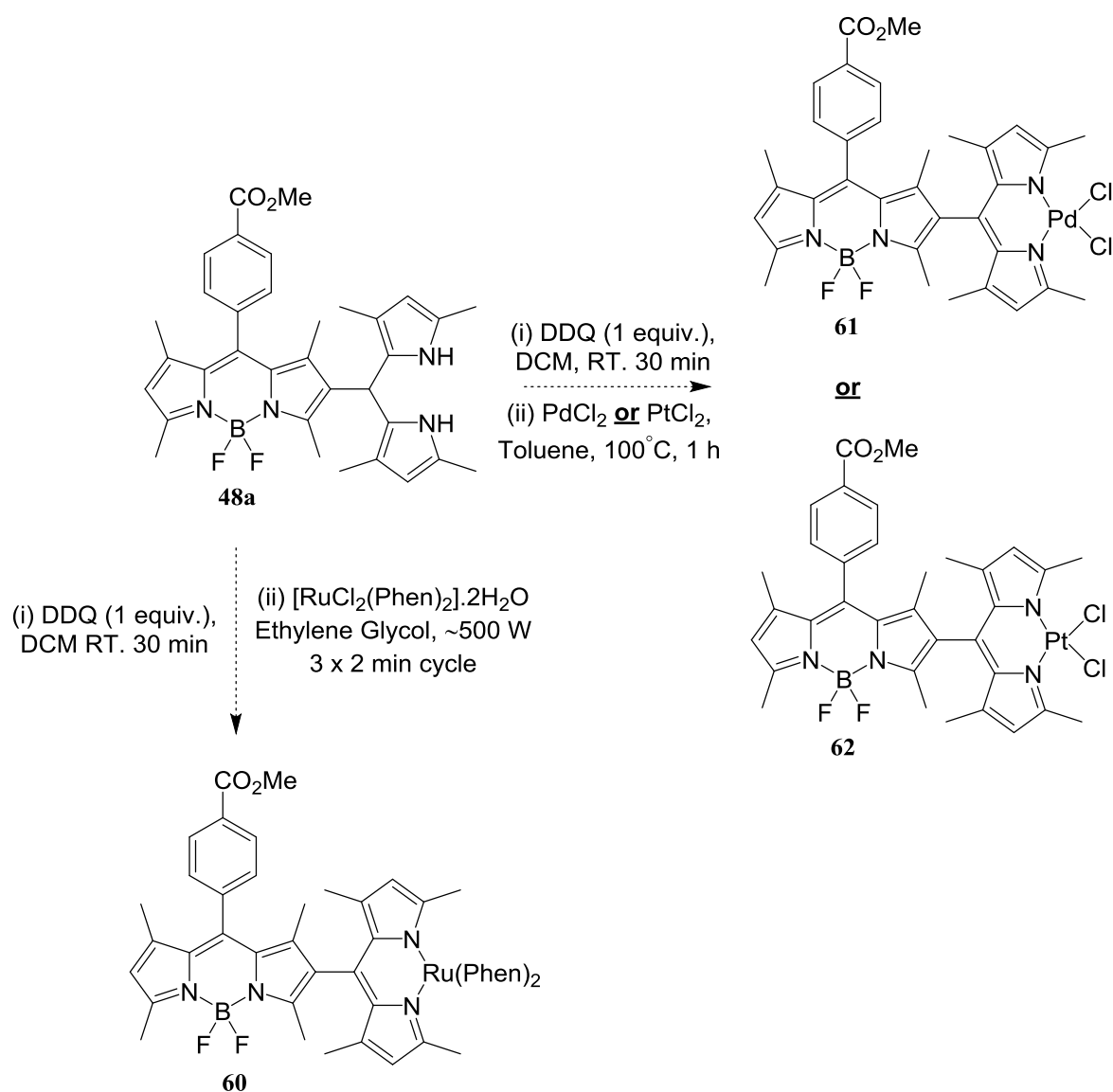


Figure 3.4. Targeted metal complexes of BODIPY **48**, with both platinum and palladium.

Both described methods are effective in different situations and were generally considered based on the expected or known stability, of both the targeted complex and the starting material itself. Obviously the gentler reflux conditions are preferred for compounds and products with expected instability's. With the known high thermal stability of most BODIPY molecules and their consequently robust nature, being a strong selling point for their fluorophore potential, the more aggressive irradiation approach was chosen. There was clear potential for an indication to be gained of its likely success within the approximate ten minute reaction timeframe and thus the gentler alternative method could be adapted if need be. Difficulties arose initially, around getting BODIPY **48a** solubilized in the ethylene glycol used as the reaction solvent, even after the first irradiation cycle at 500 W and the subsequent drastic increase in temperature associated, the reaction solution still visibly showed some insoluble material evident.

Given that the reaction was already started before it could be confirmed that even the temperature increase was going to fully solubilize the reagents, the reaction was carried out to completion anyway. TLC was attempted but was ultimately inviable due to the insolubility issue and a preliminary test of the solution mixture post-work up via the addition of potassium hexafluorophosphate, gave no rise to any precipitated complexes as would be expected, especially after H₂O was subsequently added to lower the solubility and force precipitation.

Follow-up ¹H-NMR of the crude materials also gave rise to no evidence of product formation, as well as no evidence of any peaks indicative of any BODIPY molecules present. This suggesting that the most likely the intense temperature increase created via irradiation in the microwave, caused a degradation of the starting materials. It could have been that the product was formed and broken down as well, however given that it is a ruthenium metal complex it would likely be far more stable than the starting material, and given the insolubility issue it is much more likely the reaction never occurred and that the starting material was simply thermally destroyed. What may have also complicated the reaction and helped to limit its success is the need for oxidation of the dipyrromethane framework prior to the addition of any metals or complexation

reagents. This oxidation uses *p*-chloranil to conjugate the full dipyrromethane framework, the same as for general BODIPY synthesis, however as the *p*-chloranil is not removed again from the system prior to complexation, it introduces another redox couple which undoubtedly would quench the reactions efficiency. Given more time the dipyrin would be synthesised first and isolated briefly before complexation was attempted. Given the lack of either product or reagents observed under NMR analysis post-reaction, it suggests that the thermal environment of the microwave may be too extreme and thus a more careful reflux approach may be the way forward for synthesis of BODIPY **60**.

Ruthenium generally forms extremely stable hexa-coordinate complexes. Given the high stability of these complexes, both ligand exchange and general reaction of these complexes requires significant energy input into the system, or a specific catalytic environment.¹²⁷ BODIPY complexes **61** and **62** are essentially the palladium and platinum equivalents of **60**, and were considered as two alternatives that could also be synthesised, potentially with greater ease than the ruthenium based complex. The relative reactivity rates for palladium(II) as opposed to any of the potential oxidation states for ruthenium is massive, with magnitudes of difference greater than 10^3 .¹²⁷ Along with this, both the dichloride complexes of palladium and platinum alike require minimal activation to ligand exchange compared to similar ruthenium complexes, largely as a result of the inherent lower stability of resultant complexes. Given that both platinum and palladium preferentially form four or five coordinate metal complexes also, most often the former, they offer a different angle of coordination chemistry to BODIPY **48a** also, likely a much less complicated angle. Given that the complexes proposed in Figure 3.4 are the most likely frameworks to result from reactions with the dichloride salts, the resultant analysis should be much simpler when compared to BODIPY **60**, with the phenathroline group in this structure likely to cause significant analytical issue, particularly in the NMR spectra and potentially with solubility during any physical manipulations in lab.

The synthesis of **61** and **62** proceeded using the same oxidation conditions utilised for **60** and the majority of BODIPY's synthesised up to this point within the project, with **48a** combined with one equivalent of *p*-chloranil in dichloromethane and then left stirring for approximately thirty minutes. The crude dry product mixture was then

subjected to the method of Ravikanth and co-workers, who synthesised a series of similar complexes using 3-pyrrolyl BODIPY dipyrin substituted frameworks.¹⁰¹ This method was chosen based on the similarities between the complexes formed within the paper, based around ruthenium, palladium and rhenium, to those targeted within Figure 3.4, and also due to structural similarities of the two starting materials also. Given the total reaction time of only 1.5 hours including oxidation, it also allowed for a quick indication of how **48a** may behave under such conditions and the general direction that further reactions may need to proceed. The initial attempts at synthesising the dichloride complexes **61** and **62** were unsuccessful though, however evidently due to very different reasons than those likely for BODIPY **60** [Fig. 3.4].

TLC analysis of the reaction solutions after the one hour reflux period showed some product development with a clear orange colour generated within the solution as opposed to the original purple, however starting material was still evident thus the reflux was left for a further one hour to complete the reaction. At this time the solution still indicated starting material but due to the abundance of time reacting as opposed to the literature, this could have been simply as a result of the consumption of the metal species, through a combination of quenching and actual reaction. Thus the reaction was ceased and the product mixture worked-up. This gave rise to a crude mixture which under ¹H-NMR and mass spectrometry analysis, only showed the presence of a small volume of starting material and no other BODIPY representative peaks. This despite the generation of an orange coloured species in each solution, evident through TLC. Due to a lack of time this suspected impurity was not characterised, as it could not be isolated from the crude mixture readily, however it was hypothesised that it could simply be an adduct of one of the three redox couples present within the reaction mixture, most likely the *p*-chloranil. Within the reactions is also contained the redox couples of both platinum and palladium metals respectively and also the ligand itself BODIPY **48a** and its dipyrin alternative, and these have potential to have resulted in some sort of slightly fluorescent adduct, especially given the powerful photophysical properties of BODIPY, particularly its generally associated high quantum yields and extinction coefficients, it could potentially only take a small amount of an undesired adduct to create a significant TLC observed species, that may not easily show up under NMR or fly in the mass spectrometer.

3.2 Synthesis of 2,4-Dimethylpyrrole

The synthesis of particularly BODIPY's **52** and **56** had to be repeated in order to isolate a volume of the two compounds that was suitable for setting up a series of MOF-reactions at the same time. This generated the issue of a 2,4-dimethylpyrrole shortage, due to the limited ability to purchase this compound in large quantities, largely as a result of its multiple step synthesis, which acts to raise the price significantly. Given the low yielding nature of BODIPY syntheses, BODIPY's **52** and **56** included, the scale of these reactions had to be raised upon repeats as well in order to get any appreciable quantities. When BODIPY syntheses are carried out simultaneously, 5 mL of 2,4-dimethylpyrrole could easily be used, a very large volume to consume monetarily for only one set of syntheses. Adapting on an improved two-step synthetic method for formation of the pyrrole derivative, as shown in Figure 3.5, a 15 mL volume of 2,4-dimethylpyrrole – **64**, was readily synthesised.

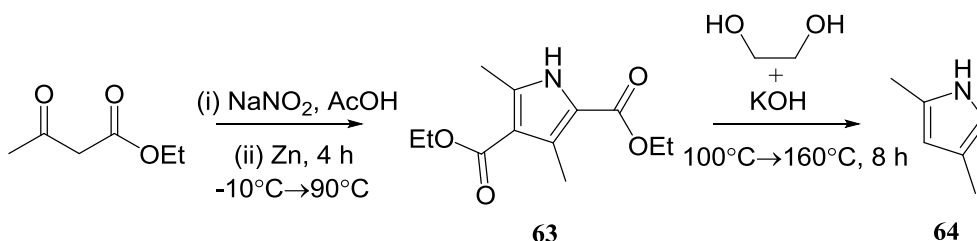


Figure 3.5. Reagents and method for two-step synthesis of 2,4-dimethylpyrrole (**64**).

Formation of the 3,5-diethyl ester precursor, molecule **63**, was very straightforward, with no purification necessary, isolated from a simple post work-up vacuum filtration and used immediately for the subsequent formation of **64**. The only difficulty was evident during the second stage of the synthesis. The use of water as the solvent when heating the reaction to the 160°C temperature proved unsuccessful. This temperature was quoted as a requirement for thermal activation of the ester group removal.¹²⁸ The hydrolysis easily occurring at lower temperatures in the presence of excess potassium hydroxide, but considerable heat required to promote the stripping of the two-functional groups from the molecule completely. Given the boiling point of water at 100°C, the

reaction never appeared to get to the required thermal barrier to result in activation of this step, until the water was substituted for ethylene glycol. This allowed for temperatures up to around 180°C and resulted in the formation of large volumes of **64** as previously stated. The desired pyrrole derivative was then isolated in pure form, through a vigorous ether extraction. The isolated 15 mL quantity was all that was required for the remainder of the project, with this being more than enough to generate gram scale quantities of both BODIPY's **52** and **56**.

Chapter Four

Dual Core BODIPY Derivatives

4.1 Dual Core BODIPY Derivatives

Development of dual core BODIPY-type derivatives were a target for this research project due to their unprecedented and interesting approach to utilising the unique properties of the BODIPY structure. The research carried out by Ziegler and co-workers to synthesise the dual core BOPHY molecule **27** [Fig. 4.1], was the inspiration for this avenue of research.⁹⁵ This BODIPY type compound exhibits particularly high quantum yields and Stoke's shifts, coupled with evidence of electronic communication between the two cores.⁹⁵ These properties, particularly the core communication, are highly desirable within the BODIPY research community as they are not a common discovery. In particular, the effects that creating such dual core molecules like **27**, is yet to be fully understood and in particular, the influence they will have on the optical properties of fluorescent compounds is still relatively unknown [Fig. 4.1].

Given the success that Ziegler et al. had in developing a dual core derivative, as opposed to a dimeric structure, some new BODIPY type structures were theorised and several synthetic methods were attempted to form similar compounds to **27**.⁹⁵ These syntheses utilise heterocyclic compounds and the standard reaction conditions for BF₂ core installation, as opposed to an intramolecular cyclisation to form the heterocyclic system used for the BOPHY system, which could be considered far more unreliable and intensive chemistry.

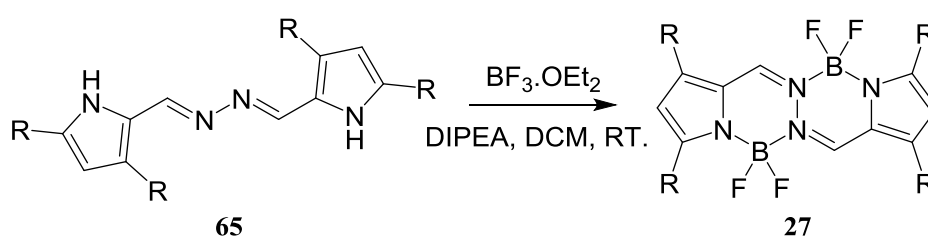


Figure 4.1. Reaction Process for Formation of BOPHY

4.2 Background to the Targeted Dual Core Functionalisation

The particular requirements for the formation of a BODIPY core is not well understood within the literature. During the early development of the BODIPY structure, shortly

after its conception, it was presumed that both the boron atom and the substituted fluorine atoms were needed to create the particular optical properties of the core. This was proven incorrect after the fluorine atoms were substituted out of the fully formed BODIPY structure and replaced with a variety of different groups, from conjugation extending functionality, to large ion coordinating probe type structures, the range of options for boron substitution is now immense and the optical characteristics of the BODIPY core are maintained.³⁰

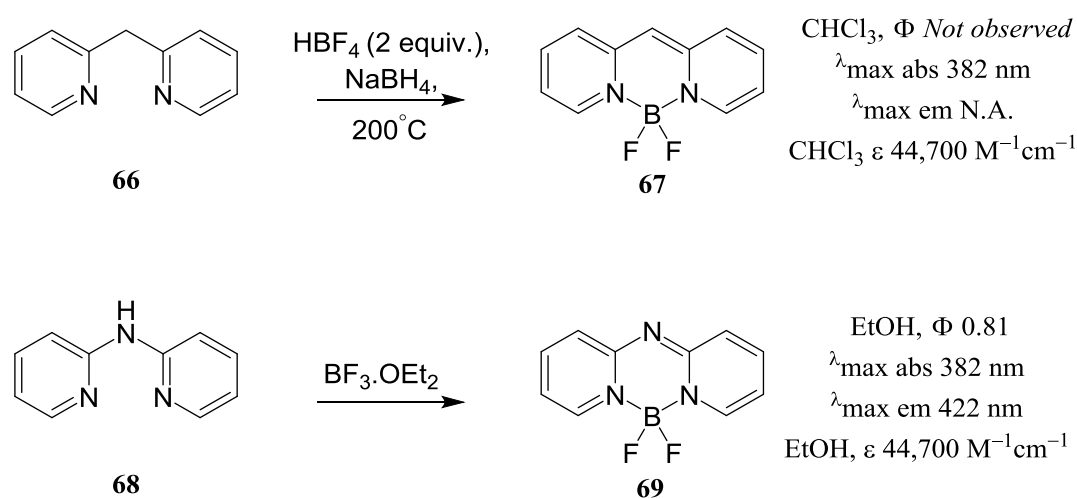


Figure 4.2. Pyridyl BODIPY (**67**), and aza-pyridyl BODIPY (**69**) molecules demonstrating their photophysical properties.

The need for a very specific level of core conjugation and aromaticity is however evident. Figure 4.2 highlights this effect very clearly, with the pyridyl based framework **67**, exhibiting no radiative emission and hence no distinguishable fluorescence quantum yield.¹²⁹ The aza-derivative **69**, is highly fluorescent however, with an intense blue shift compared to BODIPY itself, of over 100 nm for absorption spectra and 90 nm in the emission spectra in comparison to **67** [Fig. 4.2].¹²⁹ Given that the sole difference between these two systems is the absence or presence of a nitrogen atom in place of the *meso* carbon centre, these observed optical properties must be closely related to the electronic state of the core. Likely the lone pair of electrons on the nitrogen atom present in the aza-derivative, play a large role in the electronic state of **69** and help

bolster its optical properties. With molecule **69**, clearly the superior photophysically active derivative, and a good example of the fluorescence potential pyridyl rings can have in BODIPY type structures.

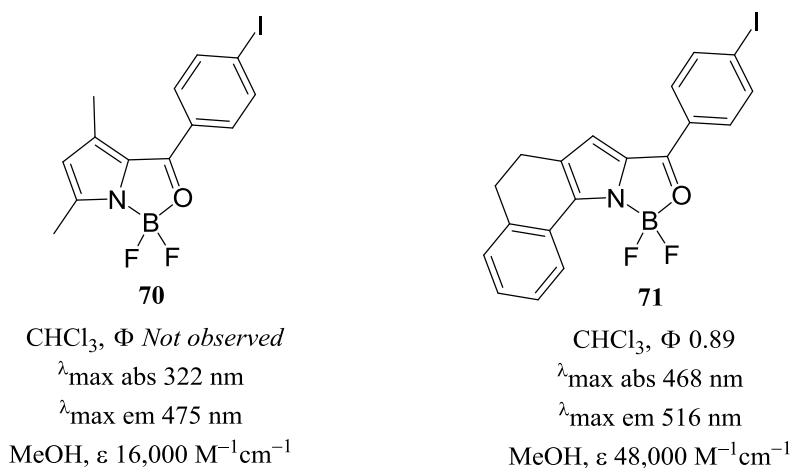


Figure 4.3. Two similar BF₂ core substituted derivatives and their highly different optical properties.

Both **70** and **71** shown in Figure 4.3, are designed with a BF₂ core moiety and have similar structures to each other, but no obvious resemblance to the classical dipyrromethane framework of BODIPY dyes. They both demonstrate the versatility of BF₂ installation, given their difference from the known BODIPY structure, with the core functionality clearly capable of being synthesised into a large variety of heterocyclic systems if the correct method is identified. When comparing their relative optical properties, they also make apparent just how important it is for the BF₂ moiety to be incorporated into a π -system with considerable core conjugation, irrelevant of the level of aromaticity. This is evident from the complete lack of fluorescence observable for **70** as opposed to **71** which has an extremely high quantum yield of 0.89. It is ring annulated to a cyclohexane ring which continues conjugation to a phenyl group, however does not create a system of three, linked, fully aromatic rings, like is the case with anthracene or phenanthrene. Anthracene in particular from these two, being a highly fluorescent simple carbon polycycle, which is largely attributed to its fully conjugated, aromatic framework. In the case of **71** however, despite the absence of such

a framework, it exhibits the same levels of intense fluorescence. It also has a relatively large extinction coefficient at $48,000\text{ M}^{-1}\text{cm}^{-1}$ and the standard BODIPY spectra around 500 nm, with a small Stokes shift, as opposed to its methylated counterpart **70**, which is blue shifted significantly to an absorption of 322 nm and a corresponding Stokes shift of 153 nm. This suggests a minimum level of conjugation is required to observe fluorescence at all with such BODIPY themed molecules, but that the particular bonds in which the BF_2 group itself are linked in, are of little concern, particularly given its position, bonded to an oxygen atom in **70** and **71**.

Ascertained across all four molecules within Figures 4.2 and 4.3, is that the specific dipyrromethane framework is not necessary in order to generate fluorophores, using this core moiety and with careful selection of the level of electron density and conjugation present within the π -systems of such frameworks, there is potential for very intense optical properties to result. Such observations, coupled with the promising photophysical properties of **27**, generates interest in terms of developing BODIPY themed structures that utilise the BF_2 core, as a means of creating fluorescence within organic frameworks. If ‘installed’ using the correct chemical synthesis, the potential should be there for multiple of these BF_2 cores to be ‘installed’ into several appropriate sites within the same molecule. Currently it is unknown if such structures would exhibit cumulative photophysical enhancement from two cores, or if they would simply exist separately. These structures branching away from the commonly observed dimeric BODIPY’s, with two separate core containing molecules, simply linked by a single bond, to a scheme involving the formation of dual core molecules, with two cores installed within a singular framework.

4.3 Proposed Dual Core BODIPY Systems

With the aim of creating dual core BODIPY-type derivatives, the ideal structures for BF_2 installation were theorised. Compound **72**, shown in Figure 4.4, was the first molecule chosen for dual core functionalization. The dihydro tetrazine group at the centre of the structure, has an abundance of nitrogen atoms, which in combination with nitrogen atoms of the pyridyl ring substituents, create two sites at either end of the tri-heterocyclic system that are viable for bonding the boron atom. This dipyridyl

substituted dihydro tetrazine, is very easily synthesised in a one pot reaction using hydrazine hydrate and 2-cyano pyridine with catalytic sulphur.¹³⁰ In installing the BF₂ moiety within **72**, the resultant structure will be that of **73**, wherein the protons on the central tetrazine ring are lost and the structure formed maintains an overall neutral charge.

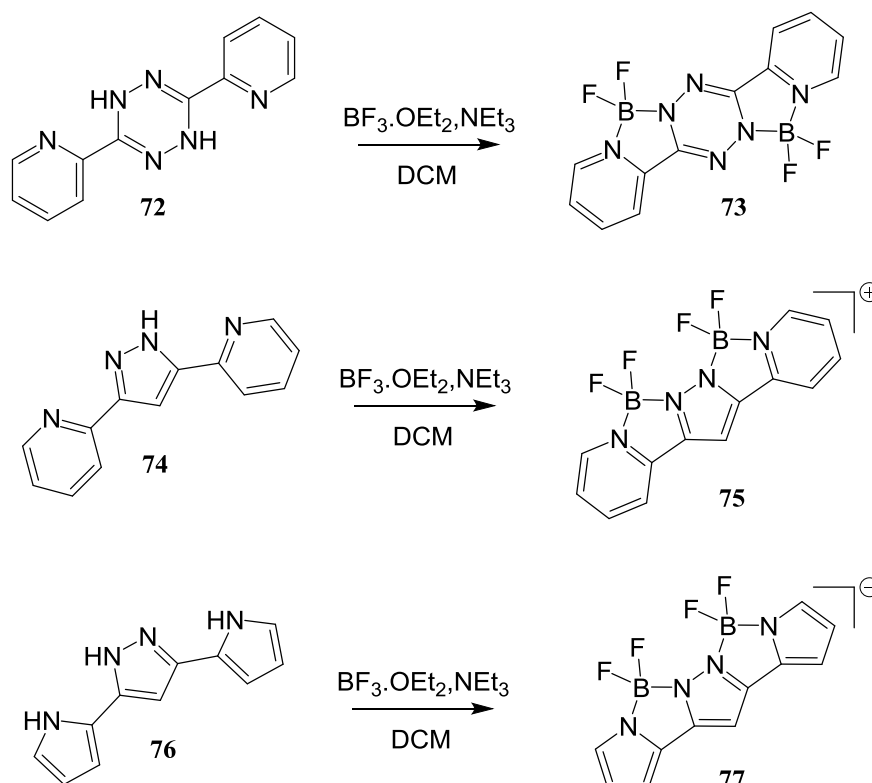


Figure 4.4. The three targeted dual core BODIPY-type systems and their precursor molecules.
*Note: Molecules **74** and **76**, were not synthesised, but are utilised from previous research within the group.*

Both the formation of a positively charged structure and the fact that the tetrazine ring is prone to chemical degradation through hydrolysing of the nitrogen-nitrogen bonds, means that formation of **73** is likely not synthetically straight forward if viable at all. Such perceived difficulties were encountered during the attempted synthesis. Using the reagents stated in Figure 4.4, core installation was attempted under the same reaction

conditions as for general BODIPY synthesis. Molecule **73** was not detected within the product material however, ^1H -NMR analysis showing no evidence of any peaks corresponding to the tetrazine starting material or any BF_2 core containing compounds. Given the absence of any starting material within the crude product mixture, it was theorized that the most likely reason for no product detection was because of the tetrazine ring breakdown, rather than unstable product formation, as an unstable product would most likely just result in BF_2 core loss and reformation of the solvolysis products.

The pyrazole centred dipyrindyl precursor **74**, also shown in Figure 4.4, was chosen as a starting material with dual core potential similar to that of **72**, but it was selected to combat the hypothesised instability problem of the tetrazine breakdown during the synthesis of **73**. Whilst not susceptible to the same ring breakdown issues as **73**, compound **75** has a different instability, due to the fact the one of the nitrogen atoms on the pyrazole ring is double bonded and thus creates a 1^+ positively charged structure wherein one BF_2 centre carries a 1^+ charge, whilst the other centre is neutral. Given the presence of charge on this framework as opposed to **73**, there will be an associated reactivity and thus a complicating element in its successful synthesis also. Precursor molecule **76** was readily available from previous research carried out within the group [Fig. 4.4], and was chosen to combat the issues associated with precursor **72** primarily as well. It contains a central pyrazole unit with peripheral pyrrole groups as opposed to the pyridine rings of **72** or **74**. The pyrazole centre circumvents the tetrazine instability once more, whilst the replacement of the peripheral pyridine groups with pyrrole units creates an overall 1^- charge on proposed product **77**, opposed to the 1^+ charge of **75** [Fig. 4.4]. It also means that there are two protonated nitrogen atoms free for boron binding, thus meaning that the resulting molecule **77**, is would only bear a 1^+ overall charge.

The attempted synthesis of dual core derivative **77** was carried out using the same method as for the previously attempted frameworks, with a maximally inert reaction environment maintained and the same reagents utilised. Given the theorised greater stability of the product and the starting material compared to the previous frameworks attempted, the exact reason behind the unsuccessful synthesis of **77** is unclear, with no product peaks observed once more in NMR or mass spectrometry analysis of potential corresponding molecular weights. Given that these reactions were trialled as the very

first avenue of the project and all attempts at synthesising even one core into the chosen frameworks were thus far unsuccessful, dual core synthesis was put on hold to identify the most likely issues and begin researching the other synthetic routes targeted in the project, primarily those of Scheme 1 and Scheme 2, as seen earlier in the chapter.

4.4 Trialling the BF₂ Core

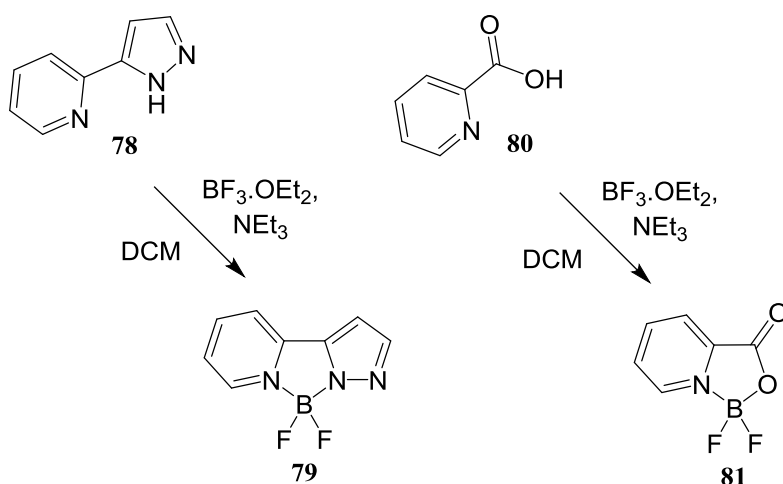


Figure 4.5. Two frameworks trialled for BF₂ core installation.

In an effort to elucidate where the exact issues were arising with the synthesis of the desired dual core frameworks and to simultaneously grasp the effect that BF₂ core formation may have on organic molecules in terms of their analytical spectra in particular, compounds **79** and **81** were targeted for synthesis. These two derivatives contain only one BF₂ core, with molecule **79** designed around the monopyridyl pyrazole framework and the other, utilising a Picolinic acid molecule as the skeleton for BF₂ installation. Given the presence of only one BF₂ group in each molecule and the smaller, less susceptible and more stable nature of these structures, the syntheses once again utilising the same reaction conditions, were thought to be more favourable. If synthesised, both **79** and **81** can act as model compounds for NMR analysis of any derivatives with a BF₂ group present, including dual core derivatives. This would also help elucidate other optical and physical properties of the BF₂ functionality, which could be invaluable for successfully forming, stabilising and ultimately characterising

the desired dual core derivatives. Unfortunately as per the previously attempted synthesis for the dual core derivatives, no product formation was ascertained through ^1H -NMR analysis and any presence of starting material was not detected.

Potentially the reason for no starting material detection is as a result of the large volume of impurities generated during BODIPY synthesis. Wagner and Lyndsay describe a very large volume of black sludge generated in their BODIPY syntheses published in 1996.¹³¹ Similarly during the synthesis of BODIPY **5** during this project, there was over 50g of crude product isolated from a 10g scale reaction, which presented initially in the form a viscous black sludge. This sludge is likely a result of the large excess volumes of triethylamine and the highly reactive BF_3 -etherate that are used installation of the BF_2 functionality. In tandem with this however, given the highly reactive nature of the Lewis acidic BF_3 -etherate and the excess it is in in these reactions, it may be that the starting material is being broken down by this species. Despite the issue of not detecting any starting material, the attempted syntheses, as per Figure 4.5 and Figure 4.4, have not generated any product formation either. With more time, repeat attempts given the insight now acquired into BODIPY chemistry, may make these all of these dual-core type derivatives more synthetically viable.

Chapter Five

Conclusions and Future Work

5.1 Conclusions and Future Work

As discussed previously there are three primary areas that were targeted for research within project. These being the HBC-coupled derivatives discussed in Chapter Two, the metal coordinating derivatives elaborated on in Chapter Three, and the dual core derivatives, as seen in Chapter Four. Each of these separate areas of BODIPY research has led to the possibility for multiple conclusions to be drawn in regards to both the specific chemistry of their synthesis and the synthesis of BODIPY molecules as a whole. Large aspects within each of the three project areas leave considerable room for future development as well, with some areas very close to considerable breakthroughs that could be elucidate given more time.

5.2 Dual Core Derivatives

For simplicity it is best to begin with the dual core derivatives discussed in the previous chapter. All three different frameworks targeted for dual core formation were synthetically inviable. In particular, given the chemical and physical similarities of compound **76** to BODIPY precursors, it is clear that there is an inherent issue reoccurring in the formation of BF₂-cores within these molecules [Fig. 4.4]. Potentially this being a result of the method being utilised or the reagents being used, or simply that having two BF₂ groups present in the such molecules is highly unfavourable.

These issues were discussed in Chapter Four, and could be as a result as any or all of these factors. Given the attempts to create these dual core derivatives as the first compounds of the research project and the associated complexity of almost all BODIPY syntheses, it is hard to rule out the possibility that it was simply the synthetic difficulty of the reactions and a lack of knowledge and experience around the chemistry of BODIPY-type molecules, that gave rise to the observed results. Similarly though, given that the only genuinely similar dual core derivative already published in the literature is that of derivative **27** – the ‘BOPHY’ molecule, we cannot rule out issues in regards to the viability of the syntheses attempted [Fig. 4.1] . BOPHY was synthesised in a much different mode and can be considered as a system with four fused heterocyclic rings, rather than the five that are created through BODIPY core formation in the proposed

structures; **73**, **75** and **77** [Fig. 4.1] [Fig. 4.4]. It may be that such molecules are not readily formed using the simple method of saturation in BF_3 -etherate and triethylamine. The precursor molecule to BOPHY, molecule **64**, also seen within Figure 4.1, has terminal pyrrole rings at either end of the molecule, the same as for **74** and **76**, however the centre of the framework revolves around a nitrogen-nitrogen bond and thus has associated free rotation and a level of flexibility far beyond that of the tri-heterocyclic precursors of the derivatives targeted in this project [Fig. 4.1] [Fig. 4.4]. The mechanism of BOPHY formation involved somewhat of an encapsulation of the BF_2 -groups by the long precursor framework, with the structure highly invested in the groups.⁹⁵ This process was also catalysed by the presence of DIPEA rather than triethylamine, suggesting that potentially triethylamine was tried first and was not viable for the reaction, although no mention of this is made in their report.⁹⁵

Given all of the differences between both the method of formation and the actual framework structure of the derivatives targeted in this project and BOPHY itself, it could be concluded that the issue with synthesising the dual core derivatives may be that they simply aren't viable for reaction with BF_3 . When hypothesising as to why the reactions have not had any success however, there are two likely reasons evident from this project and the known chemistry of BODIPY. The first of these being that the tetrazine ring of precursor **72**, is breaking down in response to the presence of such a strong Lewis acid like BF_3 -etherate as stated earlier in Chapter Four, and thus the system is simply too unstable. Secondly, that the structures of the two other precursors, **74** and **76** [Fig. 4.4], are oppositely to **73**, actually too stable, lacking either the highly reactive dipyrin system used for traditional BODIPY syntheses, or that of the very reactive imine functionalities, present in the BOPHY precursor **65** [Fig. 4.1].

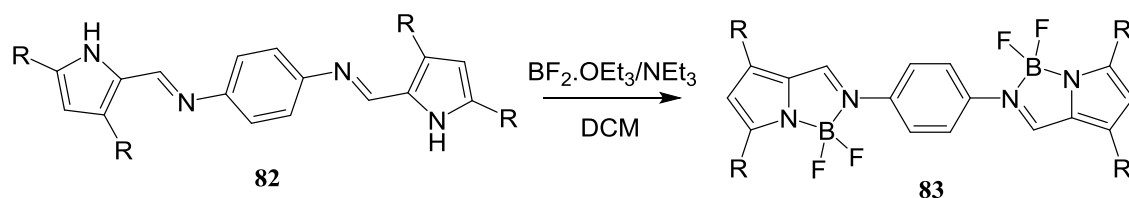


Figure 5.1. Reaction Process for formation of a derivative, crossed between BOPHY and the proposed dual core systems described in Chapter 5.

If a specific reason was to be identified, it would most likely require repeats of the three reactions and refinement of the base selection, along with a more sensitive analytical tool that can be maintained constantly throughout the reaction as opposed to TLC. For instance a real-time ^1H -NMR technique that could observe the change and/or formation of product peaks as they happen. If the syntheses were still unsuccessful as observed analytically, then their viability may be of question and confirmation of this would require the development of a structure more similar to the BOPHY molecule, such as the hypothetical structure of **82** shown in Figure 5.1. Whether or not molecule **82** would undergo reaction with BF_3 -etherate and triethylamine to form the dual core system **83**, would provide significantly more insight into the chemistry of these desired structures. Molecule **83** being somewhat of a structural compromise between the derivatives targeted in this project and the BOPHY molecule [Fig. 4.1] [Fig. 5.1].

5.3 Metal Coordinating BODIPY Derivatives

The metal coordinating derivatives made up the majority of the research focus through the second half of the project and can be considered as the area where the most success was had. Between the formation of two novel BODIPY derivatives along the way towards metal complexation in both molecules **48** and **57**, along with the formation of multiple insoluble polymers during attempted MOF synthesis, there was considerable promise shown from the chemistry undertaken during this area of the project.

5.3.1 MOF-Targeted BODIPY Ligands

From the relatively reliable synthesis of both the mono and di-ester BODIPY's, **52** and **56** [Schemes 4-5], it was evident that both the acyl chloride method of dipyrin synthesis is still effective despite its limited use in modern BODIPY synthesis, and simultaneously that the synthesis of methylated BODIPY frameworks is much more consistent than formation of the unsubstituted core system, as is described frequently within the literature.^{30-31, 35} This reliability is inferred in the way that from every repeat of these reactions, the desired BODIPY products were isolated, however with the formation of a large excess of the core absent dipyrin impurities also present, it is clear

there are still inherent issues in these syntheses. Given that the BF_3 -etherate and the triethylamine base are not the limiting reagents in this reaction, it is unlikely that there was full quenching of the approximate 40 mole excess of each and thus the reason for a large presence of the BF_2 absent dipyrins, must be attributed to the product stability rather.

As mentioned previously in Chapter Three, there is potential that rather than the BF_2 functionality not being installed in the binding site, perhaps it is actually being lost during work-up and other post-reaction procedures instead. This is problematic to determine, as analysis immediately after the reaction is quenched is limited. Only TLC gives any reliable data and even these generally only present with product spots evident amongst considerable smearing. These difficulties arising due to the large quantity of different impurities generated from the reagent excesses.

In any future work carried out on these molecules, time would clearly need to be invested into determining the exact reason for the large volume of boron free compounds isolated, as they not only do they significantly hinder the product purification process due to their similar chemical structure and properties, but it also directly restricts the potential reactions yields. Given that the synthesis of these ester derivatives **52** and **56**, could be optimized, their hydrolysis to form the carboxylic acids **46** and **47** would also require development [Schemes 4-5, Chapter. 3] [Fig. 3.1]. The current method that was utilised with limited success during the project, is both time consuming and low yielding for what should be a relatively straight forward step in the synthetic pathway. If this could be altered to a set of conditions tailored more specifically to organic molecules like BODIPY and the yields be increased, then the quantity of these BODIPY's that is required for carrying out in depth metal-coordination trials would become viable. Along with this, through the large amount of time spent attempting the purification of the BODIPY compounds in the two synthetic Schemes - 4 and 5, it is clear that there is the need for a purification method that is suited to larger scale volumes of crude material, such as the already utilised methods of recrystallization and Soxhlet extraction. This conclusion is drawn as a result of the large amount of impurities generated in the BODIPY forming reactions of these pathways and the inability to column such large amounts of crude

Despite the inherent synthetic difficulties and low yields associated with the synthesis of BODIPYs **46** and **47** [Fig. 3.1], they were still isolated in reasonable yield and metal coordination attempted. Given the large number of insoluble products formed during these attempted complexing the attempted complexations, there was clearly some sort of reaction taking place. Determining what reaction occurred would require solid state analysis, potentially infrared spectrometry and elemental analysis would help elucidate the result, but based solely on the structures of **46** and **47**, they hold potential for complexation and the insoluble products attained are a positive indication towards this. The project direction was on the right path towards identification of the suitable reaction conditions for such metal complexation, it is likely just a matter of trialling more modifications to the reaction conditions, with DMF clearly being a key component in their success and the 100°C temperature likely being where the most success will be had, given the highest percentage of insoluble polymeric species were formed there.

5.3.2 BODIPY Coordination Complexes

The generation of a MOF framework has an inherent level of serendipity and time that simply has to be invested and waited upon, however the formation of discrete metal complexes is a much more controllable process and thus the inability to isolate any from coordination with BODIPY **48** is disappointing. There are no real conclusions to be drawn from the attempts made at doing so, other than the initial reaction conditions appeared to have been unsuccessful as indicated by an absence of BODIPY characteristic peaks in NMR analysis. Thus modifications to the reaction methods will need to be made, if these compounds are to be further researched. As stated in Chapter Three earlier, the attempted synthesis at the ruthenium complex using microwave radiation is a thermally aggressive environment for the ligand to survive in, and given how reactive dipyrromethane frameworks can be potentially it caused degradation of the **48a**. The more gentle reaction conditions need to be attempted in order to determine whether or not the diphenanthroline complex [Fig. 3.3], is a viable target or if it is simply too sterically hindered, as a result of methyl substituents on the peripheral dipyrromethane moiety.

As for the two platinum and palladium complexes targeted for synthesis and also seen in Figure 3.3 of Chapter Three. It is hard to draw any discernible conclusions around these frameworks either, the synthesis of each was only attempted once due to time constraints within the project. If attempted repeats are still unsuccessful, then it would be wise to consider alternative reaction conditions with a longer reaction period coupled with a lower temperature and thus thermal input, in order to help regulate the ligand stability but still provide a reactive environment. This would be a target for optimisation, given the core absent adducts of BODIPY's **52** and **56** that were found in previous reactions of this area of the project, as these adducts likely indicated a level of core instability present in the BODIPY framework and thus creating a reaction environment that minimises any side reactions that leading to these adducts, would be a necessary step early on in the optimisation process. Given that BODIPY **48** is a novel derivative, complexation with these targeted metal centres will create an array of complexes that with full characterisation would be a notable advancement in BODIPY research.

5.4 HBC-Coupled BODIPY Derivatives

After considerable effort into the development of the two targeted HBC-coupled BODIPY derivatives **36** and **37** [Fig. 2.2], significant advances in the understanding of both the reactivity and physical properties of BODIPY dyes have been made. The insight gained into chemistry of BODIPY during this area of the research project, helped to lead the way for much of the other practical research carried out, with the knowledge of their solubility, general appearance, both in and out of solution, and their reaction particularities, all becoming useful in the progression of the other research pathways.

5.4.1 2,6-Functionalized BODIPY Derivatives of 36

Considerable advances were made along the HBC-coupled derivatives synthetic pathways themselves. Despite the arduous synthesis of the peripherally unsubstituted BODIPY **5** [Fig. 1.4], the development of a reliable, consistent, method for extracting

them from the crude product mixture was a considerable breakthrough. The use of a Soxhlet extraction set-up to automatically cycle almost 100 percent pure BODIPY from the solid phase crude material was instrumental in isolating large enough quantities of **5** to utilise for future reactions along the pathway. The selective solubility for the BODIPY molecule in Pet. Ether during these Soxhlet extractions, also lead to the simple method of Pet. Ether extraction, that helped to isolate small quantities of multiple BODIPY's and similar derivatives, throughout the research project, with the first small pure quantities of both BODIPY's **52** and **56** being isolated in this manner [Schemes 4-5].

The inability to synthesise the desired 2,6-diphenylactelyene coupled, derivative during this project (**39**), despite the array of Sonogashira reaction conditions attempted, gives inference to the probable stability of the targeted compound. Given that there are derivatives of **39** published already within the literature, such as the tetra-methylated version described by Zhang and co-workers, it speaks to the stability of the unsubstituted structure.¹¹⁶ The BODIPY molecule described within Zhang's research shares the exact same core framework, minus the methyl substituents, this suggesting that they play a pivotal role in product stability.¹¹⁶ Given the precursor they used was the 2,6-iodinated species, rather than the brominated version used within this project, there is potential that iodine is more favourable for this particular Sonogashira reaction. More likely though given the extreme difficulty groups had in successfully synthesising the fully unsubstituted BODIPY structure,⁴¹⁻⁴³ it may be that it is simply not robust enough to handle the diphenylactelyene functionality without methyl substitution present.

Both the promising ¹H-NMR and mass spectrometry data obtained during the Sonogashira reaction attempts, were indicative of both starting material loss coupled with some indistinguishable species development. It is thus hard to definitively say that **39** is not a stable product option. If future attempts at optimizing the reaction conditions were made and success was not observed, it may be a fair assumption to make though. Given the success of the second Sonogashira reaction, carried out as the first step in synthesis of **37** [Scheme 3], the best place to begin for formation of **39** in future work, may be in the form of changing the catalyst selection. One property kept constant throughout the attempted Sonogashira reactions, as seen per Table 1, was that of the

catalyst choice. Palladium(0) tetrakis(triphenylphosphine) was used each time. Success in generating the phenylactelyene coupled aldehyde species in Scheme 3 however, came from using the *in situ* activated – Palladium(II) dichloride bis(triphenylphosphine). Thus indicating that despite the recommended literature conditions described by Zhang and his team,¹¹⁶ the best catalyst for these systems may be that of the inactive palladium species, minimising the potential quenching of palladium prior to reaction activation. Along with a catalyst issue, there is potential that the mono and tetra-substituted impurities, still contained within the 2,6-dibrominated precursor, are simultaneously hindering the reaction process. If molecule **38** could be completely purified it would also remove a potential limiting factor within the reaction and allow for greater elucidation of the issues involved.

If **39** is successfully formed, the subsequent Diels-alder and cyclisation reactions to form the respective penta-phenyl benzene and HBC attenuated derivatives, will be required, as witnessed earlier in Scheme 3 also. With **39** isolated in a pure sample of reasonable size, these two reactions should pose less difficulty than previous steps, given the absence of sensitive metal catalysis and highly reactive moisture and oxygen sensitive reagents. The primary difficulty will likely be that of solubility with this being a future issue that may have to be overcome if research is to be continued and these large pentaphenyl or HBC derivatives made, as these large hydrogen carbon groups are very insoluble and can create significant synthetic and analytical issues.

5.4.2 *Meso*-Phenyl Functionalized BODIPY Derivative **37**

The major conclusion that can be drawn from development towards BODIPY **37** is that of the comparative ease, evident in the syntheses of this pathway as opposed to the peripherally unsubstituted framework [Fig. 2.2]. The method trialling of Cohen and co-workers, establishing the Sonogashira reaction as the best first reaction towards the dipyrromethane synthesis was invaluable.¹¹⁷ By comparison to the attempts at forming BODIPY **39**, only one set of reaction conditions and reagents had to be used. The absence of a complicating dipyrromethane moiety seemingly making the Sonogashira reaction much more successful, this success potentially a result of the inactive palladium(II) species used as well.

Following the successful coupling, the comparative ease of the dipyrromethane synthesis was only more evident when using 2,4-dimethyl pyrrole instead of unsubstituted pyrrole as well. Given that the synthetic pathway was abandoned post-dipyrromethane synthesis, future work here would involve formation of the BODIPY core before any further reactions to generate the hexaphenyl benzene or HBC-coupled derivatives could be undertaken. As discussed previously, this reaction usually being the step which complicates the synthetic pathways the most, for both the peripherally unsubstituted BODIPY **5** and for the two phenyl-ester BODIPY's **52** and **56**. Due to the increased stability and drastically increased practical ease of methylated dipyrromethane frameworks however, and the fact that this pathway is utilising a dipyrin as the intermediate rather than a hydrochloride salt form, the likely outcome of this BODIPY formation would likely be much more positive than the alternative reactions. For similar reasons it is hypothesised for this pathway that the ultimate target molecule, BODIPY **37**, would be much more easily attained than that of **36**. This is however the most likely reason why other research groups have already developed very similar BODIPY structures, with the relative synthetic ease, overwhelming the more interesting nature of the 2,6-HBC functionalized derivative.

Chapter Six

Experimental

6.1 General Experimental

Lab apparatus and safety equipment were used as appropriate and all precautions were followed to as per the Material Safety Data Sheet (MSDS) recommendations and the University's safety guidelines. Unless otherwise specified, all new chemicals were purchased at a reagent grade from Sigma Aldrich, and used as supplied and stored in concordance with the methods stated by both the suppliers and the MSDS guidelines. All dry solvents were obtained immediately prior to reaction from the University of Canterbury's dry-solvent system, wherein solvents are passed through high grade water absorbent alumina columns.

All flash column chromatography was carried out using Silica gel 70-230 mesh, with appropriate solvent system combinations chosen based on TLC analysis. Thin layer chromatography was performed on either foil or plastic backed F-254 Alumina and/or Silica plates, selected on a compound by compound basis, through chemical property determination and solvent system testing.

Triethylamine was purified by distillation over CaH_2 immediately prior to each reaction. Benzaldehyde was purified by washing with Na_2CO_3 followed by saturated $\text{Na}_2\text{S}_2\text{O}_3$ and H_2O , prior to vacuum distillation.

Melting points were carried out on a Modern Electrothermal Melting Point Apparatus and are stated as a range from first initial indication of melting, to time of full liquid state formation.

Nuclear Magnetic Resonance

All NMR spectra were recorded at room temperature on an Agilent 400-MR, operating at 400 MHz for all ^1H spectra, and at 100 MHz for all ^{13}C Spectra. Samples for analysis were dissolved in commercially sourced deuterated solvents; CDCl_3 , D_2O or CD_3OD , and each spectra was referenced to the corresponding residual solvent peak. Chemical shifts and coupling constants are all described in parts per million (ppm) and Hertz (Hz) respectively. HSQC and HMBC were employed as an advanced characterisation technique when required, using standard Varian and Agilent pulse sequences.

Mass Spectrometry

Data was recorded by Dr's Marie Squire and Amelia Albrett on either a DIONEX Ultimate 3000 or Bruker Maxis 4G spectrometer. All identified spectra were recorded using high resolution positive ion electrospray mode. Samples were dissolved in HPLC grade methanol only, to a targeted concentration of 20 nM.

Infrared Spectroscopy

Crystalline samples were ground using a standard mortar and pestle, to generate a fine powder suitable for solid state analysis. Infrared measurement was carried out on a Bruker ALPHA FT-IR spectrometer, with diamond ATF configuration, DTGS 4000-430 cm^{-1} . The sample was collected and peaks assigned, through 8 scans at 4 cm^{-1} resolution, using the OPUS operating program.

UV/Visible Spectroscopy

UV/Visible analysis was carried out using a Varian CARY 100 Bio UV/Visible spectrophotometer. Samples were measured with; path length constant at 1 cm, 25°C set temperature, black trimmed quartz cuvettes, and dichloromethane as the chosen solvent.

X-Ray Crystallography

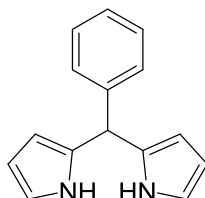
Refinement data is presented in Appendix 1. X-ray crystallographic data and refinement of **57**, was carried out with an Oxford-Agilent SuperNova instrument with a focused micro-source of Cu K α ($\lambda = 0.71073 \text{ \AA}$) radiation and an ATLAS CCD area detector. Crystal selection, preparation and analysis was done with the help of Dr Matt Polson. The structure was solved using direct methods with SHEL-XS¹³² and refined on *F*² using all data by full matrix least-squares procedures with SHEL-XL-97¹³³ within OLEX-2¹³⁴. Non-hydrogen atoms were refined with anisotropic displacement parameters where appropriate and hydrogen atoms were included in calculated positions, with isotropic displacement parameters 1.2 times the isotropic equivalent of

their carrier atoms. The functions minimised were $\Sigma w(F2o-F2c)$, with $w = [\sigma^2(F2o) + aP^2 + bP]^{-1}$, where $P = [\max(Fo)^2 + 2F2c]/3$. The graphical representation shown was created using the OLEX-2 image generator. Important bond angles, length and dimensions of the structure are discussed as part of the graphical image and the remaining structural information is stored at the University of Canterbury, Chemistry Department, and is available by request.

6.2 Compound Synthesis and Characterisation

Note: Experimental methods are described only where the method varied from that described in the literature. NMR and Mass spectrometry are described as consistent with the literature, wherein the difference between measured values and literature values are less than 0.2 ppm for NMR spectra and within 0.01 g/mol for mass analysis.

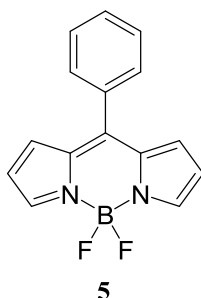
5-Phenyldipyrromethane



41

Compound **41** was synthesised as per the method described by Dehaen and co-workers.¹¹² Crude product dried and used immediately for synthesis. Stored samples degraded in response to both light and oxygen exposure. ¹H-NMR and Mass spectrometry results are both consistent with literature values.¹¹²

4,4-Difluoro-8-phenyl-4-bora-3a,4a-diaza-s-indacene

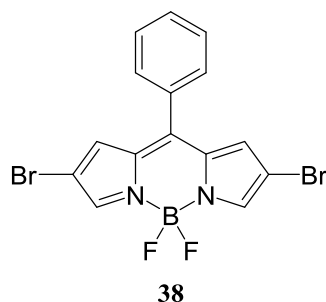


The *title compound* was obtained by modifying literature described methods for synthesising BODIPY compounds.¹³¹

A crude sample of molecule **41** (12.5 g, 56.3 mmol) was combined with *p*-chloranil (14.3 g, 58.4 mmol) under Ar gas, in a 1 L three-necked flask. The solids were placed under high vacuum, backfilled with Ar, and dissolved in dry DCM (400 mL) via cannula addition. After stirring for 30 minutes, TLC analysis showed clear loss of the starting material and the development of a bright yellow fluorescent compound (5-phenyldipyrromethene). NEt₃ (20 mL, 144 mmol) was added followed by BF₃.OEt₂ (30 mL, 243 mmol). The reaction was maintained stirring for a further 1.5 hours, until TLC showed development of a highly intense fluorescent orange compound.

The black reaction mixture was then decanted from the crude dark sludge formed and quenched with H₂O (300 mL), washed with further water (2 x 300 mL) and then extracted into DCM. The solution was then dried over Na₂SO₄ and evaporated onto silica (20 g). The free flowing impregnated silica was loaded into in a Soxhlet extraction using Pet. Ether as the solvent. Evaporation of the collected orange solvent *in vacuo* gave the *title compound* as a super fine red-orange powder. Mass: 3.11 g, Yield: 20.6%. ¹H-NMR and Mass spectrometry data are both consistent with the literature.¹³¹

2,6-Dibromo-4,4-difluoro-8-phenyl-4-bora-3a,4a-diaza-s-indacene

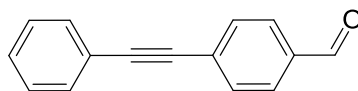


Synthesised using an adapted method of that described by Jiao, Hao and co-workers for the regioselective stepwise bromination of BODIPY dyes.¹¹⁴

BODIPY **5** (2.00 g, 7.46 mmol) was placed in a 500 mL three-necked flask under high vacuum for 30 minutes. The flask was then backfilled three times with Ar gas, before DCM (150 mL) was added via cannular addition. Under high Ar flow rate, the flask's *suba* seal was replaced with a 100 mL sealed pressure equalizing dropping funnel and a constant Ar gas flow was left passing over the equipment. In a separate 250 mL Schlenk flask, Bromine (0.75 mL, 15 mmol) was injected into a solution of DCM (75 mL), stirred until colour dissolution was evident, and then added via cannular to the sealed pressure equalizing dropping funnel. The pressure equalizing dropping funnel was then set to a flow rate of approximately 1 mL per 2 minutes. After 75 minutes and 90% Bromine/DCM solution addition, the drip was ceased and ¹H-NMR of a crude sample taken for analysis.

The NMR indicated slight formation of the tetra-brominated species, and complete consumption of mono-brominated adducts, thus the addition was ceased and the reaction quenched with 50% sodium thiosulfate (100 mL), then extracted into DCM. Recrystallization in Pet. Ether (3 x 400 mL) was carried out to increase product purity, with ¹H-NMR analysis carried out after each cycle. Semi-pure; Mass: 2.50 g, Yield: 78.7 % ¹H-NMR data is consistent with the literature quoted values, however tetra-brominated BODIPY impurities are still evident at around 10% relative to the *title compound* as per NMR integration.¹¹⁴ Mass spectrometry data unavailable due to undesired fragmentation and isotopic effects, as per the literature.¹¹⁵

4-Phenylacetylenylbenzaldehyde

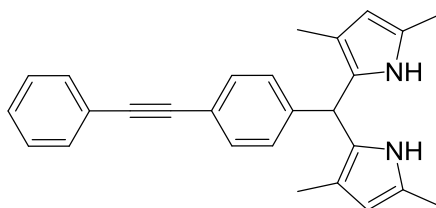


42

4-Bromobenzaldehyde (1.99 g, 10.7 mmol), [Pd(II)Cl₂(PPh₃)₂] (1.0 g, 1.43 mmol), CuI (0.050 g, 0.263 mmol) and PPh₃ (0.187 g, 0.713 mmol) were added to a 500 mL three-necked flask, *suba* sealed and placed *in vacuo*, with N₂ gas backfilled into the vessel. THF (150 mL) was added, the solution stirred and freshly distilled NEt₃, (7.50 mL, 53.8 mmol) plus phenylacetylene (3.20 mL, 29.1 mmol) were both added via syringe. Gas flow was increased, a reflux condenser substituted onto the system and the reaction left at 65°C. 48 hours later TLC indicated that product formation had levelled off with an excess of 4-bromobenzaldehyde present. Phenylacetylene (1.0 mL, 9.11 mmol) was added and the reaction left a further 24 hours until the aldehyde was fully consumed.

The resultant solution was evaporated *in vacuo* and the solid crude material was washed with hot Pet. Ether, and purified further via a silica plug, using a gradient solvent system of Pet. Ether moving to increasing DCM percentages. The final impurities were removed by trituration in Pet. Ether to afford the *title compound* as an off-white flaky solid. Mass 1.011 g, Yield: 45.6%. ¹H-NMR and Mass spectrometry both correlate to literature values.¹¹⁷

5-(Phenyl-4-acetylenyl)-1,3,7,9-tetramethyl dipyrromethane



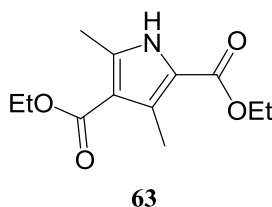
43

The *title compound* was synthesised using adapted methods from those described by Cohen and co-workers.¹¹⁷

5-(Phenyl-4-acetylenyl)-1,3,7,9-tetramethyl- dipyrromethane (0.401 g, 1.81 mmol), was placed *in vacuo* for 20 minutes and backfilled with Ar gas. DCM (100 mL) was added and the solution stirred with the addition of 2,4-dimethylpyrrole (0.60 mL, 5.83 mmol). After purging with Ar gas for 15 minutes a catalytic volume of TFA was added and the solution was left stirring at R.T. for 1.5 hours.

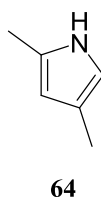
TLC analysis indicated the presence of a large 2,4-dimethylpyrrole excess., but successful development of a pale yellow fluorescent compound. After washing with NaOH (50 mL, 0.20 M) and H₂O (100 mL) with extraction into DCM, a crude pale orange brown solid was obtained. Mass: 0.2329 g, Yield: 34.1 % .¹H NMR and Mass spectrometry are consistent with the literature values.¹¹⁷

2,4-Dimethyl-3,5-dicarbethoxypyrrole



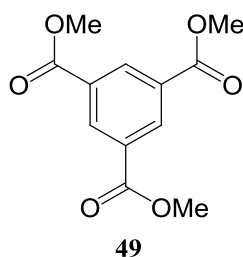
Synthesised using improved two-step method for obtaining 2,4-dimethylpyrrole, developed by Wang and co-workers.¹²⁸ ¹H-NMR spectra directly corresponds to the literature stated values.¹²⁸

2,4-Dimethylpyrrole

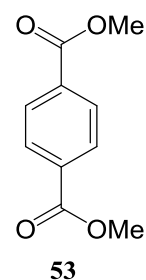


2,4-Dimethyl-3,5-dicarbethoxypyrrole (100 g, 0.418 mol) was separated into two 500 mL round bottom flasks and KOH (95 g, 1.69 mol) dissolved in 500 mL ethylene glycol was divided equally between the two flasks. The solutions were heated to 200°C for 48 hours over which time a deep brown-purple solution developed. After cooling to R.T. they were extracted with diethyl ether (3 x 150 mL) and the resulting solution was vacuum distilled to afford 16 mL of the *title compound*. Mass: 14.8 g, Yield: 37.2%. ^1H and ^{13}C -NMR correspond directly to the published 2,4-dimethylpyrrole spectra.¹²⁸

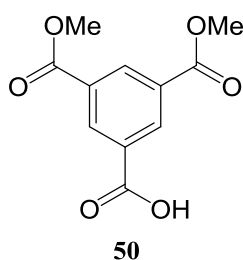
Trimethylbenzene-1,3,5-tricarboxylate



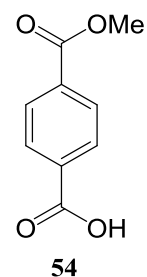
Dimethylbenzene-1,4-dicarboxylate



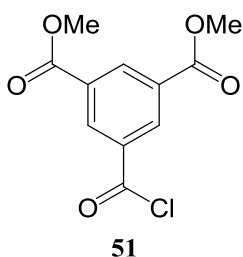
Dimethylbenzene-1,4-dicarboxylate



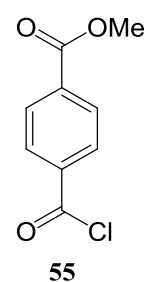
4-Methoxycarbonyl benzoic acid



2,4-Dimethoxycarbonyl benzoyl chloride

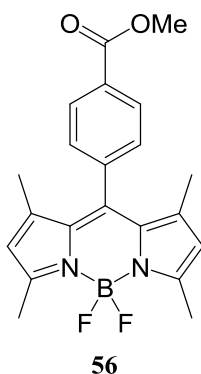


4-Methoxycarbonyl benzoyl chloride



Compounds **49** - **51** and **53** - **55** were synthesised as per methods described by Schatzschneider and co-workers, utilising esterification of the respective acid species, followed by selective hydrolysis of only one ester group to form the carboxylic acids, then converted into their respective acyl chlorides. ¹H-NMR data is consistent with the published results for all six precursor molecules.¹³⁵ Masses and yields are omitted as all products were simply dried crude and used immediately due to only low level impurities in the NMR spectra and there was no requirement for thorough purification.¹³⁵

4,4-Difluoro-8-(4-methoxycarbonyl)phenyl-1,3,5,7-tetramethyl-4-bora-3a,4a-diaza-s-indacene

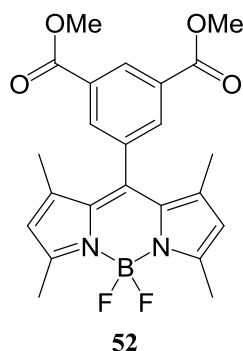


Compounds **52** and **56** were synthesised adhering to the literature methods of Chen and co-workers.¹³⁶

Compound **55** (1.86 g, 9.38 mmol) was placed in a 250 mL Schlenk flask under vacuum, then back filled with N₂ gas to create a static inert atmosphere. DCM (100 mL) was added via cannula to the flask, followed by 2,4-dimethylpyrrole (2 mL, 19.4 mmol). The solution was stirred for 24 hours at R.T., then TLC analysis performed, showing consumption of starting material and significant intermediate product development. At this stage the flask was placed in an ice-bath and NEt₃ (10 mL, 81.0 mmol) plus BF₃.OEt₂ (10 mL, 71.2 mmol) were added dropwise over five minutes. The N₂ gas was changed to a strong flowing environment to purge the system of volatile gas, then left stirring for a further 16 hours at which point TLC analysis once again showed absence of the intermediate and development of two highly fluorescent compounds.

The reaction was quenched with addition of an 80 mL solution of 25% Na₂CO₃/H₂O and stirred vigorously overnight. The resultant mixture was washed with H₂O (150 mL), extracted into DCM dried over and then evaporated under reduced pressure. Column purification was carried out on silica using 7:3 DCM/Pet. Ether as the solvent system. The product eluted off as the second compound, collected fractions were combined, concentrated and evaporated *in vacuo* to give the *title compound* as solid range-red powder. Mass: 551mg, Yield: 15.4%, ¹H-NMR and Mass spectrometry data are consistent with literature values.¹³⁶

4,4-Difluoro-8-(2,4-dimethoxycarbonyl)phenyl-1,3,5,7-tetramethyl-4-bora-3a,4a-diaza-s-indacene

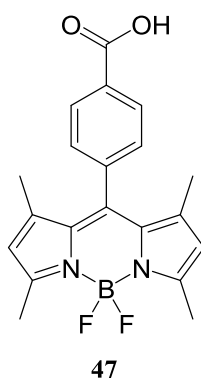


Compound **51** (1.90g, 7.39 mmol) was placed in a separate 250 mL Schlenk flask under vacuum. The flask was placed under an inert static N₂ gas atmosphere. was then dissolved in DCM (100 mL) introduced via cannula, followed by addition of 2,4-dimethylpyrrole (2.0 mL, 19.4 mmol). The mixture was left stirring at R.T. for 24 hours, then TLC analysed. TLC showed consumption of the starting material therefore NEt₃ (10 mL, 81.0 mmol) and BF₃.OEt₂ (10 mL, 71.2 mmol) were added dropwise over five minutes to the solution maintained in an ice-bath. The reaction environment was purged with N₂ gas and left stirring for another 16 hours the intermediate dipyrin salt was no longer observed under TLC, and was replaced with two highly fluorescent compounds.

25% Na₂CO₃/H₂O (80 mL) was added as a quench and the solution stirred vigorously overnight. The resultant mixture was washed with 150 mL H₂O, extracted into DCM and then evaporated under reduced pressure. Column purification was carried out on

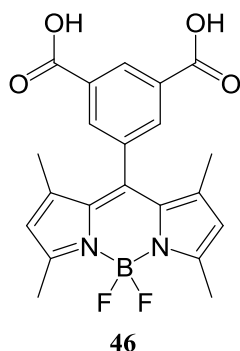
silica using 4:1 DCM/Pet. Ether as the solvent system. The product eluted off as the second compound, all pure fractions were combined and concentrated *in vacuo* to isolate **52** as a solid orange-red powder compound. Mass: 373mg, Yield: 11.5%, ¹H-NMR and Mass spectrometry analysis are in agreeance with published values.¹³⁶

4,4-Difluoro-8-(4-carboxyl)phenyl-1,3,5,7-tetramethyl-4-bora-3a,4a-diaza-s-indacene



Compound **56** (200 mg, 0.523 mmol) was stirred until almost full dissolution in MeOH (90 mL). NaOH (1.0 g, 25.0 mmol) dissolved in 10 mL H₂O was then added dropwise, over a five minute period and the solution heated to 50°C for 24 hours. Solvents were removed by evaporation at reduced pressure and the resultant crude dark red product dissolved in H₂O (50 mL) then acidified to pH: 1 via dropwise HCl addition. An immediate red precipitate was formed and collected by vacuum filtration, washed with Pet. Ether and slowly dissolved in ethyl acetate due to low solubility. The ethyl acetate was then removed *in vacuo* to give the *title compound* as a bright red-orange powder. Mass: 113 mg, Yield: 58.7% ¹H-NMR and Mass spectrometry are consistent with those quoted in the literature.¹³⁷

4,4-Difluoro-8-(2,4-dicarboxyl)phenyl-1,3,5,7-tetramethyl-4-bora-3a,4a-diaza-s-indacene

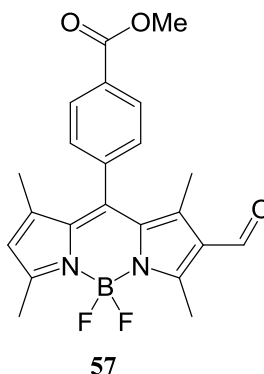


As per compound **47**, the *title compound* was synthesised from the ester precursor using a standard set of hydrolysis conditions.

Compound **52** (200 mg, 0.454 mmol) was solubilized in MeOH (90 mL). Heating to 50°C was started prior to addition of the base to assist in dissolution. Once considerably dissolved, NaOH (1.0 g, 25.0 mmol) in 10 mL H₂O was added to the warm solution over 5 minutes in a dropwise fashion. The solution was then left maintained at 50°C for 24 hours.

After the 24 hour period was up, all solvent was removed using rotary evaporation at reduced pressure and the resultant crude dark red viscous material was dissolved in H₂O (50 mL) then acidified to pH: 1 via dropwise HCl addition. An immediate red precipitate was formed and collected by vacuum filtration, washed with Pet. Ether and slowly dissolved in ethyl acetate due to significantly reduced solubility. The ethyl acetate was evaporated *in vacuo* and gave the BODIPY derivative **46** as a red powder. Mass: 159 mg, Yield: 84.9% ¹H-NMR and Mass spectrometry data are consistent with quoted literature values for the *title compound*.¹¹⁸

3-Formyl-4,4-difluoro-8-(4-methoxycarbonyl)phenyl-1,3,5,7-tetramethyl-4-bora-3a,4a-diaza-s-indacene



Synthesised using a literature preparation published in 2009 in the *Journal of Organic Chemistry* describing the β -Formylation of a variety of 1,3,5,7-tetramethyl BODIPY derivatives.¹²¹

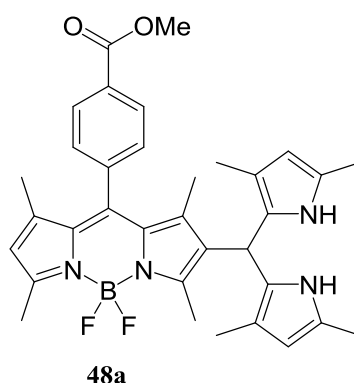
POCl_3 (6 mL, 64.4 mmol) and DMF (6 mL, 77.5 mmol) were combined in a 250 mL Schlenk flask within an ice-bath. The solution was maintained with stirring at sub 10°C for five minutes, then warmed to R.T. and left stirring for a further 30 minutes. The precursor, molecule **56** (158 mg, 0.413 mmol), was placed in a separate sealed flask, dissolved in 60 mL EDC and this solution was transferred via cannula to the Schlenk flask. The flask was transferred to a water bath and the temperature raised to 50°C . After two hours maintained like this, the reaction was quenched with addition of saturated NaHCO_3 (200 mL) and stirred for a final 30 minutes.

The resultant mixture was washed with H_2O (2 x 200 mL) extracted into excess EDC, dried over MgSO_4 and concentrated under reduced pressure. Slow evaporation of the resulting 3 mL of solution gave rise to the formation of a collection of purple-grey crystals.

Mass: 29.7 mg, Yield: 17.5%, M.P. $211\text{--}212^\circ\text{C}$, $^1\text{H-NMR}$ (400 MHz, CDCl_3) δ/ppm 10.01(s, 1H), 8.23(d, $J=7.0$ Hz) 2H), 7.42(d, $J=6.3$ Hz) 2H), 6.17(s, 1H), 3.99(s, 3H), 2.83(s, 3H), 2.63(s, 3H), 1.65(s, 3H), 1.40(s, 3H), $^{13}\text{C-NMR}$ (100 MHz, CDCl_3) δ/ppm 185.78, 166.19, 162.23, 156.91 142.65, 142.05, 138.86, 131.36, 130.76, 130.63, 129.24, 125.45, 128.14, 124.33, 52.48, 15.13, 14.97, 13.01, 11.75, m/z ESI-MS (MeOH) Found

[MH]⁺ 411.1694 [C₂₂H₂₂BF₂N₂O₃]⁺ requires 411.1692, IR ν/cm^{-1} : 2952w, 1720s, 1541s, 1403s, 1311s, 1275s, 1083br/s, 1014s, 979s, 822m, 737s, UV/Visible (CH₂Cl₂) λ_{max} (ϵ) 499 nm (34485).

3-(1,3,7,9-Tetramethyl)dipyrrol-4,4-difluoro-8-(4-methoxycarbonyl)phenyl-1,3,5,7-tetramethyl-4-bora-3a,4a-diaza-s-indacene

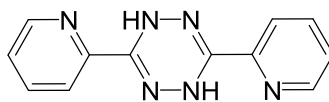


Compound **47** (103 mg, 0.251 mmol) was placed *in vacuo* in a 100 mL Schlenk flask. The flask was back-filled with Ar gas to create a flowing inert environment and dry DCM (50 mL) was added via syringe. 2,4-Dimethylpyrrole (0.052 mL, 0.505 mmol) was injected into the solution, followed by five drops of TFA to catalyse the reaction. After 30 minutes of intense stirring TLC showed the formation of two deep pink, highly fluorescent compounds and the solution was quenched with H₂O (50 mL) washed with a further 50 mL and extracted into DCM. The resultant dilute solution was dried over Na₂SO₄ and concentrated *in vacuo*.

Chromatographic purification on silica using straight DCM, eluted an impure mixture of the *title compound* and its mono-pyrrole adduct, as evidenced by TLC. Mass: 72.0 mg, Yield: 54.5% ¹H NMR peaks evident are consistent with 3-(2,4-dimethyl)pyrrol-4,4-difluoro-8-(4-methoxycarbonyl)phenyl-1,3,5,7-tetramethyl-4-bora-3a,4a-diaza-s-indacene, as the observed impurity.

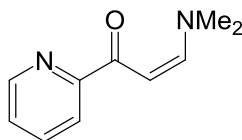
Mass: 72.0 mg, Yield: 54.5% $^1\text{H-NMR}$ (400 MHz, CDCl_3) δ /ppm 8.15(d, $J=7.8$ Hz, 2H), 7.40(d, $J=8.2$ Hz, 2H), 7.21(s, 1H) 5.98(s, 1H), 5.65(s, 1H), 3.95(s, 3H), 2.73(s, 3H), 2.55(s, 3H), *2.14(s, 6H)*, *1.77(s, 6H)*, 1.33(s, 3H), 1.08(s, 3H), m/z ESI-MS (MeOH) Found $[\text{M}]^+$ 581.2916 $[\text{C}_{34}\text{H}_{36}\text{BF}_2\text{N}_4\text{O}_2]^+$ requires 581.2899 and Found $[\text{M}-(2,4\text{-dimethylpyrrole})]^+$ 488.2329 $[\text{C}_{28}\text{H}_{29}\text{BF}_2\text{N}_3\text{O}_2]^+$ requires 488.2321. Note: $^1\text{H-NMR}$ and Mass spectrometry impurities are indicated with italics.

3,6-Di(2-pyridinyl)-1,4-dihydro-1,2,4,5-tetrazine



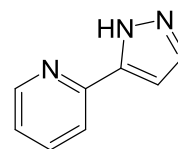
71

2-Propen-1-one, 3-(dimethylamino)-1-(2-pyridinyl)



84

3-(2-Pyridinyl)pyrazole



77

The *title compound's* **71**, **77**, and **84** were synthesised using methods adapted from previous research within the group. $^1\text{H-NMR}$ results are consistent for all molecules with the literature values, as is Mass spectrometry of compound **71**.^{130, 138} Mass spectrometry of **77** and **84**, were unavailable due to mass limitations.

References

1. Albrecht, C. *Anal. Bioanal. Chem.* **2008**, 390 (5), 1223-1224.
2. Lichtman, J. W.; Conchello, J. A. *Nat. Methods* **2005**, 2 (12), 910-919.
3. Thomson, T. *Annal Phil.* **1819**, 14, 34-36.
4. Mishra, A.; Behera, R. K.; Behera, P. K.; Mishra, B. K.; Behera, G. B. *Chem. Rev.* **2000**, 100 (6), 1973-2012.
5. Wright, P.; Staff, U. B. In *Kirk-Othmer Encycl. Chem. Technol.*; John Wiley & Sons, Inc.: **2000**.
6. Benniston, A. C.; Copley, G. *PCCP* **2009**, 11 (21), 4124-4131.
7. Baeyer, A. V. *Ber. Dtsch. Chem. Ges.* **1871**, 4, 555-558.
8. Zheng, H.; Zhan, X.-Q.; Bian, Q.-N.; Zhang, X.-J. *Chem. Commun.* **2013**, 49 (5), 429-447.
9. C.H.G., W. *Trans. R. Soc. Edinburg* **1856**, 21, 377.
10. Noelting, E.; Dziewoński, K. *Ber. Dtsch. Chem. Ges.* **1905**, 38 (3), 3516-3527.
11. Beija, M.; Afonso, C. A. M.; Martinho, J. M. G. *Chem. Soc. Rev.* **2009**, 38 (8), 2410-2433.
12. Santra, S.; Yang, H.; Dutta, D.; Stanley, J. T.; Holloway, P. H.; Tan, W.; Moudgil, B. M.; Mericle, R. A. *Chem. Commun.* **2004**, (24), 2810-2811.
13. Dong, S.; Roman, M. *J. Am. Chem. Soc.* **2007**, 129 (45), 13810-13811.
14. Okanobo, A.; Chauhan, S. K.; Dastjerdi, M. H.; Kodati, S.; Dana, R. *Am. J. Ophthalmol.* **2012**, 154 (1), 63-71.
15. Alford, R.; Simpson, H. M.; Duberman, J.; Hill, G. C.; Ogawa, M.; Regino, C.; Kobayashi, H.; Choyke, P. L. *Mol. Imaging* **2009**, 8 (6), 341-354.
16. Hoebe, R. A.; Van Der Voort, H. T. M.; Stap, J.; Van Noorden, C. J. F.; Manders, E. M. M. *J. Microsc.* **2008**, 231 (1), 9-20.
17. Zheng, Q.; Jockusch, S.; Rodriguez-Calero, G. G.; Zhou, Z.; Zhao, H.; Altman, R. B.; Abruna, H. D.; Blanchard, S. C. *Photochem. Photobiol.* **2016**, 15 (2), 196-203.
18. Kuhn, M. A.; Hoyland, B.; Carter, S.; Zhang, C.; Haugland, R. P. *Handbook of Biological Stains and Dyes* **1995**, 238-244.
19. Weiss, S. *Science* **1999**, 283 (5408), 1676-1683.
20. Yang, Y.; Zhao, Q.; Feng, W.; Li, F. *Chem. Rev.* **2013**, 113 (1), 192-270.
21. Berezin, M. Y.; Achilefu, S. *Chem. Rev.* **2010**, 110 (5), 2641-2684.

22. Wagnieres, G. A.; Star, W. M.; Wilson, B. C. *Photochem. Photobiol.* **1998**, 68 (5), 603-632.
23. Kobayashi, H.; Ogawa, M.; Alford, R.; Choyke, P. L.; Urano, Y. *Chem. Rev.* **2010**, 110 (5), 2620-2640.
24. Tsien, R. Y. *Annu. Rev. Biochem* [Article] **1998**, 67 (1), 509.
25. Wu, L.; Burgess, K. *J. Am. Chem. Soc.* **2008**, 130 (12), 4089-4096.
26. Zimmer, M. *Chem. Rev.* **2002**, 102 (3), 759-782.
27. Arun, K. H. S.; Kaul, C. L.; Ramarao, P. J. *Pharmacol. Toxicol. Methods* **2005**, 51 (1), 1-23.
28. Wouters, F. S.; Verveer, P. J.; Bastiaens, P. I. H. *Trends Cell Biol.* **2001**, 11 (5), 203-211.
29. Hoffman, R. M. *Lab. Invest.* **2015**, 95 (4), 432-452.
30. Loudet, A.; Burgess, K. *Chem. Rev.* **2007**, 107 (11), 4891-4932.
31. Ziessel, R.; Ulrich, G.; Harriman, A. *New J. Chem.* **2007**, 31 (4), 496-501.
32. Thoresen, L. H.; Kim, H.; Welch, M. B.; Burghart, A.; Burgess, K. *Synlett* **1998**, 1998 (11), 1276-1278.
33. Entwistle, A.; Noble, M. J. *Microsc.* **1992**, 168 (3), 219-238.
34. Umezawa, K.; Matsui, A.; Nakamura, Y.; Citterio, D.; Suzuki, K. *Chem. Eur. J.* **2009**, 15 (5), 1096-1106.
35. Boens, N.; Leen, V.; Dehaen, W. *Chem. Soc. Rev.* **2012**, 41 (3), 1130-1172.
36. Nepomnyashchii, A. B.; Bard, A. J. *Acc. Chem. Res.* **2012**, 45 (11), 1844-1853.
37. Ulrich, G.; Ziessel, R.; Harriman, A. *Angew. Chem. Int. Ed.* **2008**, 47 (7), 1184-1201.
38. Ni, Y.; Wu, J. *Org. Biomol. Chem.* **2014**, 12 (23), 3774-3791.
39. Treibs, A.; Kreuzer, F. H. *Justus Liebigs Ann. Chem.* **1968**, 718 (1), 208-223.
40. Kang, H. C.; Haugland, R. P.; Fisher, P. J.; Prendergast, F. G. 1989; pp 68-73.
41. Arroyo, I. J.; Hu, R.; Merino, G.; Tang, B. Z.; Peña-Cabrera, E. J. *Org. Chem.* **2009**, 74 (15), 5719-5722.
42. Schmitt, A.; Hinkeldey, B.; Wild, M.; Jung, G. *J. Fluoresc.* **2009**, 19 (4), 755-758.
43. Tram, K.; Yan, H.; Jenkins, H. A.; Vassiliev, S.; Bruce, D. *Dyes Pigm.* **2009**, 82 (3), 392-395.

44. Thermo Fisher Scientific Inc. BODIPY FL in Bovine pulmonary artery endothelial cells. www.thermofisher.com/nz/en/home/life-science/cell-analysis/fluorophores/bodipy-fl (accessed 23.03.17, 2017).
45. Urano, Y.; Kamiya, M.; Kanda, K.; Ueno, T.; Hirose, K.; Nagano, T. *J. Am. Chem. Soc.* **2005**, *127* (13), 4888-4894.
46. Bandichhor, R.; Thivierge, C.; Bhuvanesh, N. S. P.; Burgess, K. *Acta Crystallogr. Sect. E* **2006**, *62* (10), 4310-4311.
47. de Wael, E. V.; Pardoën, J. A.; van Koeveringe, J. A.; Lugtenburg, J. *Recl. Trav. Chim. Pays-Bas* **1977**, *96* (12), 306-309.
48. Bröring, M.; Krüger, R.; Link, S.; Kleeberg, C.; Köhler, S.; Xie, X.; Ventura, B.; Flamigni, L. *Chem. Eur. J.* **2008**, *14* (10), 2976-2983.
49. Kee, H. L.; Kirmaier, C.; Yu, L.; Thamyongkit, P.; Youngblood, W. J.; Calder, M. E.; Ramos, L.; Noll, B. C.; Bocian, D. F.; Scheidt, W. R.; Birge, R. R.; Lindsey, J. S.; Holten, D. *J. Phys. Chem. B* **2005**, *109* (43), 20433-20443.
50. Ueno, T.; Urano, Y.; Setsukinai, K.-i.; Takakusa, H.; Kojima, H.; Kikuchi, K.; Ohkubo, K.; Fukuzumi, S.; Nagano, T. *J. Am. Chem. Soc.* **2004**, *126* (43), 14079-14085.
51. Zhang, D.; Martin, V.; Garcia-Moreno, I.; Costela, A.; Perez-Ojeda, M. E.; Xiao, Y. *PCCP* **2011**, *13* (28), 13026-13033.
52. Mula, S.; Elliott, K.; Harriman, A.; Ziessel, R. *J. Phys. Chem. A* **2010**, *114* (39), 10515-10522.
53. Sabatini, R. P.; McCormick, T. M.; Lazarides, T.; Wilson, K. C.; Eisenberg, R.; McCamant, D. W. *J. Phys. Chem. Lett.* **2011**, *2* (3), 223-227.
54. Ji, S.; Ge, J.; Escudero, D.; Wang, Z.; Zhao, J.; Jacquemin, D. *J. Org. Chem.* **2015**, *80* (11), 5958-5963.
55. Lakshmi, V.; Rajeswara Rao, M.; Ravikanth, M. *Org. Biomol. Chem.* **2015**, *13* (9), 2501-2517.
56. Rey, Y. P.; Abradelo, D. G.; Santschi, N.; Strassert, C. A.; Gilmour, R. *Eur. J. Org. Chem.* **2017**
57. Kim, H.; Burghart, A.; B. Welch, M.; Reibenspies, J.; Burgess, K. *Chem. Commun.* [10.1039/A905739K] **1999**, (18), 1889-1890.
58. Yin, Z.; Tam, A. Y.-Y.; Wong, K. M.-C.; Tao, C.-H.; Li, B.; Poon, C.-T.; Wu, L.; Yam, V. W.-W. *Dalton Trans.* **2012**, *41* (37), 11340-11350.

59. Ma, X.; Azeem, E. A.; Liu, X.; Cheng, Y.; Zhu, C. *J. Mat. Chem. C* **2014**, 2 (6), 1076-1084.
60. Moriarty, R. D.; Martin, A.; Adamson, K.; O'Reilly, E.; Mollard, P.; Forster, R. J.; Keyes, T. E. *J. Microsc.* **2014**, 253 (3), 204-218.
61. Díaz-Moscoso, A.; Emond, E.; Hughes, D. L.; Tizzard, G. J.; Coles, S. J.; Cammidge, A. N. *J. Org. Chem.* **2014**, 79 (18), 8932-8936.
62. Albrecht, M.; Lippach, A.; Exner, M. P.; Jerbi, J.; Springborg, M.; Budisa, N.; Wenz, G. *Org. Biomol. Chem.* **2015**, 13 (24), 6728-6736.
63. Donuru, V. R.; Zhu, S.; Green, S.; Liu, H. *Polymer* **2010**, 51 (23), 5359-5368.
64. Brizet, B.; Bernhard, C.; Volkova, Y.; Rousselin, Y.; Harvey, P. D.; Goze, C.; Denat, F. *Org. Biomol. Chem.* **2013**, 11 (44), 7729-7737.
65. Yu. Schmidt, E.; Zorina, N. V.; Yu. Dvorko, M.; Protsuk, N. I.; Belyaeva, K. V.; Clavier, G.; Méallet-Renault, R.; Vu, T. T.; Mikhaleva, A. b. I.; Trofimov, B. A. *Chem. Eur. J.* **2011**, 17 (11), 3069-3073.
66. Buyukcakil, O.; Bozdemir, O. A.; Kolenen, S.; Erbas, S.; Akkaya, E. U. *Org. Lett.* **2009**, 11 (20), 4644-4647.
67. Vives, G.; Giansante, C.; Bofinger, R.; Raffy, G.; Guerzo, A. D.; Kauffmann, B.; Batat, P.; Jonusauskas, G.; McClenaghan, N. D. *Chem. Commun.* **2011**, 47 (37), 10425-10427.
68. Liu, S.; Shi, Z.; Xu, W.; Yang, H.; Xi, N.; Liu, X.; Zhao, Q.; Huang, W. *Dyes Pigm.* **2014**, 103 (0), 145-153.
69. Volkova, Y.; Brizet, B.; Harvey, P. D.; Denat, F.; Goze, C. *Eur. J. Org. Chem.* **2014**, 2014 (11), 2268-2274.
70. Liao, J.; Wang, Y.; Xu, Y.; Zhao, H.; Xiao, X.; Yang, X. *Tetrahedron* **2015**, 71 (31), 5078-5084.
71. Shimizu, S.; Iino, T.; Saeki, A.; Seki, S.; Kobayashi, N. *Chem. Eur. J.* **2015**, 21 (7), 2893-2904.
72. Mao, M.; Zhang, X.; Cao, L.; Tong, Y.; Wu, G. *Dyes Pigm.* **2015**, 117 (0), 28-36.
73. Chen, W.; Zhang, J.; Mack, J.; Kubheka, G.; Nyokong, T.; Shen, Z. *RSC Adv.* **2015**.

74. Yamamura, M.; Yazaki, S.; Seki, M.; Matsui, Y.; Ikeda, H.; Nabeshima, T. *Org. Biomol. Chem.* [10.1039/C4OB02351J] **2015**, *13* (9), 2574-2581.
75. Yuan, L.; Lin, W.; Zheng, K.; He, L.; Huang, W. *Chem. Soc. Rev.* **2013**, *42* (2), 622-661.
76. Poirel, A.; Nicola, A. D.; Retailleau, P.; Ziessel, R. *J. Org. Chem.* **2012**, *77* (17), 7512-7525.
77. Nagai, A.; Chujo, Y. *Macromol.* **2010**, *43* (1), 193-200.
78. Chu, G. M.; Guerrero-Martínez, A.; Fernández, I.; Sierra, M. Á. *Chem. Eur. J.* **2014**, *20* (5), 1367-1375.
79. Kowada, T.; Maeda, H.; Kikuchi, K. *Chem. Soc. Rev.* **2015**, *44* (14), 4953-4972.
80. Lakshmi, V.; Shaikh, M. S.; Ravikanth, M. *J. Fluoresc.* **2013**, *23* (3), 519-525.
81. Zatsikha, Y. V.; Yakubovskiy, V. P.; Shandura, M. P.; Kovtun, Y. P. *Dyes Pigm.* **2015**, *114* (0), 215-221.
82. Chen, J.; Burghart, A.; Derecskei-Kovacs, A.; Burgess, K. *J. Org. Chem.* **2000**, *65* (10), 2900-2906.
83. Boens, N.; Leen, V.; Dehaen, W.; Wang, L.; Robeyns, K.; Qin, W.; Tang, X.; Beljonne, D.; Tonnelé, C.; Paredes, J. M.; Ruedas-Rama, M. J.; Orte, A.; Crovetto, L.; Talavera, E. M.; Alvarez-Pez, J. M. *J. Chem. Phys. A* **2012**, *116* (39), 9621-9631.
84. Dost, Z.; Atilgan, S.; Akkaya, E. U. *Tetrahedron* **2006**, *62* (36), 8484-8488.
85. Wang, L.; Fang, G.; Cao, D. *Sens. Actuators, B.* **2015**, *221* (0), 63-74.
86. Kamkaew, A.; Lim, S. H.; Lee, H. B.; Kiew, L. V.; Chung, L. Y.; Burgess, K. *Chem. Soc. Rev.* **2013**, *42* (1), 77-88.
87. Ortiz, M. J.; Agarrabeitia, A. R.; Duran-Sampedro, G.; Bañuelos Prieto, J.; Lopez, T. A.; Massad, W. A.; Montejano, H. A.; García, N. A.; Lopez Arbeloa, I. *Tetrahedron* **2012**, *68* (4), 1153-1162.
88. Adarsh, N.; Avirah, R. R.; Ramaiah, D. *Org. Lett.* **2010**, *12* (24), 5720-5723.
89. Baruah, M.; Qin, W.; Basarić, N.; De Borggraeve, W. M.; Boens, N. *J. Org. Chem.* **2005**, *70* (10), 4152-4157.
90. Juarez, L. A.; Costero, A. M.; Parra, M.; Gil, S.; Sancenon, F.; Martinez-Manez, R. *Chem. Commun.* **2015**, *51* (9), 1725-1727.
91. Duan, W.; Wei, H.; Cui, T.; Gao, B. *J. Mat. Chem. B* **2015**, *3* (5), 894-898.
92. Li, Q.; Guo, Y.; Shao, S. *Analyst* **2012**, *137* (19), 4497-4501.

93. Ahrens, J.; Böker, B.; Brandhorst, K.; Funk, M.; Bröring, M. *Chem. Eur. J.* **2013**, *19* (34), 11382-11395.
94. Nakamura, M.; Tahara, H.; Takahashi, K.; Nagata, T.; Uoyama, H.; Kuzuhara, D.; Mori, S.; Okujima, T.; Yamada, H.; Uno, H. *Org. Biomol. Chem.* **2012**, *10* (34), 6840-6849.
95. Tamgho, I.-S.; Hasheminasab, A.; Engle, J. T.; Nemykin, V. N.; Ziegler, C. J. *J. Am. Chem. Soc.* **2014**, *136* (15), 5623-5626.
96. Jones, L. J.; Upson, R. H.; Haugland, R. P.; Panchuk-Voloshina, N.; Zhou, M.; Haugland, R. P. *Anal. Biochem.* **1997**, *251* (2), 144-152.
97. Huaultmé, Q.; Mirloup, A.; Retailleau, P.; Ziessel, R. *Org. Lett.* **2015**, *17* (9), 2246-2249.
98. Yamaguchi, Y.; Matsubara, Y.; Ochi, T.; Wakamiya, T.; Yoshida, Z.-i. *J. Am. Chem. Soc.* **2008**, *130* (42), 13867-13869.
99. Wan, C.-W.; Burghart, A.; Chen, J.; Bergström, F.; Johansson, L. B. A.; Welford, M. F.; Kim, T. G.; Topp, M. R.; Hochstrasser, R. M.; Burgess, K. *Chem. Eur. J.* **2003**, *9* (18), 4430-4441.
100. Madhu, S.; Kumar, S.; Chatterjee, T.; Ravikanth, M. *New J. Chem.* **2014**, *38* (11), 5551-5558.
101. Lakshmi, V.; Lee, W.-Z.; Ravikanth, M. *Dalton Trans.* **2014**, *43* (42), 16006-16014.
102. Baudron, S. A. *Cryst. Eng. Comm.* **2016**, *18* (25), 4671-4680.
103. Cui, Y.; Yue, Y.; Qian, G.; Chen, B. *Chem. Rev.* **2012**, *112* (2), 1126-1162.
104. James, S. L. *Chem. Soc. Rev.* **2003**, *32* (5), 276-288.
105. Eddaoudi, M.; Moler, D. B.; Li, H.; Chen, B.; Reineke, T. M.; O'Keeffe, M.; Yaghi, O. M. *Acc. Chem. Res.* **2001**, *34* (4), 319-330.
106. Allendorf, M. D.; Bauer, C. A.; Bhakta, R. K.; Houk, R. J. T. *Chem. Soc. Rev.* **2009**, *38* (5), 1330-1352.
107. Stock, N.; Biswas, S. *Chem. Rev.* **2012**, *112* (2), 933-969.
108. Furukawa, H.; Cordova, K. E.; O'Keeffe, M.; Yaghi, O. M. *Science* **2013**, *341* (6149).

109. Hayashi, Y.; Obata, N.; Tamaru, M.; Yamaguchi, S.; Matsuo, Y.; Saeki, A.; Seki, S.; Kureishi, Y.; Saito, S.; Yamaguchi, S.; Shinokubo, H. *Org. Lett.* **2012**, *14* (3), 866-869.
110. Zhao, N.; Xuan, S.; Fronczek, F. R.; Smith, K. M.; Vicente, M. G. H. *J. Org. Chem.* **2017**.
111. Boyle, R. W.; Bruckner, C.; Posakony, J.; James, B. R.; Dolphin, D. *Org. Synth.*; John Wiley & Sons, Inc.: **2003**.
112. Dehaen, W.; Maes, W.; Ngo, T. H.; Dolusic, E.; Rohand, T. *ARKIVOC* **2007**, *2007* (10), 307-324.
113. Parees, D. M. *Anal. Chem.* **1979**, *51* (11), 1675-1679.
114. Jiao, L.; Pang, W.; Zhou, J.; Wei, Y.; Mu, X.; Bai, G.; Hao, E., Regioselective Stepwise Bromination of Boron Dipyrromethene (BODIPY) Dyes. *J. Org. Chem.* **2011**, *76* (24), 9988-9996.
115. Qi, Y.; Geib, T.; Huynh, A.-M.; Jung, G.; Volmer, D. A. *Rapid Commun. Mass Spectrom.* **2015**, *29* (9), 885-890.
116. Zhang, D.; Wen, Y.; Xiao, Y.; Yu, G.; Liu, Y.; Qian, X. *Chem. Commun.* **2008**, (39), 4777-4779.
117. Halper, S. R.; Cohen, S. M. *Chem. Eur. J.* **2003**, *9* (19), 4661-4669.
118. Pradhan, T.; Maiti, S.; Kumar, R.; Lee, Y. H.; Kim, J. W.; Lee, J. H.; Kim, J. S. *Dyes Pigm.* **2015**, *121*, 1-6.
119. Baudron, S. A. *Dalton Trans.* [10.1039/C3DT50493J] **2013**, *42* (21), 7498-7509.
120. Zhu, S.; Zhang, J.; Janjanam, J.; Vegesna, G.; Luo, F.-T.; Tiwari, A.; Liu, H. *J. Mat. Chem. B* **2013**, *1* (12), 1722-1728.
121. Yu, C.; Jiao, L.; Yin, H.; Zhou, J.; Pang, W.; Wu, Y.; Wang, Z.; Yang, G.; Hao, E. *Eur. J. Org. Chem.* **2011**, *2011* (28), 5460-5468.
122. Jiao, L.; Yu, C.; Li, J.; Wang, Z.; Wu, M.; Hao, E. *J. Org. Chem.* **2009**, *74* (19), 7525-7528.
123. Ni, F.; Cotton, T. M. *Anal. Chem.* **1986**, *58* (14), 3159-3163.
124. Geissman, T. A. In *Organic Reactions*; John Wiley & Sons, Inc.: **2004**.
125. Corey, E. J.; Gilman, N. W.; Ganem, B. E. *J. Am. Chem. Soc.* **1968**, *90* (20), 5616-5617.

126. Sedelmeier, J.; Ley, S. V.; Baxendale, I. R.; Baumann, M. *Org. Lett.* **2010**, *12* (16), 3618-3621.
127. Livingstone, S. E. In *The Chemistry of Ruthenium, Rhodium, Palladium, Osmium, Iridium and Platinum*; Pergamon: **1973**; Vol. 25, p ii.
128. Meng, G.; Zheng, M. L.; Wang, M. *Org. Prep. Proced. Int.* **2011**, *43* (3), 308-311.
129. Sathyamoorthi, G.; Soong, M. L.; Ross, T. W.; Boyer, J. H. *Heteroat. Chem.* **1993**, *4* (6), 603-608.
130. Das, S.; Samanta, S.; Ray, S.; Biswas, P. *RSC Adv.* **2015**, *5* (92), 75263-75267.
131. Wagner, R. W.; Lindsey, J. S. *Pure Appl. Chem.* **1996**, *68* (7), 1373-1380.
132. Sheldrick, G. *Acta Crystallogr. Sect. A* **2008**, *64* (1), 112-122.
133. Sheldrick, G. *Bruker AXS Inc., Madison, Wisconsin, USA* **1997**.
134. Dolomanov, O. V.; Bourhis, L. J.; Gildea, R. J.; Howard, J. A. K.; Puschmann, H. *J. Appl. Crystallogr.* **2009**, *42* (2), 339-341.
135. Splith, K.; Neundorf, I.; Hu, W.; N'Dongo, H. W. P.; Vasylyeva, V.; Merz, K.; Schatzschneider, U. *Dalton Trans.* **2010**, *39* (10), 2536-2545.
136. Chen, Y.; Zhao, J.; Guo, H.; Xie, L. *J. Org. Chem.* **2012**, *77* (5), 2192-2206.
137. Ekmekci, Z. *Tetrahedron Lett.* **2015**, *56* (14), 1878-1881.
138. Wang, J.; Su, D.; Wang, D.; Ding, S.; Huang, C.; Huang, H.; Hu, X.; Wang, Z.; Li, S. *Inorg. Chem.* **2015**, *54* (22), 10648-10655.

Appendices

Crystallographic Data for BODIPY 57

Identification code	jfb64-507-1
Empirical formula	C ₄₄ H ₄₂ B ₂ F ₄ N ₄ O ₆
Formula weight	820.43
Temperature/K	120.01(10)
Crystal system	triclinic
Space group	P-1
a/Å	9.5020(3)
b/Å	11.5184(4)
c/Å	18.4106(7)
α/°	85.924(3)
β/°	75.831(3)
γ/°	88.388(2)
Volume/Å ³	1948.64(12)
Z	2
ρ _{calc} /cm ³	1.398
μ/mm ⁻¹	0.880
F(000)	856.0
Crystal size/mm ³	0.425 × 0.224 × 0.186
Radiation	CuKα (λ = 1.54184)
2θ range for data collection/°	7.696 to 153.816
Index ranges	-11 ≤ h ≤ 9, -13 ≤ k ≤ 14, -23 ≤ l ≤ 23
Reflections collected	18776
Independent reflections	8065 [R _{int} = 0.0257, R _{sigma} = 0.0277]
Data/restraints/parameters	8065/0/551
Goodness-of-fit on F ²	1.014
Final R indexes [I ≥ 2σ (I)]	R ₁ = 0.0412, wR ₂ = 0.1104
Final R indexes [all data]	R ₁ = 0.0478, wR ₂ = 0.1169
Largest diff. peak/hole / e Å ⁻³	0.32/-0.30